République Algérienne Démocratique et Populaire

Ministère de l'Enseignement Supérieur et de la Recherche Scientifique

Université Larbi Tébessi –Tébessa-

Faculté des Sciences Exactes et des Sciences de la Nature et de la Vie Département :

Science de la Terre et de l'Univers

MEMOIRE DE MASTER

Domaine: Science de la Terre et l'Univers Filière: Géologie

Option: Géologie de l'ingénieur et géotechnique :

Thème:

Stability analysis of some landslides around Zâarouria. W of Souk Ahras

Présenté par:

ALLOUANE Amira

Devant le jury:

FEHDI chemseddine	**Professeur**	**Présidant**	**Université Larbi Tebessi**
DJABRI mohamed	**M.C.B**	**Examinateur**	**Université larbi Tebessi**
BOUMEZBEUR Abd Rahmen	**Professeur**	**Rapporteur**	**Université larbi tebessi**

Date de soutenance : 17-06-2021

THANKS

I want to thank Dr BOUMEZBEUR for believing in me and for being everything I wished in a teacher and the best mentor

I want to thank all my teachers for their efforts for bringing this department up to a great level.

I am also thanking my best friends Djohra, Mariama, Maroua, Nihad, Kaouter, Sara, Nourlhouda, Ibtissem and all others for being the best friends I will ever wish for.

I want to thank my parents for being the light of this modest path.

DEDICATION

It is an honor for me to dedicate this modest work:

To my dear parents

To my sister and her my brothers

To all my friends and colleagues

To my favorite teacher Dr

BOUMEZBEUR A To everyone who

helped me do this job.

TABLE OF CONTENT

CHAPTER II

INTRODUCTION TO LAND SLIDES HAZERDS

CHAPTER III

STABILITY ANALYSIS AND FACTOR OF SAFTY

CHAPTER IV

SHEET PILE DESIGN

TABLE OF FIGURES

CHAPTER I: PRESENTATION OF THE REGION OF SOUK AHRAS

CHAPTER II: INTRODUCTION TO LAND SLIDES HAZERDS

CHAPTER III: STABILITY ANALYSIS AND FACTOR OF SAFTY.

CHAPTER IV: SHEET PILE DESIGN

LIST OF TABLES

CHAPTER I: PRESENTATION OF THE REGION OF SOUK AHRAS

CHAPTER II: INTRODUCTION TO LAND SLIDES HAZERDS

Abstract

Landslides are natural phenomena that occur in mountainous and hilly terrains like our study area Zaarouria. They occur very often when the rainfall exceeds some threshold and they reoccur despite the remedial measures undertaken every time they happen. They caused severe damage to houses and the road network. They are frequent mainly along the road side slopes. They are the result of interplay between the geological, geomorphologically, hydrological parameters. The identification of the conditions that lead to instability helps to propose adequate remedial measures and design efficient stabilizing structures such as sheet piles. The studied slope is located in the entrance north of Zaarouria. Before any stability analysis, the geological model, soil properties, type of instability were carefully determined. First soil properties and geometry were used to design a sheet pile wall for slope stabilization. Second these soil properties and parameters were used in Geoslope and Plaxis to assess the stability of the studied slope. Second, the cantilever sheet pile with the required flexural stiffness, normal stiffness, pile length, and so on, were applied as reinforcement. The safety factor increases significantly, showing the stabilizing effect of the proposed solution.

Résume

Les glissements de terrain sont des phénomènes naturels qui se produisent dans des terrains montagneux et vallonnés comme notre zone d'étude Zaarouria. Ils surviennent très souvent lorsque les précipitations dépassent un certain seuil et ils se reproduisent malgré les mesures correctives prises à chaque fois qu'ils se produisent. Ils ont causé de graves dommages aux maisons et au réseau routier. Ils sont fréquents principalement le long des pentes en bord de route. Ils sont le résultat de l'interaction entre les paramètres géologiques, géomorphologiques, hydrologiques. L'identification des conditions qui conduisent à l'instabilité permet de proposer des mesures correctives adéquates et de concevoir des structures stabilisatrices efficaces telles que des palplanches. Le versant étudié est situé à l'entrée nord de Zaarouria. Avant toute analyse de stabilité, le modèle géologique, les propriétés du sol, le type d'instabilité ont été soigneusement déterminés. Les premières propriétés et géométries du sol ont été utilisées pour concevoir un mur de palplanches pour la stabilisation des pentes. Deuxièmement, ces propriétés et paramètres du sol ont été utilisés dans Geoslope et Plaxis pour évaluer la stabilité de la pente étudiée. Deuxièmement, la palplanche en porte-à-faux avec la rigidité à la flexion requise, la rigidité normale, la longueur du pieu, etc., a été appliquée comme renfort. Le facteur de sécurité augmente considérablement, montrant l'effet stabilisant de la solution proposée.

ملخص

الانهيارات الأرضية هي ظاهرة طبيعية تحدث في التضاريس الجبلية والتلال مثل منطقة دراستنا الزعرورية. تحدث في كثير من الأحيان عندما يتجاوز هطول الأمطار بعض العتبة وتتكرر على الرغم من التدابير العلاجية المتخذة في كل مرة تحدث. وألحقت أضرارا بالغة بالمنازل وشبكة الطرق. هم متكررون بشكل رئيسي على طول منحدرات جانب الطريق. إنها نتيجة التفاعل بين المعلمات الجيولوجية والجيومرفولوجية والهيدرولوجية. يساعد تحديد الظروف التي تؤدي إلى عدم الاستقرار في اقتراح تدابير علاجية مناسبة وتصميم هياكل استقرار فعالة مثل ركائز الألواح.

يقع المنحدر المدروس في المدخل شمال الزعرورية. قبل إجراء أي تحليل للثبات ، تم تحديد النموذج الجيولوجي وخصائص التربة ونوع عدم الاستقرار بعناية. تم استخدام خصائص التربة وهندستها أولاً لتصميم جدار كومة صفائحية لتثبيت المنحدر. ثانياً ، تم استخدام خواص ومعايير التربة في Geoslope وPlaxis لتقييم ثبات المنحدر المدروس. ثانيًا ، تم تطبيق كومة الصفائح الكابولية مع صلابة الانحناء المطلوبة ، والصلابة العادية ، وطول الوبر ، وما إلى ذلك ، كتعزيز. يزداد عامل الأمان بشكل كبير ، مما يدل على تأثير التثبيت للحل المقترح.

Landslides are natural hazardous phenomenon that usually occurs in hills and mountain sides, they are usually the result of the interplay of natural and / or anthropogenic factors. Since this phenomenon occurs sometimes in human developed areas they make an even bigger risk of destruction and sometimes death.

The wilaya of Souk Ahras is a region that is highly exposed to landslide hazards because of its morphology, geology and climate. It is a mountainous area with large and long slopes, a deeply incised water streams, high rise escarpments and scattered hills. The area contains forested, bare and cultivated lands. The rejuvenation of the slope inclinations and the climate play in a way that landslide and erosion will never stop and mitigation measures can only reduce the consequences of the phenomenon.

The recent development has made a great pressure on the authorities to put in action urgent plans to meet the population requirements. The planning process has considered zones of marginal stability which have been previously considered inadequate for house construction or road development. These developments have in fact enhanced and instabilities and caused problems to traffic flow and main supplies.

Therefore, in order to understand the causes of the phenomenon of landslides and propose the adequate mitigation measures in this wilaya we need to take a close look to its geology, geographic location, and climate conditions. The work is undertaken according to this reasoning where a first chapter is elaborated acquaint the reader with the area and presents its main geographical and geological characteristics. The second chapter is an attempt to introduce the reader to the realm of landslide, how they occur, where they occur, their types and processes. The third chapter is mainly a presentation of the methods of slope stability computation. Sheet pile role, characteristics and design in slope stability engineering is the subject of the fourth chapter. This chapter includes also the study of the stability of a slope in Zaarouria by the use of sheet piles. The stability computation using Geoslope 2020 and Plaxis 8.2 softwares was carried out. They both showed a significant increase in the factor of safety upon the use of sheet piles with adequate characteristics. Indeed in the field, the studied slope has been efficiently stabilized by the sheet piles in conformity with our computations.

I. Introduction

The souk ahras region is well known with the occurrence of landslide phenomenon due to its morphology and other factors, in this chapter we are going to study the geological, topographic, hydrological and climate conditions to take better idea on the study area Zaarouria and relate some triggering mechanisms to these factors.

II. Presentation of the study area

1. Geographic location of souk ahras

The wilaya of Souk Ahras is located in the far east of the country, near the Tunisian border, 640 kilometers from Algiers. It is bounded to the northeast by the wilaya of Taraf, to the northwest by the wilaya of Guelma, to the south by the wilaya of Tébessa, to the southwest by the Republic of Tunisia. It occupies a strategic position between the north, the highlands and the south of the country.

The wilaya of souk Ahras covers a total area of approximately 4359.65 km², its surface area covering almost 0.18% of the entire national territory. Distributed administratively over 28 municipalities and 10 daïras. Its forest cover, made up of breads, Aleppo, cypress and eucalyptus, is estimated at over 97,280 ha. The wilaya is characterized by a resident population of more than 438,127 inhabitants, giving a density of 101 inhabitants / km², with an average annual growth rate equal to 1.8% (2008 statistics). Its climate is semi-arid with a Mediterranean dominance in the North, and continental in the South (hamed, 2004; Fahdi, 2008; Demdoum et al; 2013). Crossed by important Maghreb wadis, the Seybouse, the Medjerda, and the Mellègue; the wilaya has two large dams (Ain Dalia and OuedCharef, whose total capacity exceeds 240 million m³) and several hill reservoirs meeting the needs of the wilaya in PDO and irrigation. Its main mountains are Dj. Meida (1423m), Dj. Kelaia (1286m), Dj. Zouara (1292m) and Dj. Dekma (1120m). The wilaya of souk ahras has a dense and well-maintained road network of more than 1,200 linear km, with very dense electrification, affecting more than 90% of its territory. The geomorphological configuration of the wilaya reveals two main groups:

A mountainous and forested north made up of 12 municipalities with a total area of 1879.58 km², characterized by an average altitude of (1000 m), high rainfall and dominance in cattle breeding and fruit trees.

A south in high plains and pastures encompassing 16 municipalities with an area of 2480.07 km², the average rainfall is 350 mm / year. This area is characterized by an average altitude of (650m) and a strong dominance of sheep farming and cereal production.

2. Geographical location of the study region " Zaarouria"

The area concerned by the landslide risk study is located 8 km south of Souk Ahras in the municipality of Zaarouria shown in figure 1, between 36 ° 13 ′ 38 ″ north, 7 ° 57 ′ 28 ″ east it is spread over a surface of: 196 M² and a population of 11 234 ha. It is characterized by strong demographic and agricultural dynamics.

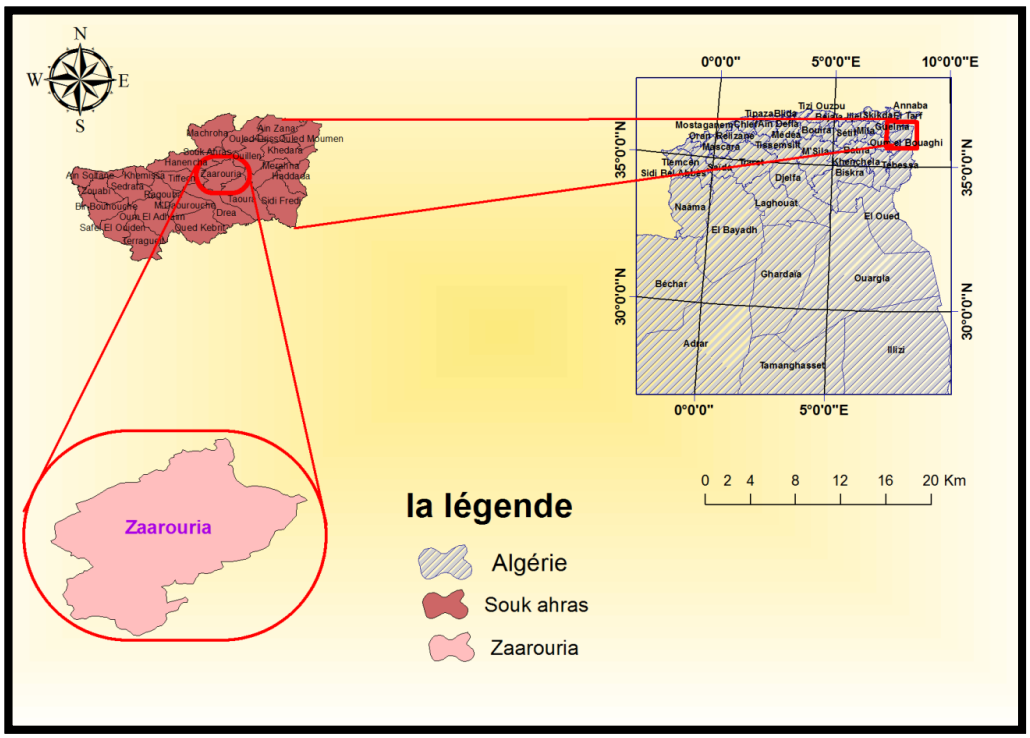

Figure1: The geographical location of the study area

3. Topography

The study area Zaarouria can be gemorphologically considered to be a large slope facing North West. This slope is essentially composed of two parts, the upstream part steeper than the downstream part, the average slope of which varies from 10° to 25° and ends in an order three stream which downpour into Oued Medjerda. The steep part constitutes the mountain side of Djebel Chouga, the maximum altitude of which is 1098m. The digital terrain model in figure 2 illustrates the geomorphology of the terrain. It is made up of a certain number of altitude sections including 2% for the section between 400 - 500m.

The slopes vary between 0 and 60°, the parts considered to be gentle have slopes less than 10°, they constitute the major parts of the land oriented towards the east and made up of Triassic materials. The slopes developed on Mio-Pliocene materials have more accentuated inclination varying from approximately the steepest slopes and has the characteristics of mountain side slopes.

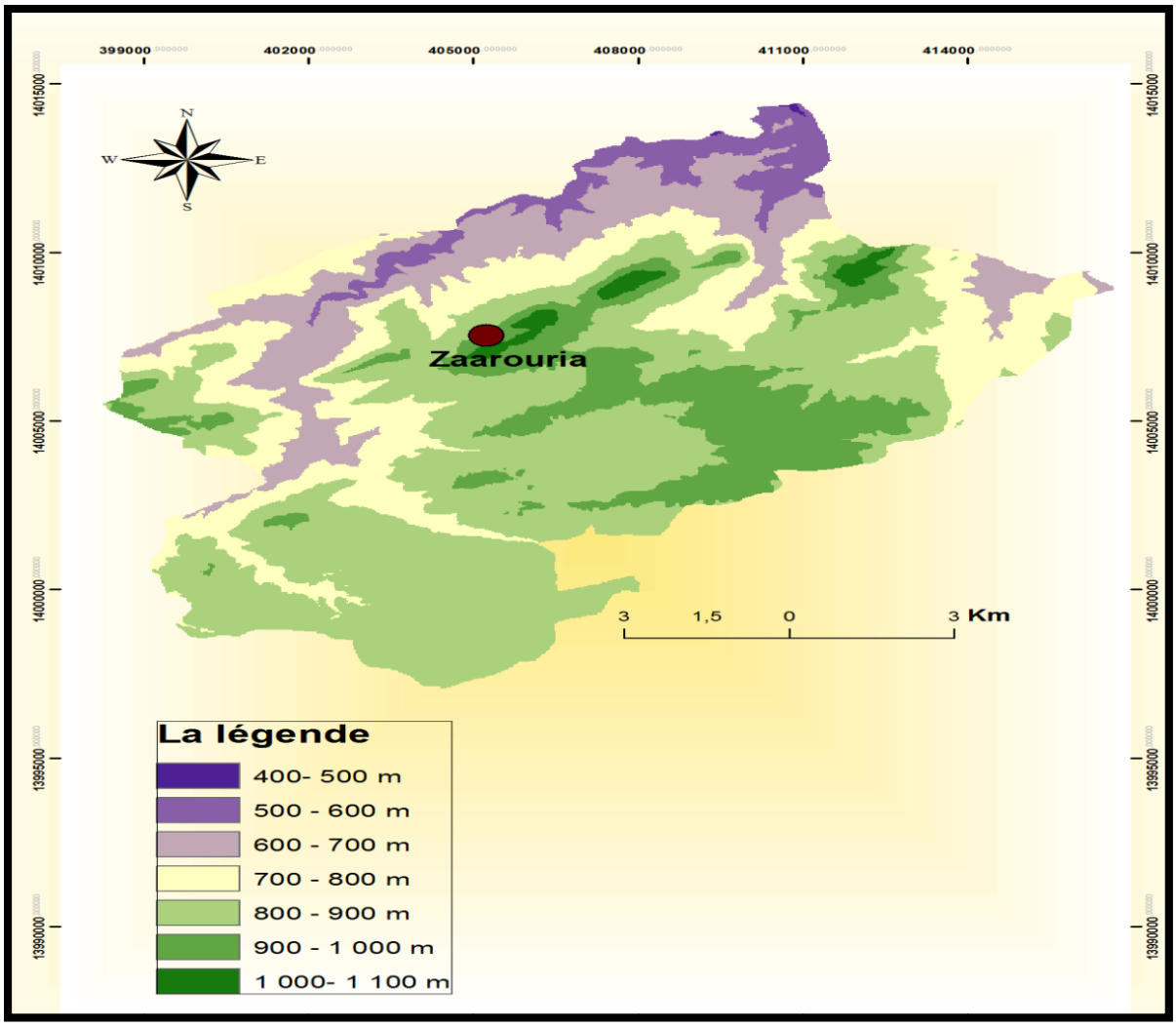

Figure2: The digital terrain model illustrates the geomorphology of the terrain

4. The hydrographic network:

The study area is part of the upper Medjerda Mountains. The hydrographic network there is well developed; it is represented by small temporary rivers on the sides of the embankments, flowing into the large wadis, the most important of which are wadi Medjerda, wadi Mellégue.

The hydrographic network of the study area is relatively undeveloped given the amounts of precipitation that the region receives. This is in our opinion due to the fact that mass movements and erosion phenomena prevail over incision and drainage path development.

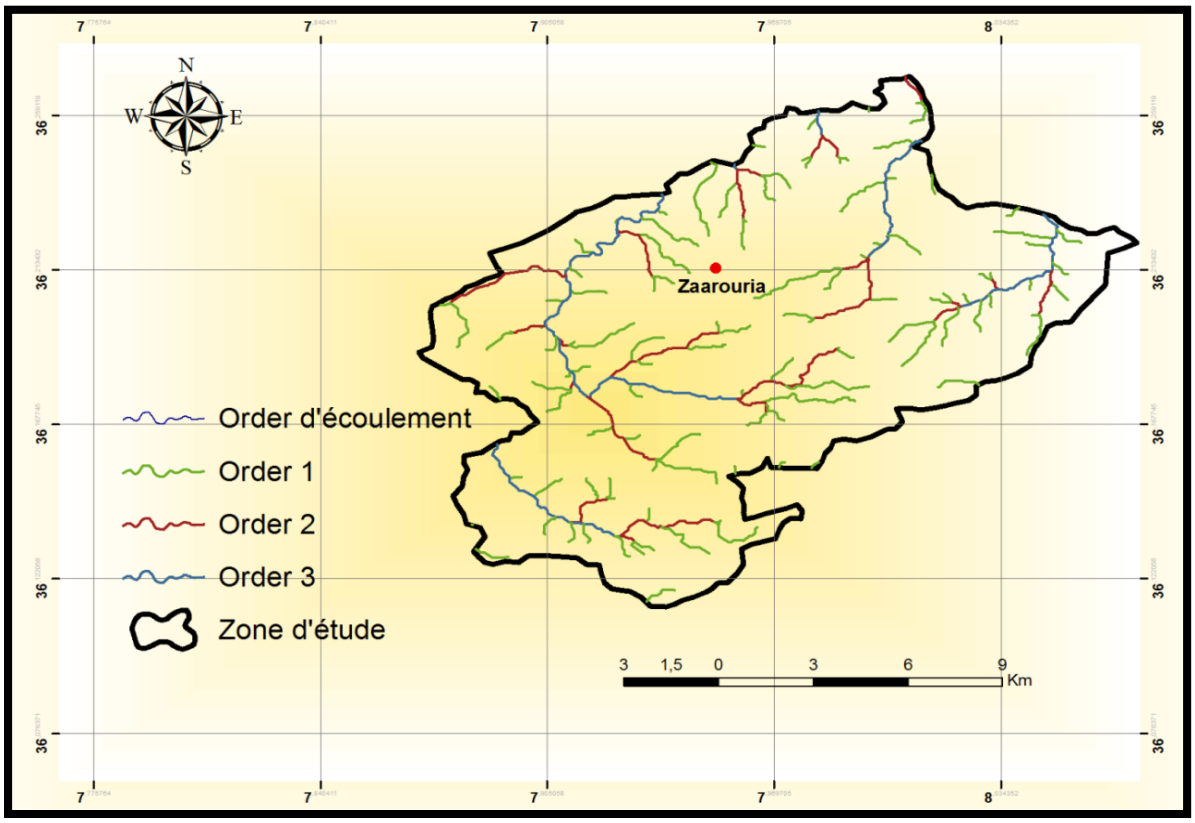

Figure 3: orders of the hydrographic network of Zaarouria:

5. Geological setting

The study area is part of the Maghrebids basin which stretches over 2000 km long, from the Strait of Gibraltar to the North of Calabria (Italy), passing through the Moroccan Rif, the Atlas littoral from Algeria (Kabyle of Tell), from Tunisia (Kroumirie-Nefza), Sicily and finally Calabria. The Tell was essentially structured during the tertiary movements, especially the Miocene. From north to south, three paleogeologeographic domains can be distinguished.

a. The internal domain

The northern domain, it is made up of Paleozoic crystallophyllian terrains of varied nature. From the Triassic to the Upper Oligocene, the internal massifs of the Maghrebids constitute a high zone, often emerged. It constitutes a string of coastal massifs bordered to the south by their sedimentary cover formed mainly of carbonate rocks of secondary to tertiary age called Dorsal Kabyle. It was the platform of the Thetis Sea. This intensely deformed limestone ridge extends from Sicily in the East to the Betic Cordilleras in the 'West through northern Rif

b. **The Flyschdomain**:

This area is characterized by flysch-type sediments ranging from the Lower Cretaceous to Upper Miocene. These are deep sea deposits, set up, generally under Lysocline, by turbidity

currents. It seems to be mostly abyssal plain formation (Bouillin, 1986). We distinguish from north to south of the flysch basin: the Mauritanian flyschs and the Massylian flyschs, differing from each other by their geographical position and slightly by the nature of the sediments.

c. The External domain:

The Tellian units constitute a complex stack of thrust sheets in the south of the Para-autochthonous foreland, also known under the name of the `` pre-Saharan " domain of the high plains. The allochthonous Tellian results from the detachment and cleavage of the Meso-Cenozoic sedimentary cover deposited on the northern margin of the African plate.

In this work, it will not be dealt with the geological details of the entire region rather than the geological nature of the area of study.

6. Local geology

In souk Ahras area, the successions of the geological formations start with the trias evaporitic formations up to the plio-quaternary. In the study area, which is a north facing slope, the trias formation is mainly composed of dark brown sticky Lithology which corresponds to what is known by “argile du trias”. It is covered by cretaceous marls on top of which comes the Miocene with loose yellowish sand. This side hill slope is in fact the northern flank of a NE SW anticline. This northern flank upon which stretchs the studied slope is covered by a mantle of silt clay and marl.

.

Age	Dominante Lithology
Quaternaire	Alluvions, terrasses
Moi-pliocène, Continental	Argiles rouge, sables, agglomérats
Miocène supérieur	Argiles et argiles sableuses
Miocène inferieur	Argiles sableuses. Argiles et calcaire lacustres
Oligocène	Argiles rouge et argile sableuses de Numidie
Eocène moyen	Marnes et nappes de calcaires
Eocène inferieur	Marnes et nappes de calcaires
Crétacé supérieur	Calcaire sénonien et marnes
Crétacé inferieur et moyen	Marnes et calcaire marneux Turoniens
Trias	Marnes gypses, calcaires et dolomie

Table 1: Representation of stratigraphic scale

III. Hydrogeology and hydrology of the region:

Hydrological and hydrogeological conditions coming together with weather conditions to confirm the importance of water in the alteration process, surface water acts mechanically, physically and chemically as the number one responsible of surface erosion, when same water infiltrates it changes the hydrogeological conditions by increasing the pore pressure which is the most important factor trigger for landslides coming as a result of heavy rainfall.

1. Hydrology:

The wilaya of Souk Ahras has a large enough hydrographic network that can be used to promote any agricultural speculation requiring the use of irrigation. We note the presence of two large watersheds within the limits of the wilaya (Figures 5): the watershed of the Seybouse and that of Medjerda. In fact, the high chain of the Souk Ahras Mountains stretched NE-SW, represents a barrier constituting a watershed line and the limit between these two large watersheds.

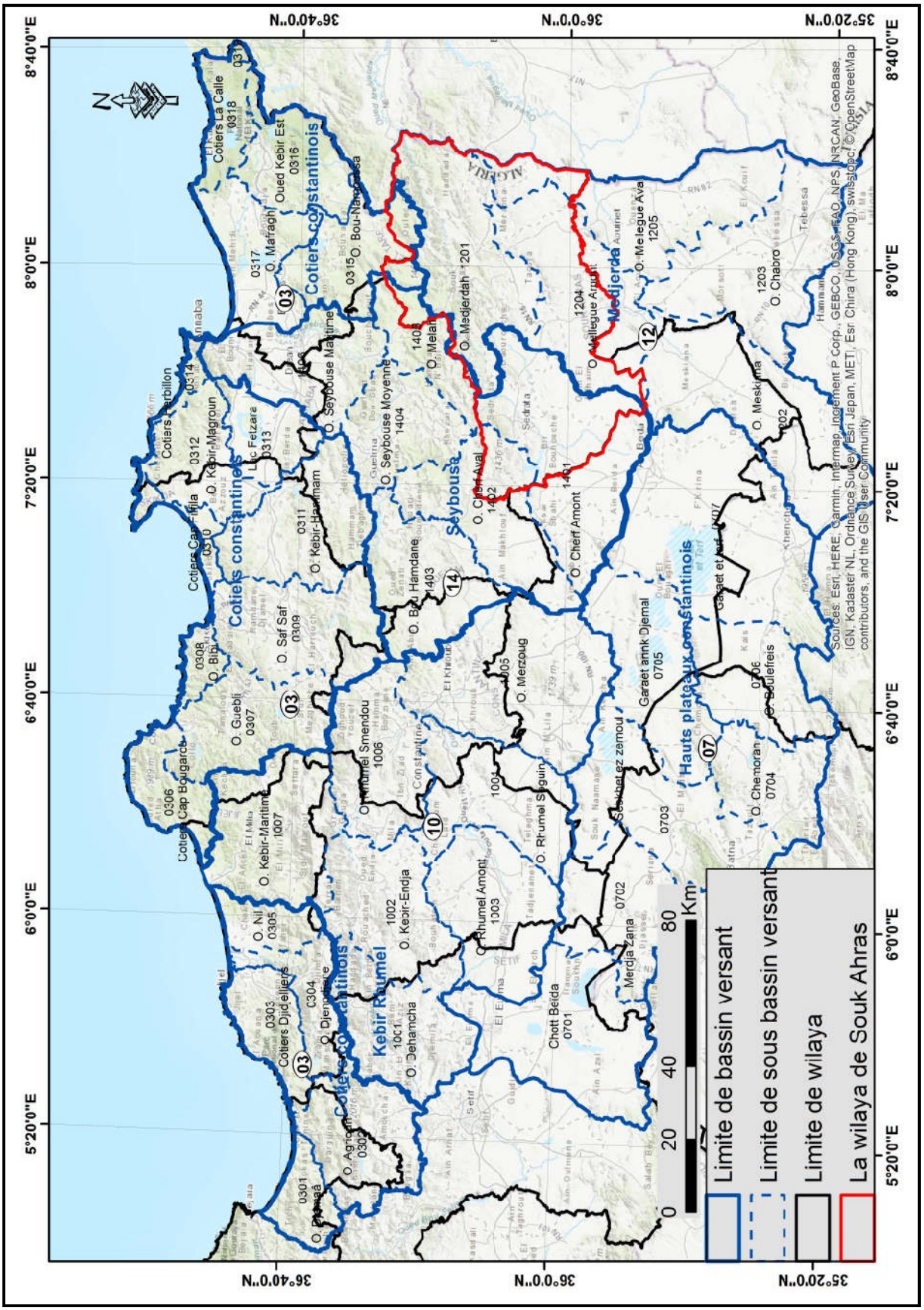

Figure 4: geographic location of watersheds of the Este of Algeria**.**

2. Hydrogeology:

Geological framework and tectonic, the features of the landscape and the climate of the territory have already determined the hydrogeological conditions of the region (B. Kriviakine, et al., 1989b). The study region is characterized by formations ranging from the Triassic to Quaternary, generally made up of limestone, clays, marls, sandstones and gravel. The hydrogeological characteristics of the different areas of the wilaya of Souk Ahras (Figure 6) are represented as follows:

- ✓ The scree and the breccias of slopes sometimes create sources of weak importance.
- ✓ Miocene and Pliocene sandstones and conglomerates are also store rocks for excellent filtering properties (B. Kriviakine, et al., 1989b).
- ✓ Red Numidian clays, on which low permeability sandstone rests fragmented into numerous independent panels. The sources are numerous, but their flow rates are low. There are also outcrops of marl and marly limestone from Eocene, almost impermeable.
- ✓ The main aquifer levels are linked to the Campanian and Maestrichtian. They have the highest water content. These cracked and porous limestones lying on waterproof marl. It contains pure water which has a good taste and which is discharged thanks to sources with a flow rate of 0.5 - 1.0 l / S (in H. Djaba, 2010).
- ✓ The Triassic diapir: they correspond to outcrops of marl, gypsum and rocks more resistant. They are very poor in groundwater, only a few large limestone "blocks" (1 to 2 km2)contain small slicks that give rise to small springs with varying flow ratesfrom 0.1 to 0.3 l / s. they often mark out large faulty areas, highlighting theTriassic contact Senonian series "diapir de Tifech" (B. Kriviakine, et al., 1989b).

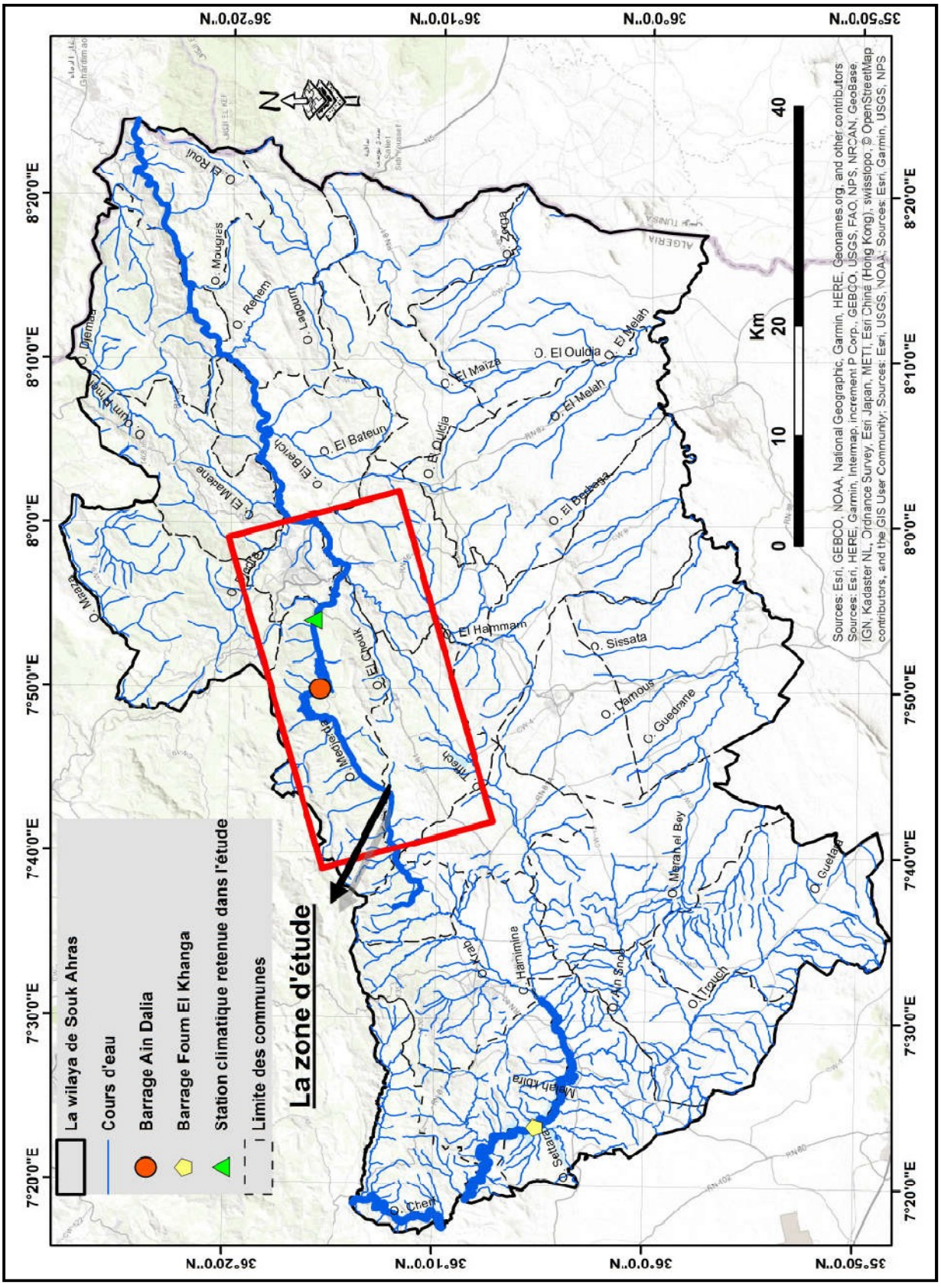

Figure 5: Aquifers of souk ahras region

IV. Weather:

Since souk Ahras is located in the North Est. part of Algeria then there is no doubt that it has a continental climate« semi-wet »with a Mediterranean influence on the north part and a desert « semi-arid »one on the south part, with rainfall varies between 300 et 1 100 mm/year (figure 1and 2). January and December days are encountered to be the heaviest wintery rainy and windy days; it is caused by the successive passage of the W depression, of some Mediterranean depression and by the passage of cold fronts as per the least rainy days are days of July and august with precipitation of6,04 et 16,83 mm, the majority of the rains of these dry months is caused mainly by violent thunderstorms and sometimes by the passage of cold fronts associated with northerly winds (in W. Khoualdia, 2017).

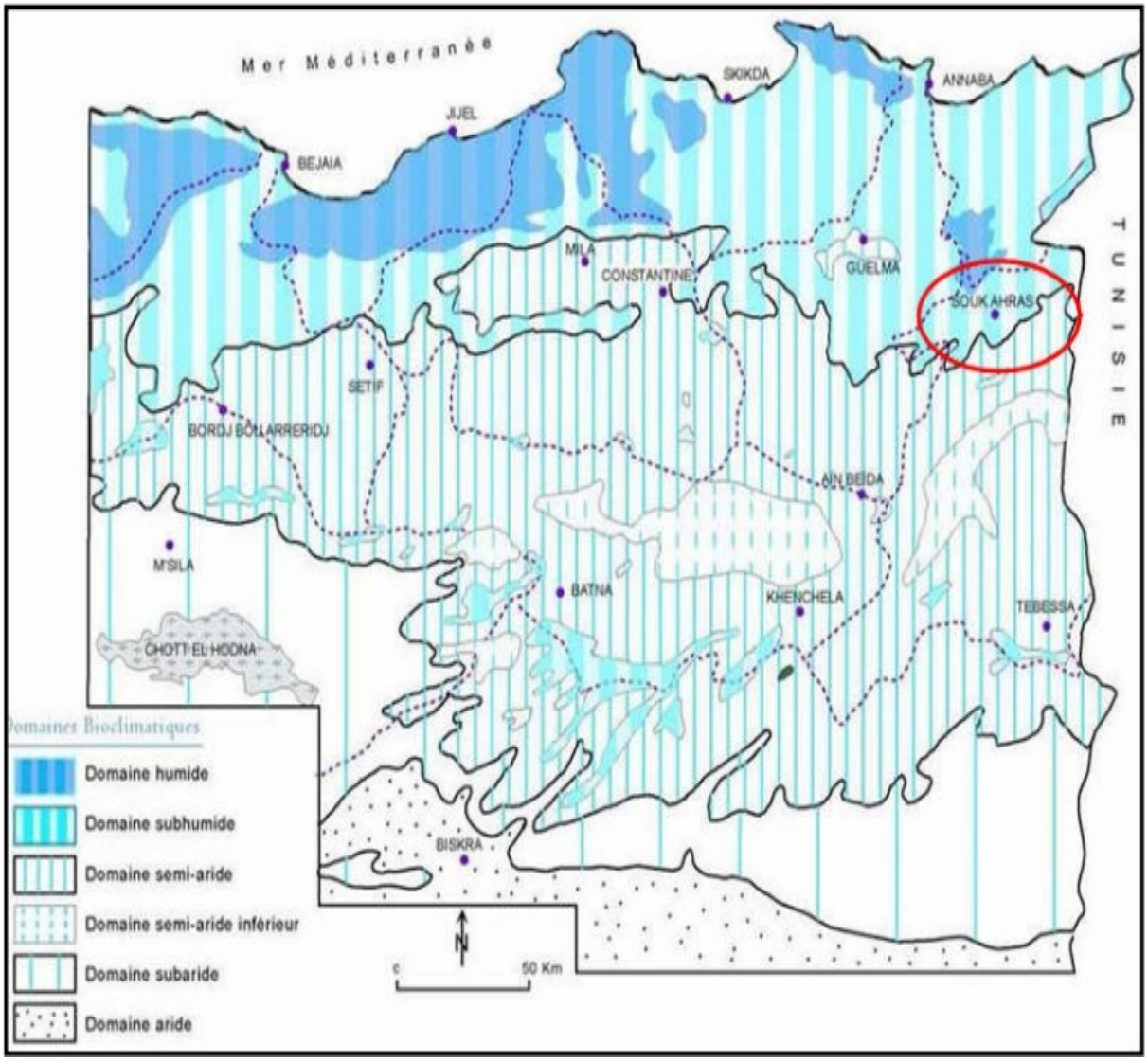

Figure6: Simplified map of bioclimatic zones of the Algerian E (established according to Côte M., 1998a in Mébarki, 2005).

1. Hydro climatic analysis:

Climate particularities and properties are a very important part in the geological or geotechnical studies because it allows us to assess the effects of climatologically factors on the mechanical behavior of soil. Precipitations in the region of Souk ahras are relatively high in the northern part but variable and irregular from year to year; two seasons are marked by the temperature a cold one in winter and the hot season in summer (in Y.Bouroubi, 2017).

In this chapter we are going through the work made by Dr MAHDADI fatnain 2018 /2019 which is based on the analysis of climate characteristics of fiveelements: precipitation, temperature, air humidity ,aridity and evaporation, for a determined period of time

2. Precipitation:

Precipitation is the amount of meteoric water liquid or solid that falls in to a determined horizontal surface called pluviometric section. The map of rainfall in northern Algeria carried out by AZHR 1993 Figure 2 shows that the rainfall in the wilaya of Souk ahras is characterized by precipitation values varies from 300 mm in the south of the wilaya in M'daourouch to 1200 mm in the north of the wilaya in El Mechrouha which represents the most wet aria of the wilaya

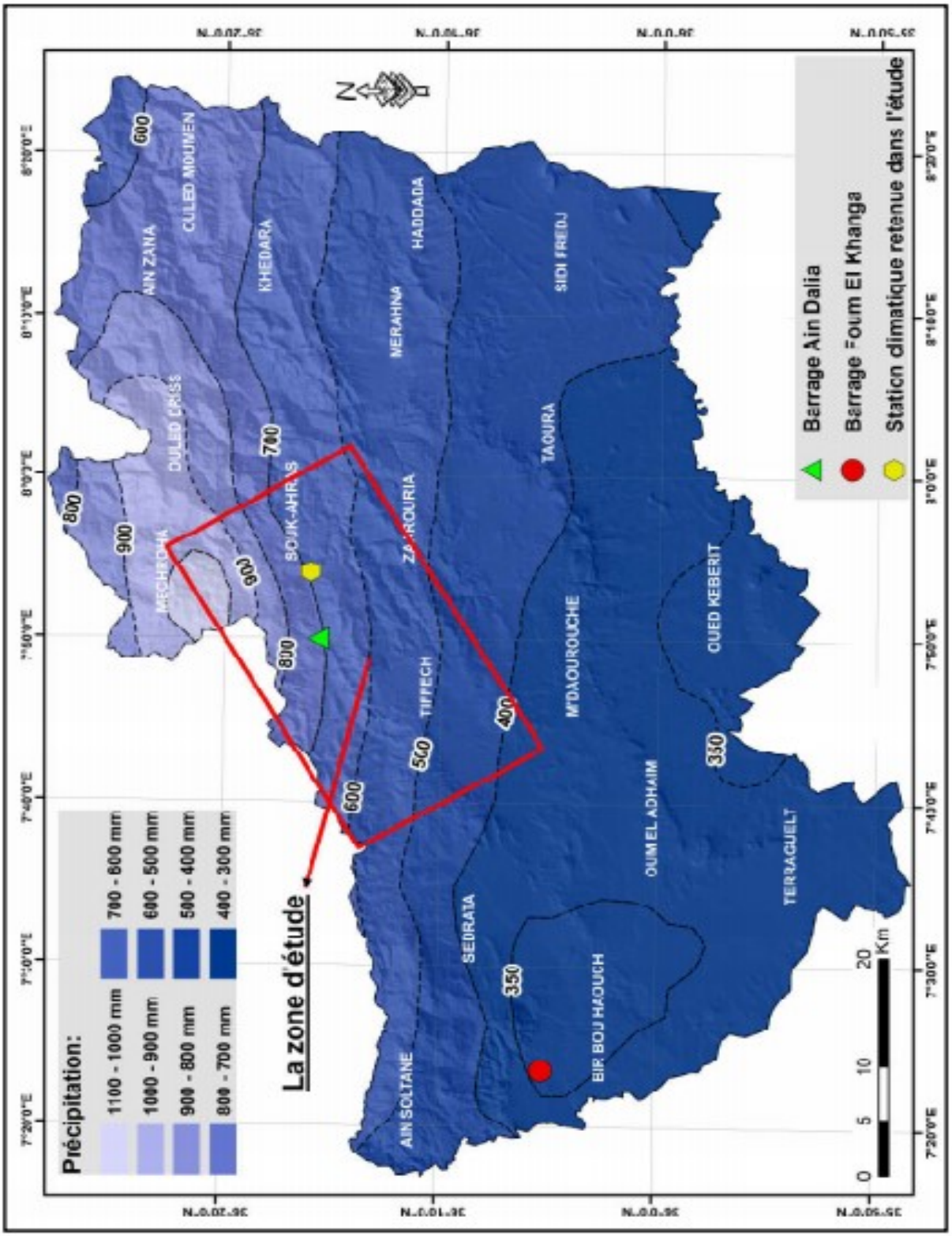

Figure 7: Map of the main annual precipitation of the Souk Ahras region. Extract from the rainfall map of Northern Algeria at 1: 500,000. ANRH, 1993 (Average data for 60 years, 1921 to 1960 and 1968 to 1989).

The analysis of precipitation is carried out using data from the Souk station Ahras (Table 1), collected in the period from 1990 to 2017 (Table 2) summarizes the average values of monthly and seasonal precipitation:

Table N °2: Coordinate of Souk Ahras station

Station	State	Code	**X**(m)	Y(m)	Z(m)
Souk ahras	Functional	12.01.01	967,25	342,25	590

Table N °3: Average monthly and seasonal precipitation for the station (Period: 1990-2017).

	Sep.	Oct.	Nov.	Déc.	Jan.	Feb.	Mar.	Apr.	Mai	Jun	Jul.	Aug	
Moyennes	40,26	49,48	87,51	120,44	132,78	103,79	85,1	75,87	59,05	19,83	6,04	16,83	**Moyennei nterannuelll** = 797 mm
Moyennessa isonnière	**Automne**			**winter**			**spring**			**Summer**			
	177,24 mm/22,2 %			357,02 mm/44,8 %			220,02 mm/27,6 %			42,7m /5,4%			

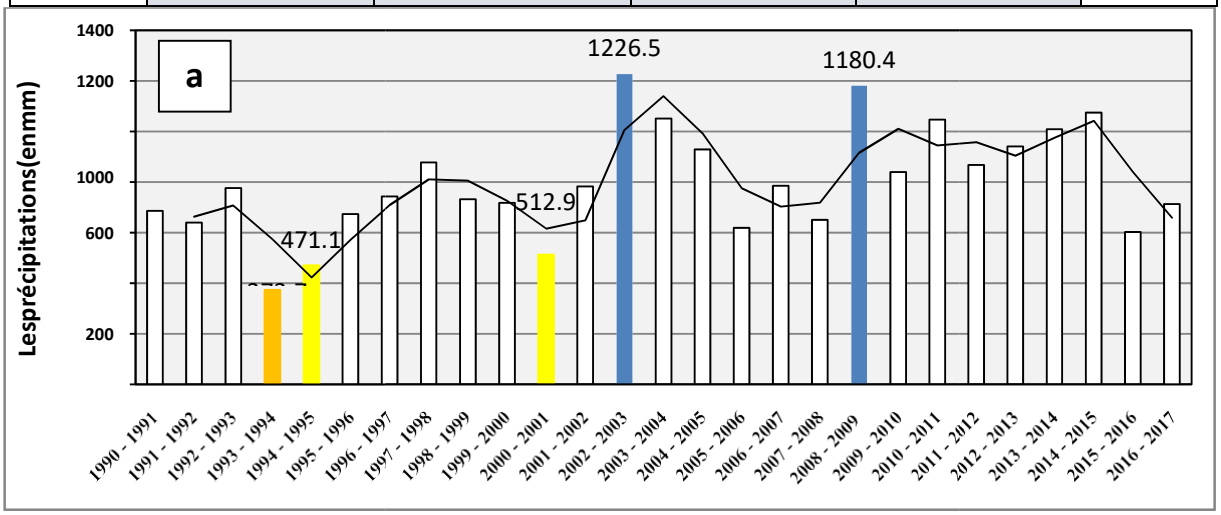

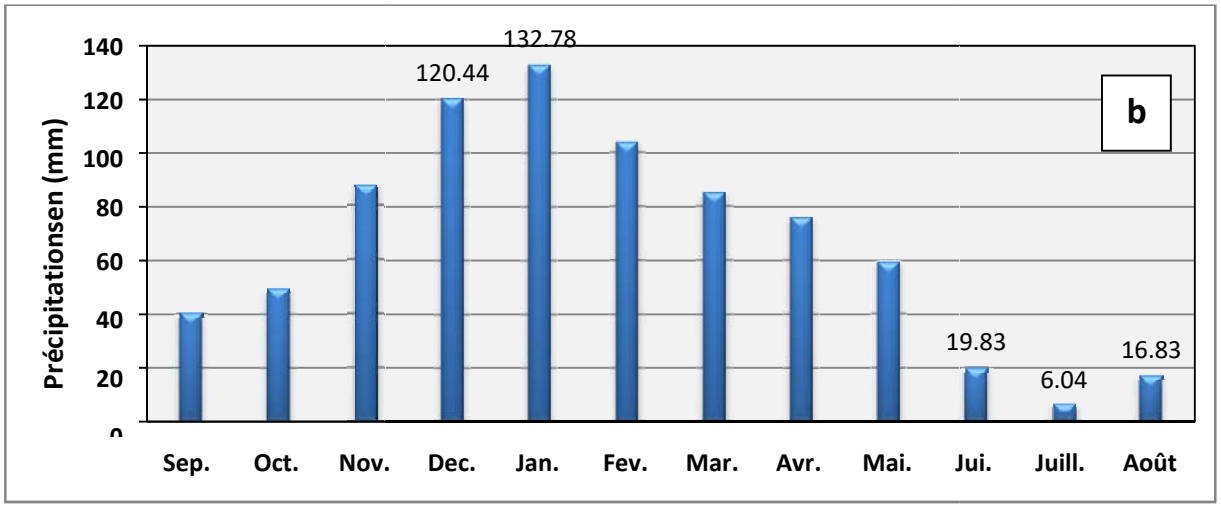

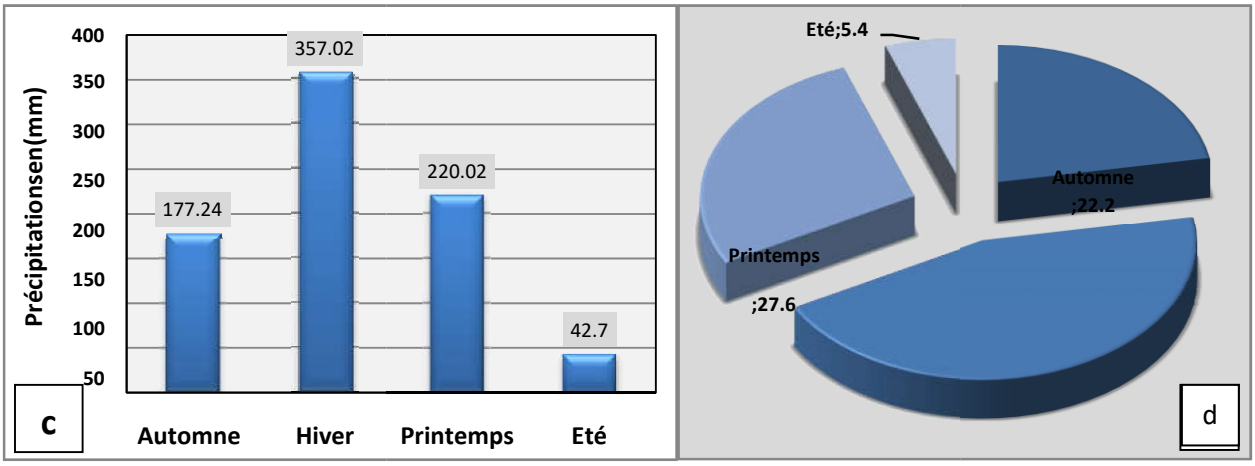

Figure 8: Variation of precipitation of recent series (1990-2017) of souk ahras station;**a**: interannual precipitation in mm; **b**: monthly average precipitation in mm; **c**: seasonal precipitation en mm; **d**: seasonal precipitation en %.

Results obtained from the examination of histograms in figure 3 are:

- For a period of 27 years the interannual precipitation variation shows that the most watered years are 2002-2003 and 2008-2009 with precipitation values of 1 226,5 mm/year et 1 180,4 mm/year; on the other hand the year 1993 is the most dry with 373,7 mm/year, Noting that the average annual precipitation is the order of 790 mm /year.
- The variation in average monthly precipitation shows a maximum of the order of 132.78 mm observed in January and a minimum of around 6.04 mm characterizes the month of July. For the monthly variation in precipitation, the months of December and January were the rainiest months with a monthly average of 120.44 mm and 132.78 mm respectively. While the months of June, July and August being the least rainy months with a monthly average of 19.83 mm, 6.04 mm and 16.83 mm respectively, which makes summer the least rainy season in the series of measures
- The seasonal distribution of precipitation shows that the the rainiest season is winter, in total 357.02 mm, or 44.8% of annual rainfall. In spring, the total precipitation is around 220 mm, or 27.6% of the annual total, and in autumn, the total precipitation is around 177 mm, or 22.2% of the annual total. The summer season is the driest; the recorded rainfall is the lowest, around 42 mm, or 5.4% of all rainfall.

3. Temperature:

The air temperature has a great influence on the evapotranspiration which favors the flow deficit; It also influences the hydrological balance. We also note that the significant temperature contrasts (considerable temperature difference) between day and night have a negative effect on the mechanical behavior of the slopes. It intensifies the phenomenon of surface alteration of formations by the evaporation of water, which can be at the origin of its exfoliation or an expansion of water molecules in the pores of the soil which can locally produce fairly strong pressures.

Next table (3) shows the The monthly average thermometric measurements of data from the Souk Ahras station for a period of 27 years:

Table N°4: Average monthly and seasonal temperatures for the Sous Ahras station (Period: 1990-2017)

	Sep.	Oct.	Nov.	Déc.	Jan.	Fév.	Mar.	Avr.	Mai	Juin	Juill.	Août	
Moyennes	22,27	18,72	12,87	10	8,66	8,86	12,08	14,3	17,71	23,28	26,23	26,56	**Moyennei nterannuelle** =16,795 °C
Moyennessai sonnière	**Automne**			**Hiver**			**Printemps**			**Et é**			
	17,95 °C			9,17 °C			14,7°C			25,36 °C			

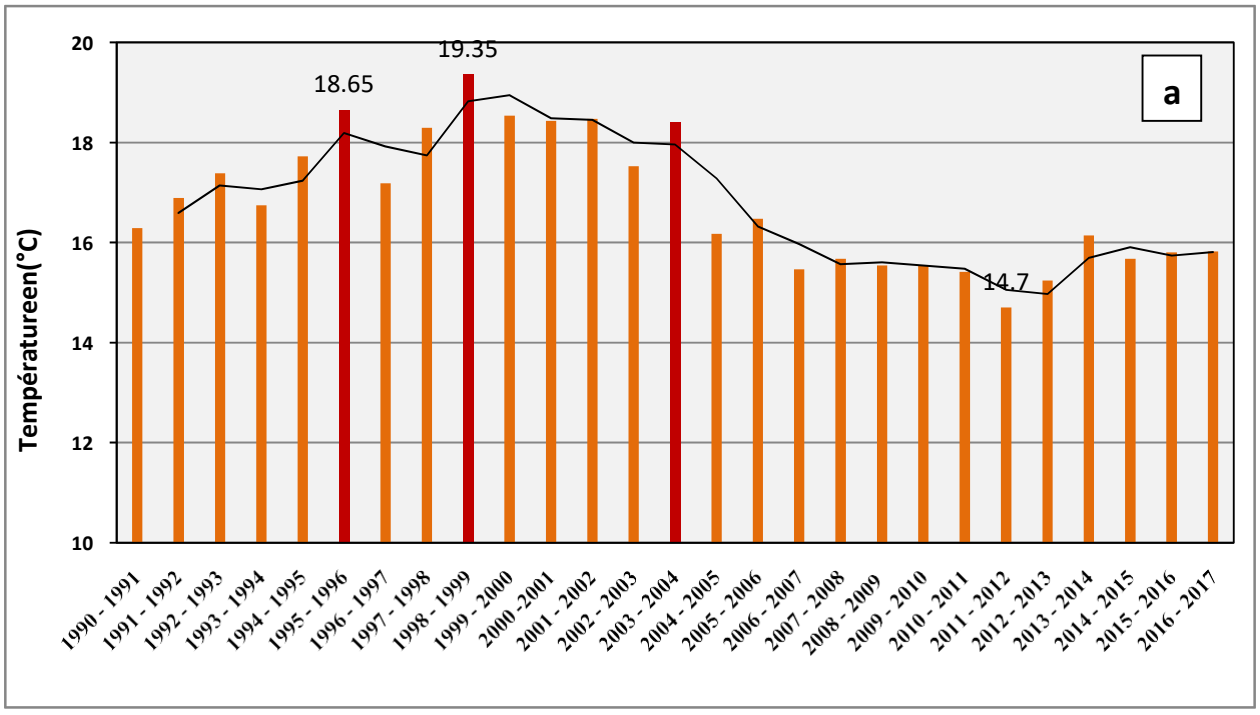

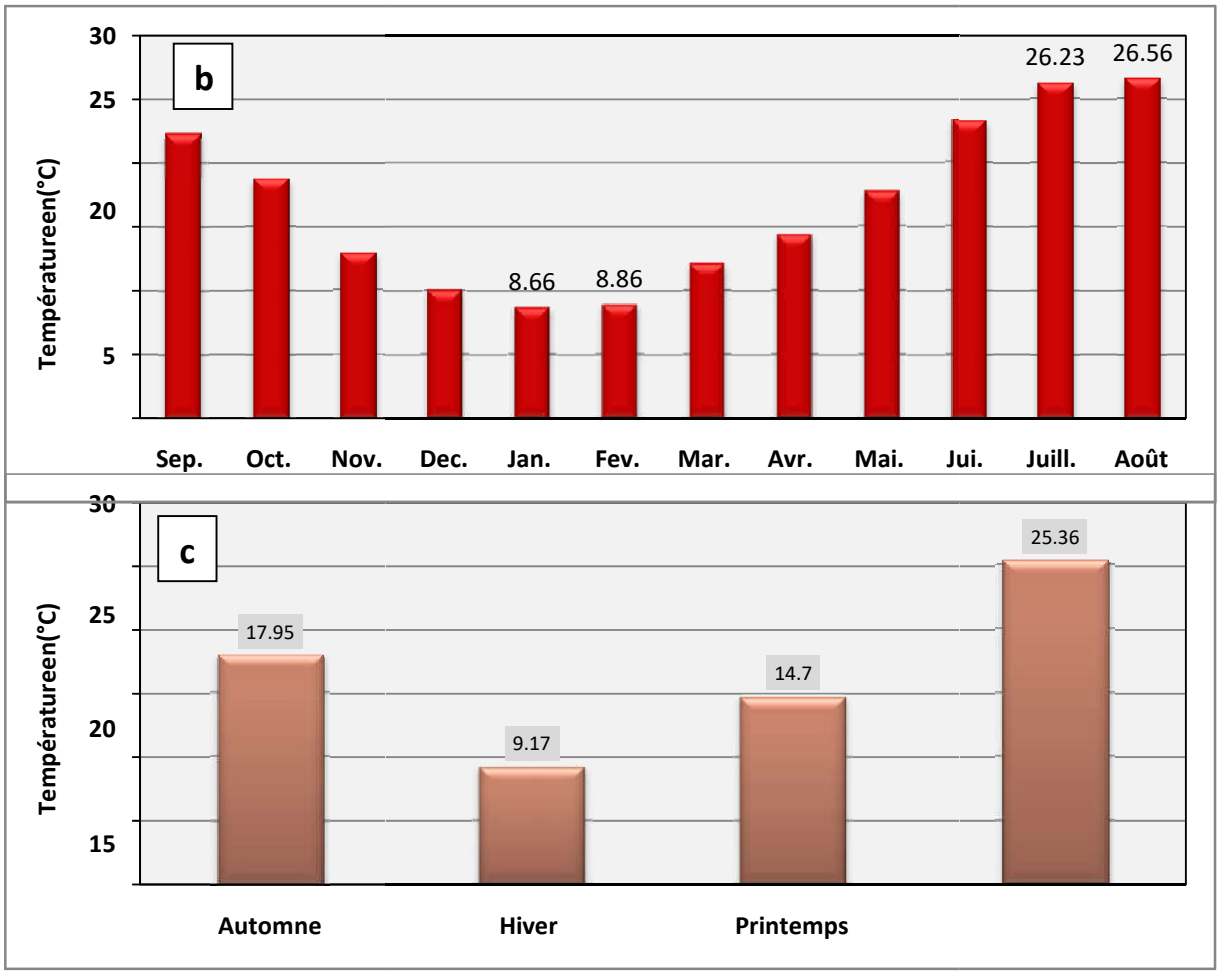

Figure 9: Temperature variation for a recent series (1990-2017) from the Souk Ahras station; **a**: interannual temperatures in °C; **b**: monthly average temperatures in °C; **c**: seasonal average temperatures in °C.

Examination of monthly average thermometric measurements of data from the Souk Ahras station for a period of 27 years 1990-2017, allows us to draw the following results:

- The interannual temperature variation over a 27-year period (1990-2017) shows that the average temperature is around 16.8 °C, fluctuating between 19.35 °C in 1998-1999 and 14.7 °C in 2011-2012;
- The variation in monthly average temperatures shows a maximum of around 26.56 ° C observed in August and a minimum of 8.66 ° C characterizes the month of January. The months of July and August were the hottest months with a monthly average of 26.23 ° C and 26.56 ° C respectively. While the months of January and February were the coldest with a monthly average of 8.66 ° C and 8.86 ° C respectively.

- The seasonal average temperature variation from one season to another shows that Summer is the hottest season with an average of 25.36 ° C; while the coldest season is Winter with an average of 9.17 ° C (we calculate in this case a difference of 16.19 ° C). The association of this discrepancy with the provocative factors. could cause mobility of vulnerable boulders.

4. Air humidity:

It is a state of climate corresponding to the amount of water vapor in the air. It can act as a catalytic factor for chemical weathering reactions in rocks at the surface, such as the phenomenon of oxidation. The monthly and annual average air humidity is given from the results of observations on the Souk Ahras station, for the period 1990-2017.

Table N°5: Average monthly and interannual humidity for the SougAhras station (Period: 1990-2017).

	Sep.	Oct.	Nov.	Déc.	Jan.	Fév.	Mar.	Avr.	Mai	Juin	Juill.	Août	
Moyennes	61,64	67,74	71,5	74,3	75,41	72,98	72,36	69,81	65,07	59,6	50,56	51,19	
Moyennessaisonnière	**Automne**			**Hiver**			**Printemps**			**Eté**			**Moyenneinterannuelle = 66,01%**
	66,96%		25,36%	74,23%		28,12%	69,09%		26,16%	53,78%		20,37%	

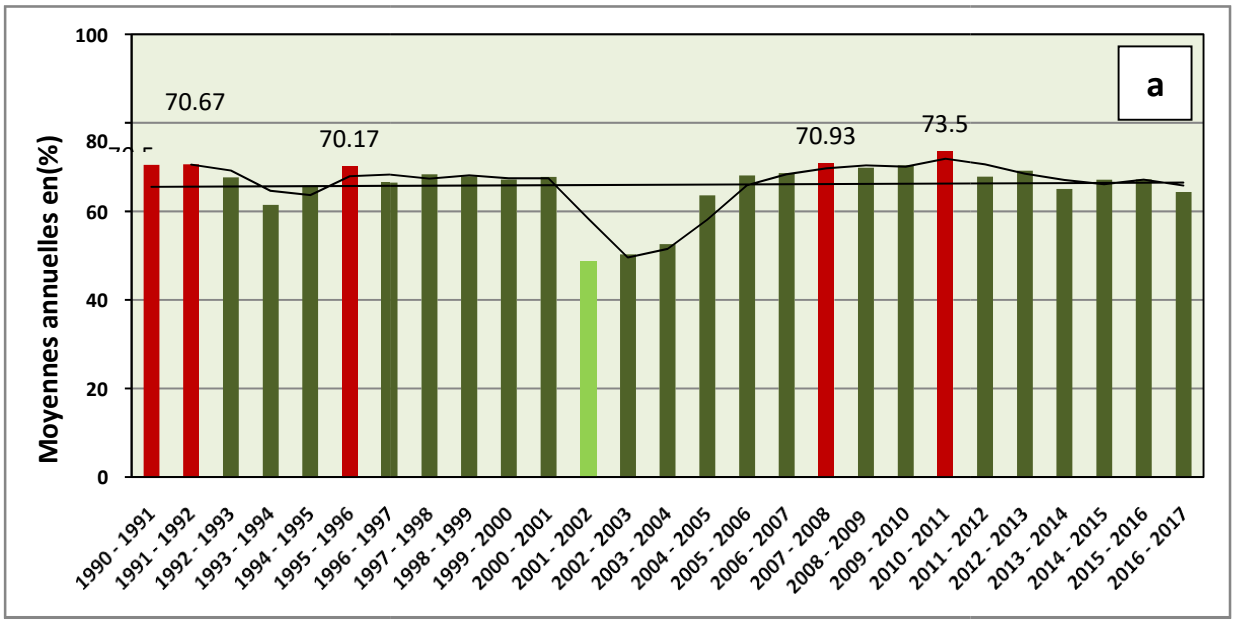

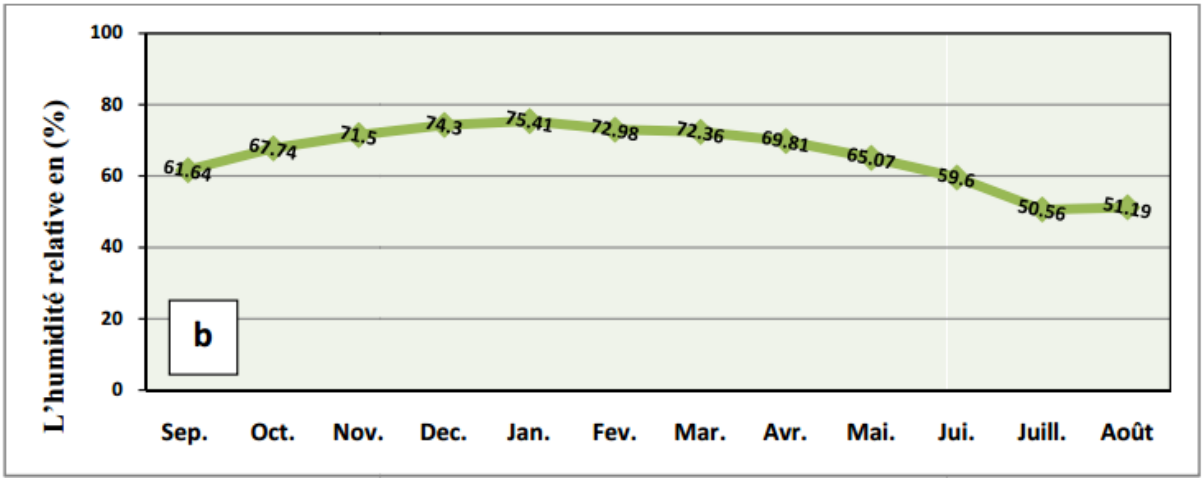

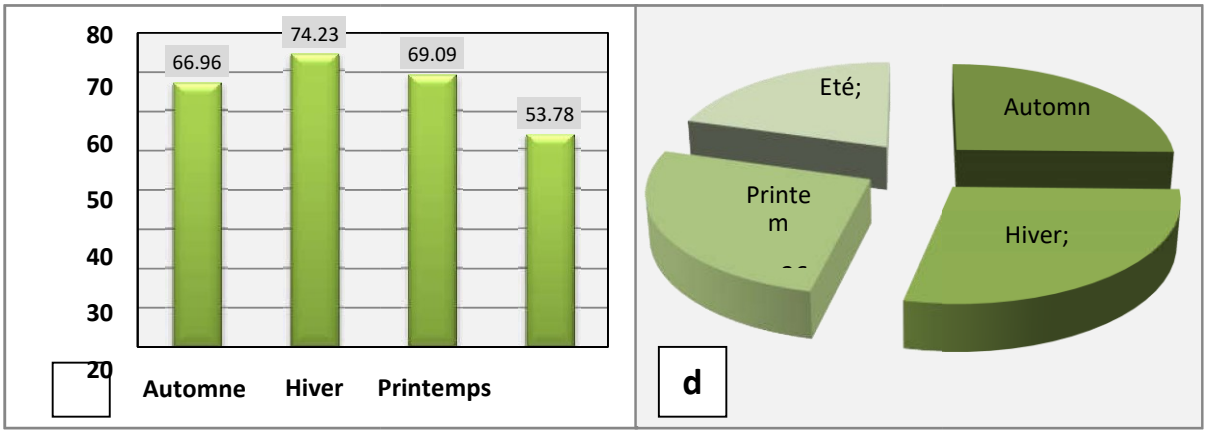

Figure 10: Change in relative humidity (in%) for a recent series (1990-2017) from the Souk Ahras station; **a**: interannual variation in relative humidity; **b**: variation of monthly means of relative humidity;**c**: variation of seasonal averages; **d**: the percentages of changes in seasonal averages of relative humidity.

Analysis of the data in Table4 and Figure 5, shows that the relative humidity in the Souk Ahras region varies between a minimum of 50.56% in July and a maximum of 75 , 41% in January, with an interannual average of 66.01%. The driest season of the year is summer with an average relative humidity of 53.78%. While the wettest season is winter, with relative humidity reaching 74.23%.

5. Evaporation:

Is the amount of water evaporated or transpired by the soil and plants. In this study, they used interannual and monthly values of evaporation from a recent 10-year series from 2008 to 2017, measured at the Souk Ahras station, using a "Colorado" type evaporation basin. Analysis of the data

in Table 5 and Figure6, shows that the average monthly evaporation in the Souk Ahras region varies between a minimum of 43.9 mm in the month of January; and a maximum of 182.98 mm in July; with an interannual average of 91.6 mm.

Table N °6: Evaporation in mm and in% measured at the Souk Ahras station (Period: 2008-2017).

	Sep.	Oct.	No.	Déc.	Jan.	Fév.	Mar.	Avr.	Mai	Juin	Juill.	Août
Moyennes	111,68	90,66	60,54	44,35	43,9	44,41	56,54	68,58	89,61	30,67	182,98	175,62
Moyennessaisonnière	**Automne**			**Hiver**			**Printemps**			**Eté**		
	87,63 mm		23,91%	44,22 mm		12,06%	71,58 mm		19,53%	163,09mm		44,53%
Moyenneinterannuelle =191,6mm												

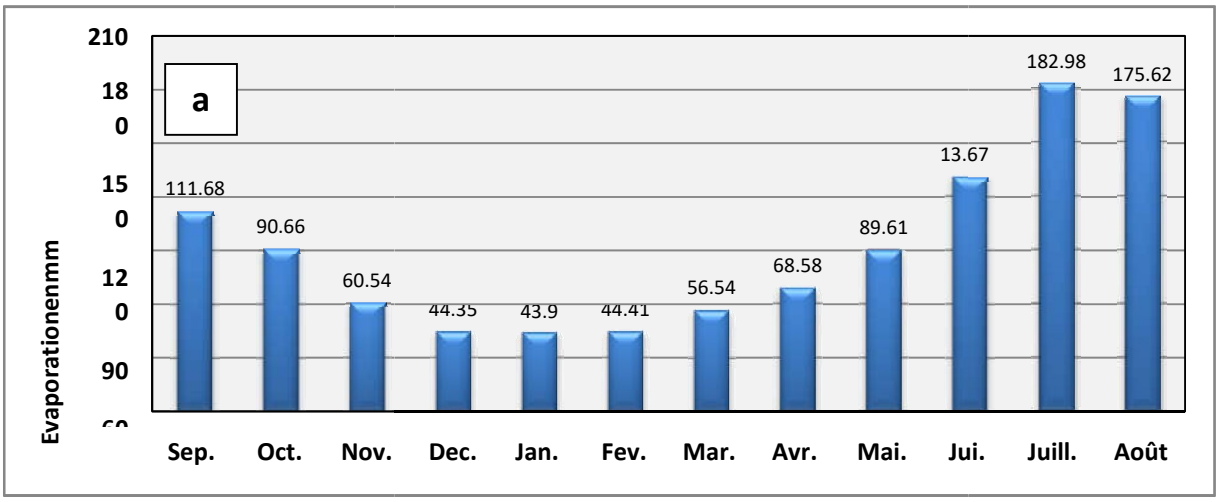

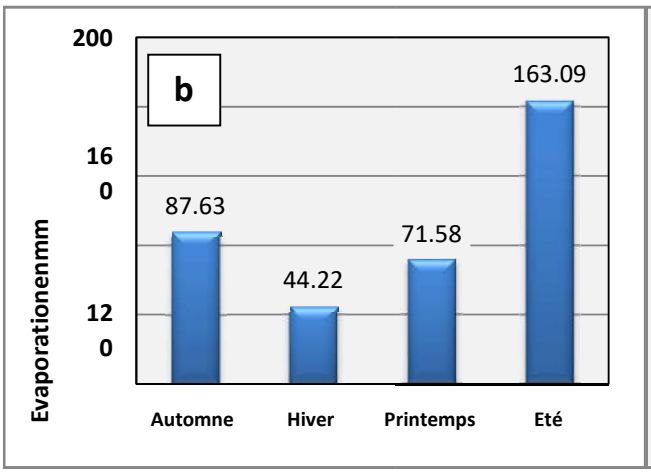

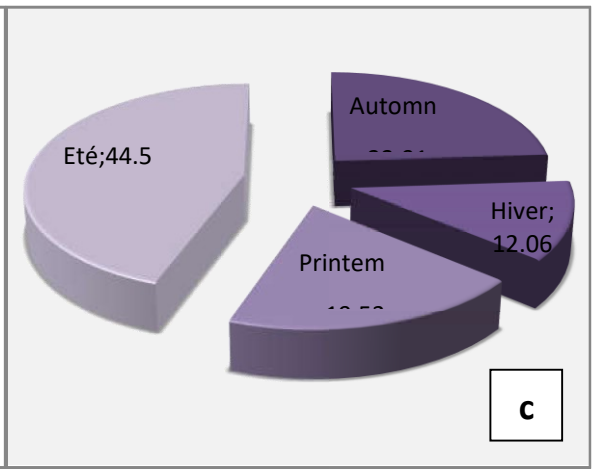

Figure 11: Variation in evaporation (in mm) for a recent series (2008-2017) from the Souk Ahras station; **a**: variation in monthly evaporation averages **b**: variation in seasonal averages in mm; **c**: the percentages of variation of the seasonal averages of evaporation.

6. Aridity and its index:

Unlike humidity aridity is a climate condition where water lacks at all cycles, to characterize the type of climate of a region and classify it in a bioclimatic stage we use the aridity index table 6; based on values mean annual precipitation and mean annual temperatures. It is calculated by Martonne's formula (1923): **I = P / T ° + 10**; of which **P**: average annual rainfall in mm, **T °:** annual average temperature in C °.

For the Souk Ahras station: **P = 797.0 mm, T = 16.795 ° C,** while **I = 29.74. Hence 20 <I <30** we find that our study area is characterized by a temperate climate according to the Martonne.

Table N° 7: Type of climate according to the Martonne aridity index (1923).

Indice d'aridité de MORTONNE	Type de Climat
I< 5	Climat hyper aride
5 < I< 7.5	Climat désertique
7.5 <I<10	Climat steppique
10 <I<20	Climat semi-aride
20 <I<30	Climat tempéré

7. Water budget calculations:

Water Budget calculations allows us to assess the process of a quantity of water arriving on the ground by precipitation or snow before returning to the atmosphere, it can be calculated by the following formula (G. Castany, 1982): **P = ETR + R + I** Of which **ETR**: annual evapotranspiration (mm). **I**: infiltration. **P**: precipitation**. A**: runoff.

a. Study of evapotranspiration:

It is the combination of phenomena of evaporation which is a physical process and transpiration a biological one, it is a function of many factors (humidity, temperature, sunshine and plant cover), it is expressed by mm of water for a given period of time it can occur at any time of the water cycle provided that there is enough water to be evapotranspiredand sufficient energy (in M. Bourouga, 2015). The term evapotranspiration encompasses two types: Potential

evapotranspiration (ETP) and real evapotranspiration (ETR), first one is the evapotranspiration of a surface that would be sufficiently supplied with water to evaporate the maximum quantity of water allowed by the given climatic conditions, and second is is the amount of water effectively evaporated by the soil, plants and open water surfaces, for a given area and a defined period.

Water losses from a soil reach ETP if they are greater than or equal to the water stock of the RFU (the easily usable reserve).

In case of insufficiency they are limited to a smaller quantity or ETR (G. Castany, 1982). A water balance has been established based on the formulas proposed by Thorntwait. The results are shown in Table N°7:

Table N °8: Water balance of the Souk Ahras region according to Thorntwait (Souk Ahras station: 1990-2017).

Mois	T(° C)	IT	K	ETP $_{nc}$(mm)	ETP$_C$ (mm)	P (mm)	P- ETP	BH (mm)	CH	VR (mm)	RFU (mm)	ETR (mm)	Défi.(mm)	Exc.(mm)
S	22,27	9,6	1,03	89,73	92,42	40,26	-52,16	-49,47	-0,54	0	0	40,26	52,16	0
O	18,72	7,38	0,97	67,12	65,11	49,48	-15,63	-15,63	-0,24	0	0	49,48	15,63	0
N	12,87	4,18	0,86	35,9	30,88	87,51	56,63	56,63	1,83	56,63	56,63	30,88	0	0
D	10,01	2,86	0,84	23,59	19,82	120,44	100,62	100,62	5,08	13,37	70	19,82	0	87,25
J	8,66	2,3	0,87	18,53	16,12	132,78	116,65	116,65	7,24	0	70	16,12	0	116,65
F	8,86	2,38	0,85	19,24	16,36	103,8	87,44	87,44	5,35	0	70	16,36	0	87,44
M	12,08	3,8	1,03	32,31	33,28	85,1	51,82	51,82	1,56	0	70	33,28	0	51,82
A	14,3	4,91	1,1	42,84	47,12	75,87	28,75	28,75	0,61	0	70	47,12	0	28,75
M	17,71	6,78	1,21	61,17	74,02	59,05	-14,97	-14,97	-0,2	-14,97	55,03	74,02	0	0
J	23,28	10,27	1,22	96,63	117,89	19,83	-98,06	-98,06	-0,83	-55,03	0	74,86	43,03	0
J	26,23	12,3	1,24	117,93	146,24	6,04	-140,2	-140,2	-0,96	0	0	6,04	140,2	0
A	26,56	12,53	1,26	120,37	151,66	16,83	-134,84	-134,84	-0,89	0	0	16,83	134,84	0
Annuel	**16,8**	**79,29**		**725,39**	**810,93**	**796,98**		**-11,25**				**425,07**	**385,85**	**371,91**

T: monthly temperature in (° C); **P**: monthly precipitation in (mm); **IT**: thermal index; **K**: correction coefficient; ETPnc: uncorrected potential evapotranspiration in (mm); **ETPC**: potential evapotranspiration corrected in (mm); **BH**: Water Balance; **RFU**: easily usable reserves in (mm); **ETR**: real evapotranspiration in (mm); Challenge. : Agricultural deficit in (mm); **Exc**.: exceed in (mm).

b. Interpretation of the results from the table:

The interpretation of the results allows us to conclude the next :

- The deficit period begins in June and ends in October of the following year with a maximum of 140.20 mm recorded in July and a maximum of 15.63 mm in October. During this period the physical disintegration is considerable, the ground becomes tired by the deficit in the volume of water, manifested by the shrinkage of clays and the appearance of cracks generated by traction.
- The excess water is spread from the month of December with 87.25 mm until the month of April with 28.75 mm, it is during this period that the stability is threatened and that the risk of movement of land rises by increasing the volume of water in the soil and in the subsoil;
- Precipitation reaches its maximum in January (132.78 mm)
- Evapotranspiration peaks in August (151.66 mm) when precipitation reaches (16.83 mm). During the month of December the stock is reconstituted where the RFU reaches its maximum (70 mm) until the month of April, then remains until the month of May with a value of 55.03 mm, then decreases until the month of April. 'total exhaustion in June.

V. Vegetation:

Vegetation plays the role of a screen which conditions the speed of surface runoff and reduces its aggressiveness. It is closely linked to the nature of the soil and the climate. Thus, the forms and extent of water erosion are directly related, in addition to other factors, to the distribution of vegetation cover on the ground.

the northern part where the elevations and the crests are marked by an important pluviometry and dense forests of cork oak,zeen oak and afered oak constituting dense forest especially of Djregoune, Djkelia and Djzaarouria.The climate becomes less humid as it moves southwards, where the vegetation cover is mainly based on alpine pine and Mediterranean crops. Sheep farming is more abundant whereas cereal crops, on marly formations, are dominant agriculture in the northern part of the souk ahrasregion.On limestone,However, under grown pine forests, and maquis dominate. Stony areas and calcareous crusts are covered with steppe-type vegetation.

VI. Conclusion

In this chapter we took a close look on the region of souk ahras and Zaarouria and now we can understand its geological context and climate conditions along with hydrological and hydrogeological features, viewed topographic and morphological factors of the region

I. Introduction

Landslides occur when part of a natural slope is unable to support its own weight. For example, soil material on a slippery surface underneath, can become heavy with rainwater and slide down due to its increased weight. A landslide is a downward or outward movement of soil, rock or vegetation, under the influence of gravity. This movement can occur in many ways. It can be a fall, topple, slide, spread or flow. The speed of the movement may range from very slow to rapid. The mass of moving material can destroy property along its path of movement and cause death to people and livestock. Although landslides usually occur on relatively steep slopes, they may also occur in areas with low relief or slope gradient. The following are some examples of landslides and the areas when they occur: Road cut slope failure, river bank failures, lateral spreading of soil material under earthquake loading, collapse of mines roofs side walls, slope failures associated with quarries and open-pit mines and underwater (submarine) landslides.

For a landslide to occur there must be some predisposing factors that prepare the soil or rock mass to fail as well as some triggering factors which starts the movement of a marginally stable body. Predisposing factors (quasi static variables) are inherent to the geology, lithology, structure and the physical and mechanical properties of the soil or rock. The triggering factors, however, are mainly external factors which are usually earthquakes, rainfall.

In a landslide, soil masses can move along a planar surface, a curvilinear or complex. The different parts of a rotational landslide is shown below in figure 1

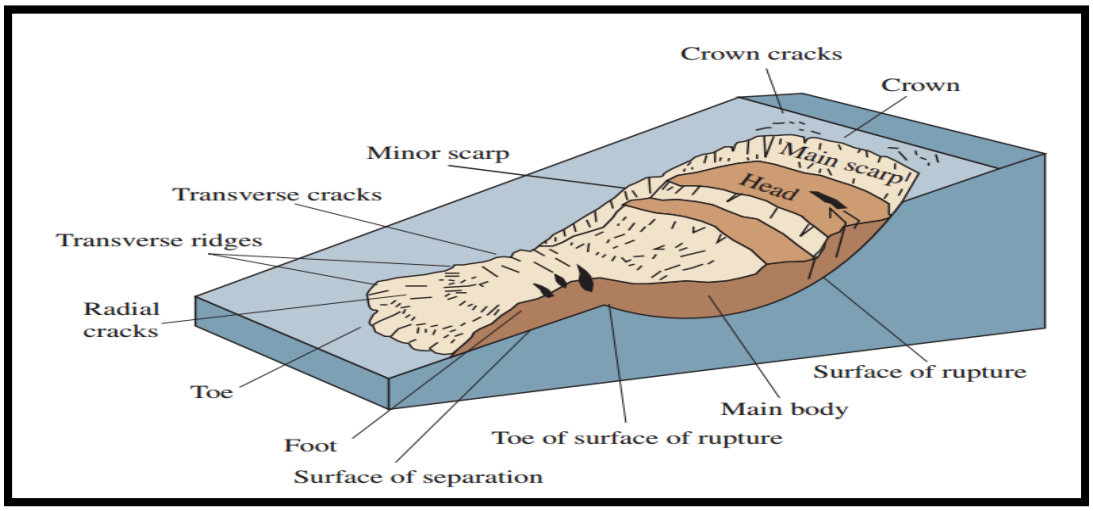

Figure 1: shows a graphic illustration of a landslide, with the commonly accepted terminology describing its features

I. Signs of landslides activity:

When an area has been hit by a landslide or is currently experiencing it some relevant signs which the specialist should not ignore. These are:

- Cracks in soil
- Tilted or bent trees
- Increased spring activity or newly wet ground
- Hummocky or uneven terrain
- Sagging or taut utility lines
- Sunken or broken road beds
- Movement of soil away from foundations
- Leaking or broken water pipes

II. Landslide prone areas

Some areas are more likely to be affected by landslides more than others. It has been observed that areas wherepre-existing landslides are highly susceptible to develop new ones, they are associated with a relief showing irregular surface often called hummocky topography. The base of the slopes, the landfill slopes, steep cut slopes and hillsides near leach field septic systems.

III. Basic Landslide Types :

Landslides can be classified into different types (Varnes et al 1978). On the basis of the type of movement and the type of material involved (please see References 9 and 39). In brief, material in a landslide mass is either ***rock*** or ***soil*** (or both); the latter is described as ***earth*** if mainly composed of sand-sized or finer particles and ***debris*** if composed of coarser fragments. The type of movement describes the actual internal mechanics of how the landslide mass is displaced can be classed as***fall***, ***topple, slide, spread,*** or ***flow.*** Thus, landslides are described using two terms that refer respectively to material and movement (that is, rockfall, debris flow, and so forth). Landslides may also form a complex failure encompassing more than one type of movement (that is, rock slide—debris flow).A classification system based on these parameters is shown in table 1

Table N ° 1: Types of landslides. Abbreviated version of Varnes' classification of slope movements (Varnes, 1978)

TYPE OF MOVEMENT		TYPE OF MATERIAL		
		BEDROCK	ENGINEERING SOILS	
			Predominantly coarse	Predominantly fine
FALLS		Rock fall	Debris fall	Earth fall
TOPPLES		Rock topple	Debris topple	Earth topple
SLIDES	ROTATIONAL	Rock slide	Debris slide	Earth slide
	TRANSLATIONAL			
LATERAL SPREADS		Rock spread	Debris spread	Earth spread
FLOWS		Rock flow (deep creep)	Debris flow (soil creep)	Earth flow
COMPLEX		Combination of two or more principal types of movement		

1. Falls:

A fall begins with the detachment of soil or rock, or both, from a steep slope along a surface on which little or no shear displacement has occurred. They are abrupt, downward movements of rock or earth, or both, that detach from steep slopes or cliffs. The falling material usually strikes the lower slope at angles less than the angle of fall, causing bouncing. The falling mass may break on impact, may begin rolling on steeper slopes, and may continue until the terrain flattens.

❖ Occurrence and relative size/range:

They are known worldwide, they occuron steep or vertical slopes also in coastal areas, and along rocky banks of rivers and streams. The volume of material in a fall can vary substantially, from individual rocks or clumps of soil to massive blocks thousands of cubic meters in size.

❖ Velocity of travel

Very rapid to extremely rapid, free-fall; bouncing and rolling of detached soil, rock, and boulders. The rolling velocity depends on slope steepness.

❖ Triggering mechanism:

Undercutting of slope by natural processes such as streams and rivers or differential weathering (such as the freeze/thaw cycle), human activities such as excavation during road building and (or) maintenance, and earthquake shaking or other intense vibration.

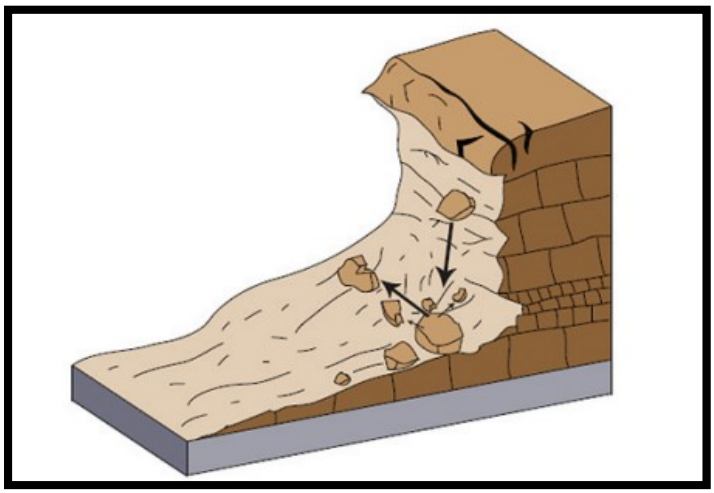

Figure 2: Schematic of a rock fall

Figure 3: A rock fall/slide that occurred in Clear Creek Canyon, Colorado, USA,

2. Topple

A topple is recognized as the forward *rotation* out of a slope of a mass of soil or rock around a point or *axis* below the *center of gravity* of the displaced mass. Toppling is sometimes driven by gravity exerted by the weight of material upslope from the displaced mass. Sometimes toppling is due to water or ice in cracks in the mass. Topples can consist of rock, debris (coarse material), or earth materials (finegrained material). Topples can be complex and composite.

❖ Occurrence

Known to occur globally, often prevalent in columnar-jointed volcanic terrain, as well as along stream and river courses where the banks are steep.

❖ **Velocity of travel**

Extremely slow to extremely rapid, sometimes accelerating throughout the movement depending on distance of travel.

❖ **Triggering mechanism**

Sometimes driven by gravity exerted by material located upslope from the displaced mass and sometimes by water or ice occurring in cracks within the mass; also, vibration, undercutting, differential weathering, excavation, or stream erosion.

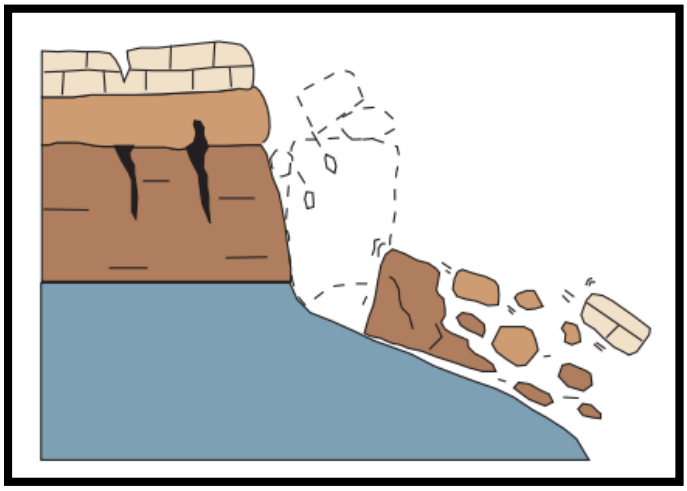

Figure 4: Schematic of a topple.

Figure 5: Photograph of block toppling at Fort St. John, British Columbia, Canada.
(Photograph by G. Bianchi Fasani.)

3. Slides

A slide is a downslope movement of a soil or rock mass occurring on surfaces of rupture or on relatively thin zones of intense shear strain. Movement does not initially occur simultaneously over the whole of what eventually becomes the surface of rupture; the volume of displacing material enlarges from an area of local failure

a) Rotational Landslide

A landslide on which the surface of rupture is curved upward (spoon-shaped) and the slide movement is more or less rotational about an axis that is parallel to the contour of the slope is called a rotational landslide. The displaced mass may, under certain circumstances, move as a relatively coherent mass along the rupture surface with little internal deformation. The head of the displaced material may move almost vertically downward, and the upper surface of the displaced material may tilt backwards toward the scarp. If the slide is rotational and has several parallel curved planes of movement, it is called a slump

- **Occurrence**

Because rotational slides occur most frequently in homogeneous materials, they are the most common landslide occurring in “fill” materials.

- **Relative size/range**

Rotational sliding is usually associated with a slope inclination ranging from about 20 to 40 degrees. In soils, thesurface of rupture generally has a depth-to-length ratio between 0.3/ 0.1.

- **Velocity of travel**

Rotational slides affect cohesive material and are relatively slow (less than 0.3 meter or 1 foot every 5 years) to moderately fast (1.5 meters or 5 feet per month) to rapid.

- **Triggering mechanism**

Many triggering mechanisms can be identified in different geotechnical environments. Intense and (or) sustained rainfall or rapid snowmelt can lead to the saturation of slopes and increased groundwater levels within the mass induce an increase in pore pressure. Among other mechanisms we can number thhe rapid drop in river level following floods, the ground-water levels rising as a result of filling reservoirs, or the rise in level of streams, lakes, and rivers, which cause erosion at the base of slopes. These types of slides can also be earthquake-induced

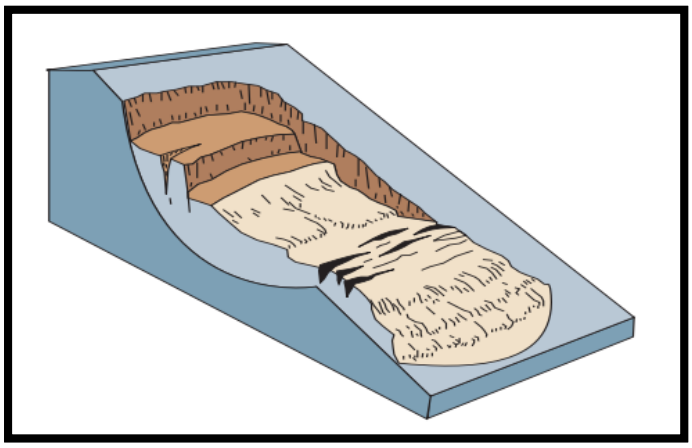

Figure 6: Schematic diagram showing a rotational landslide.(Modified from Reference 9.

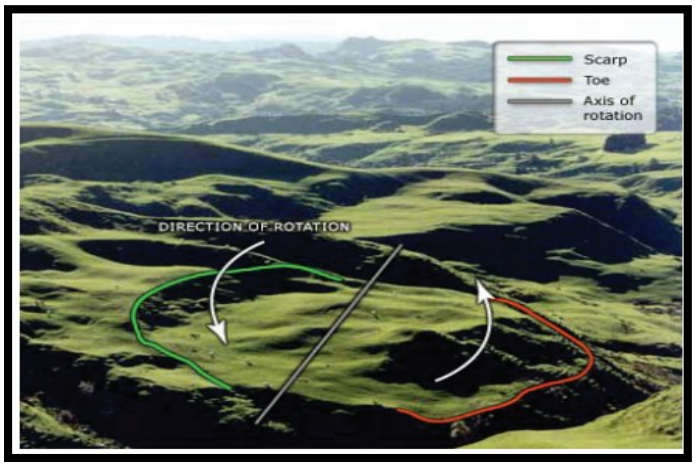

Figure 7: Photograph of a rotational landslide which occurred in New Zealand. The green curveat center leftis the scarp

b) Translational Landslide

The mass in a translational landslide moves out, or down and outward, along a relatively planar surface with little rotational movement or backward tilting. This type of slide may progress over considerable distances if the surface of rupture is sufficiently inclined, in contrast to rotational slides, which tend to restore the slide equilibrium. The material in the slide may range from loose, unconsolidated soils to extensive slabs of rock, or both. Translational slides commonly fail along geologic discontinuities such as faults, joints, bedding surfaces, or the contact between rock and soil. In northern environments the slide may also move along the permafrost layer

- **Occurrence**

They are among the most common types of landslides, worldwide. They are found globally in all types of environments and conditions.

❖ **Relative size/range**

They are generally shallower than rotational slides. The surface of rupture has a distance-to-length ratio of less than 0.1 and can range from small (residential lot size) failures to very large, regional landslides that are kilometers wide.

❖ **Velocity of travel**

The movement may initially be slow (5 feet per month or 1.5 meters per month) but many are moderate in velocity (5 feet per day or 1.5 meters per day) to extremely rapid. With increased velocity, the landslide mass of translational failures may disintegrate and develop into a debris flow.

❖ **Triggering mechanism**

The main triggering factors are intense rainfall, rise in ground water within the slide due to rainfall, snowmelt, flooding, or other inundation of water resulting from irrigation, or leakage from pipes or human-related disturbances such as undercutting. These types of landslides can be earthquake-induced.

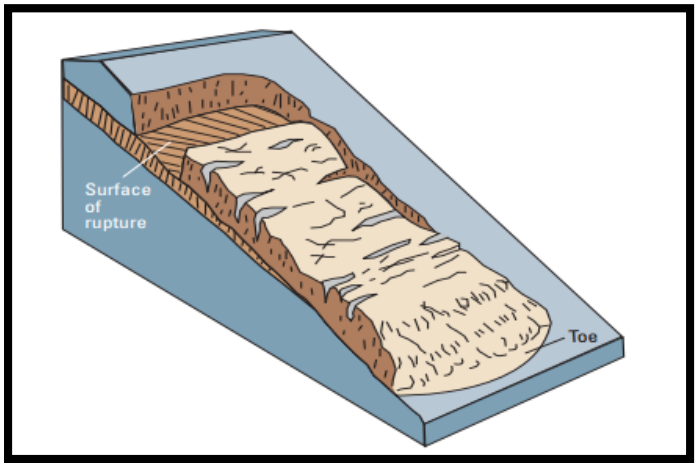

Figure 8: Schematic diagram of a translational landslide.(modified from Reference 9.)

Figure 9: A translational landslide that occurred in 2001 in the Beatton River Valley, British Columbia, Canada.(Photograph by Réjean Couture,

4. Spreads:

An extension of a cohesive soil or rock mass combined with the general subsidence of the fractured mass of cohesive material into softer underlying material. Spreads may result from liquefaction or flow (and extrusion) of the softer underlying material. Types of spreads include block spreads, liquefaction spreads, and lateral spreads.

a) Lateral Spreads

They usually occur on very gentle slopes or essentially flat terrain, especially where a stronger upper layer of rock or soil undergoes extension and moves above an underlying softer, weaker layer. Such failures commonly are accompanied by some general subsidence into the weaker underlying unit. In rock spreads, solid ground extends and fractures, pulling away slowly from stable ground and moving over the weaker layer without necessarily forming a recognizable surface of rupture. The softer, weaker unit may, under certain conditions, squeeze upward into fractures that divide the extending layer into blocks. In earth spreads, the upper stable layer extends along a weaker underlying unit that has flowed following liquefaction or plastic deformation. If the weaker unit is relatively thick, the overriding fractured blocks may subside into it, translate, rotate, disintegrate, liquefy, or even flow.

❖ **Occurrence**

They are known to occur where there are liquefiable soils. Common, but not restricted, to areas of seismic activity.

❖ **Relative size/range**

The area affected may start small in size and have a few cracks that may spread quickly, affecting areas of hundreds of meters in width.

❖ **Velocity of travel**

Slow to moderate and sometimes rapid after certain triggering mechanisms, such as an earthquake. Ground may then slowly spread over time from a few millimeters per day to tens of square meters per day.

❖ **Triggering mechanism**

Triggers that destabilize the weak layer include:

Liquefaction of lower weak layer by earthquake shaking, Natural or anthropogenic overloading of the ground above an unstable slope, saturation of underlying weaker layer due to precipitation, snowmelt, and(or) ground-water changes, liquefaction of underlyingsensitive marine clay following an erosionaldisturbance at base of a riverbank/slope, plastic deformation of unstable material at depth (for example, salt).

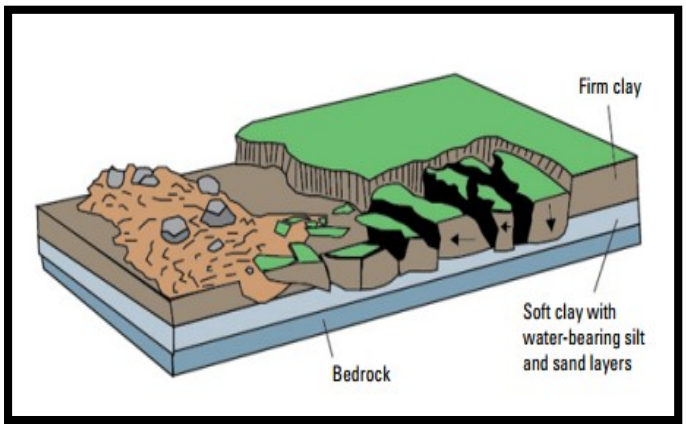

Figure 10: Schematic diagram of a lateral spread. A liquefiable layer underlies the surface layer.(Schematic modified from Reference 9.

Figure 11: Photograph of lateral spread damage to a roadway as a result of the 1989 Loma Prieta, California,USA, earthquake. (Photograph by Steve Ellen, U.S. Geological Survey.)

5. **Flows**

A flow is a spatially continuous movement in which the surfaces of shear are short-lived, closely spaced, and usually not preserved. The component velocities in the displacing mass of a flow resemble those in a viscous liquid. Often, there is a gradation of change from slides to flows, depending on the water content, mobility,and evolution of the movement.

a) **Debris Flows**

A form of rapid mass movement in which loose soil, rock and sometimes organic matter combine with water to form a slurry that flows downslope. They have been informally and inappropriately called “mudslides” due to the large quantity of fine material that may be present in the flow. Occasionally, as a rotational or translationalslide gains velocity and the internal mass loses cohesion or gains water, it may evolve into a debris flow. Dry flows can sometimes occur in cohesion less sand (sand flows). Debris flows can be deadly as they can be extremely rapid and may occur without any warning.

❖ **Occurrence**

Debris flows occur around the world and are prevalent in steep gullies and canyons; they can be intensified when occurring on slopes or in gullies that have been denuded of vegetation due to wildfires or forest logging. They are common in volcanic areas with weak soil.

❖ **Relative size/range**

These types of flows can be thin and watery or thick with sediment and debris and are usually confined to the dimensions of the steep gullies that facilitate their downward movement. Generally the movement isrelatively shallow and the runout is both long and narrow, sometimes extending for kilometers in steep terrain. The debris and mud usually terminate at the base of the slopes and create fanlike, triangular deposits called debris fans, which may also be unstable.

❖ **Velocity of travel**

Can be rapid to extremely rapid (35 miles per hour or 56 km per hour) depending on consistency and slope angle.

❖ **Triggering mechanisms**

Debris flows are commonly caused by intense surface-water flow, due to heavy precipitation or rapid snowmelt, that erodes and mobilizes loose soil or rock on steep slopes. Debris flows also commonly mobilize from other types of landslides that occur on steep slopes, are nearly saturated, and consist of a large proportion of silt- and sand-sized material.

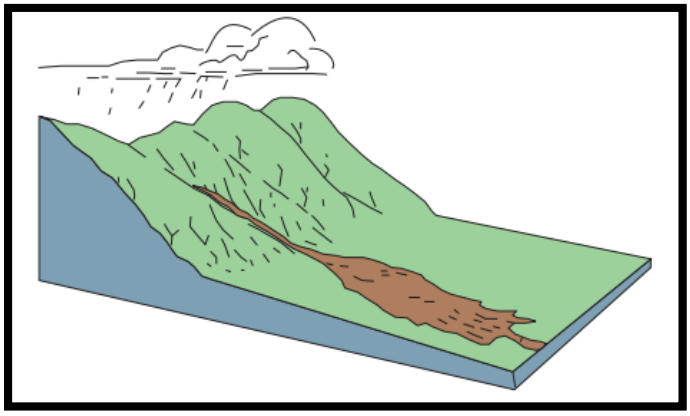

Figure 12: Schematic of a debris flow.

Figure 13: Debris-flow damage to the city of Caraballeda

b) Debris Avalanche

Debris avalanches are essentially large, extremely rapid, often open-slope flows formed when an unstable slope collapses and the resulting fragmented debris is rapidly transported away from the slope. In some cases, snow and ice will contribute to the movement if sufficient water is present, and the flow may become a debris flow and (or) a lahar.

❖ **Occurrence**

Occur worldwide in steep terrain environments. Also common on very steep volcanoes where they may follow drainage courses.

❖ **Relative size/range**

Some large avalanches have been known to transport material blocks as large as 3 kilometers in size, several kilometers from their source.

❖ **Velocity of travel**

Rapid to extremely rapid; such debris avalanches can travel close to 100 meters/sec.

❖ **Triggering mechanism**

In general, the two types of debris avalanches are those that are “cold” and those that are “hot.” A cold debris avalanche usually results from a slope becoming unstable, such as during collapse of weathered slopes in steep terrain or through the disintegration of bedrock during a transform into a debris avalanche. A hot debris avalanche is one that results from volcanic activity including volcanic earthquakes or the injection of magma, which causes slope instability.

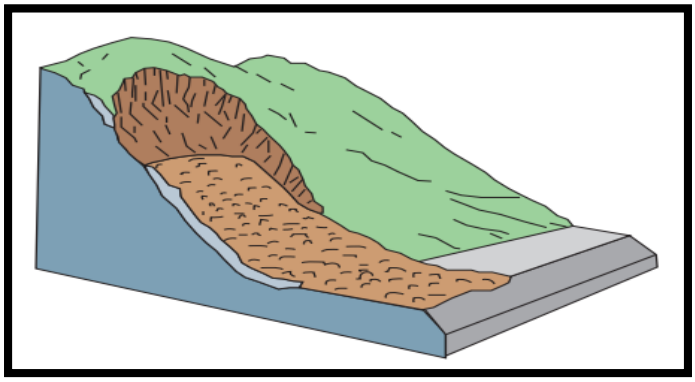

Figure 14: Schematic of a debris avalanche.

Figure 15: A debris avalanche that buried the village of Guinsaugon, Southern Leyte, Philippines, in February 2006.

6. **Earthflow**

Earthflows can occur on gentle to moderate slopes, generally in fine-grained soil, commonly clay or silt, but also in very weathered, clay-bearing bedrock. The mass in an earthflow moves as a plastic or viscous flow with strong internal deformation. Susceptible marine clay (quick clay) when disturbed is very vulnerable and may lose all shear strength with a change in its natural moisture content and suddenly liquefy, potentially destroying large areas and flowing for several kilometers. Size commonly increases through headscarp retrogression. Slides or lateral spreads may also evolve downslope into earthflows. Earthflows can range from very slow (creep) to rapid and catastrophic. Very slow flows and specialized forms of earthflow restricted to northern permafrost environments are discussed elsewhere.

❖ **Occurrence**

Earthflows occur worldwide in regions underlain by fine-grained soil or very weathered bedrock. Catastrophic rapid earthflows are common in the susceptible marine clays of the St. Lawrence Lowlands of North America, coastal Alaska and British Columbia, and in Scandinavia.

❖ **Relative (size/range)**

Flows can range from small events of 100 square meters in size to large events encompassing several square kilometers in area. Earthflows in susceptible marine clays may runout for several kilometers. Depth of the failure ranges from shallow to many tens of meters.

❖ **Triggering mechanisms**

Triggers include saturation of soil due to prolonged or intense rainfall or snowmelt, sudden lowering of adjacent water surfaces causing rapid drawdown of the ground-water table, stream erosion at the bottom of a slope, excavation and construction activities, excessive loading on a slope, earthquakes, or human-induced vibration

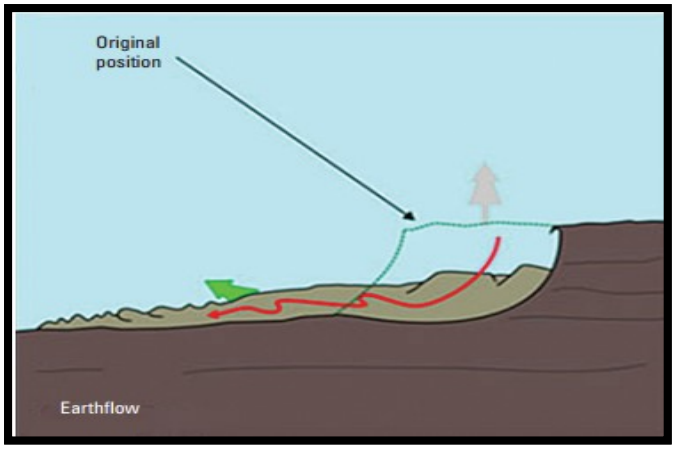

Figure 16. Schematic of an earthflow.(Schematic from Geological Survey of Canada.)

Figure 17: The 1993 Lemieux landslide—a rapid earthflow in sensitive marine clay near Ottawa, Canada.

IV. Causes of landslides

Many of the landslides are natural phenomenon that occurs independently of any human actions. There are also landslides that have been induced by the very actions taken to make land suitable for some human purposes. Landslides can be triggered due to external causes or internal causes.

1. External Causes

- Undercutting of the foot of the hill slope due to river erosion, quarrying, excavation for canals and roads, etc.
- External loads such as buildings, reservoirs, highway traffic, stockpiles of rocks, accumulation of alluvium on slopes, etc.
- Increase in unit weight of slope material due to increased water content.
- Vibrations due to earthquakes, blasting, traffic, etc., causing increase in shearing stresses.
- Entropic changes caused by deforestation
- Undermining caused by tunneling, collapse of underground caverns, seepage erosion, etc.

2. Internal Causes

- Increase in pore water pressure.
- Reduction in cohesive strength caused by progressive laterization.
- Hair cracks due to alternate swelling and shrinkage from tension.
- Presence of faults, joints, bedding planes, cleavage etc., and their orientation.
- Freezing and thawing of rocks and soils.
- Material properties such as compressive strength, shearing strength, etc., of earth material.

3. Effect of Increase in Water Content:

Increasing water levels is the most common trigger of landslides. Increased water pressure decreases the effective stress and the factor of safety of a slope. The Oso landslide in Washington was likely triggered by increased precipitation in the weeks before the slide occurred (Henn et al, 2015). Precipitation can also trigger landslides destabilized by a
previous event such as an earthquake, as seen in the landslides triggered by a rainstorm after the Wenchuan earthquake

4. Increase in Slope Gradient

Steeper the slope, greater is the chances of its failure. An increase in the steepness or gradient, of a slope leads to an increase in shear stress on the potential rupture plane and to a

decrease in normal stress. Such increase in slope gradient may be due to undermining of the foot of the slope by stream erosion or by excavation. Exceptionally, the change of slope gradient may be produced by subsidence and upliftment of the earth's surface. When the slope are designed, a factor of safety has to be computed and efforts are to be made to construct the slope in such a way as to maintain a factor of safety greater than 1.

5. Earthquake Vibrations:

Vibration due to earthquakes not only triggers devastating landslides but also rock falls and the like. Earthquake shocks, particularly those of shorter duration, acceleration of ground motion, tilt of the slope, modifies the system of forces in a manner that driving forces get the upper hand. The vibrations generated by the vehicular traffic create oscillation of different frequency in rocks and they change the stress pattern, reducing shear strength and inducing mass movement. Loosely deposited, fully saturated sand (void ratio larger than critical void ratio) may be compacted by seismic tremors (contractant deformation) so that the increased pore water pressure practically balances the effective stress and the soil liquefies, causing grave damages to the construction, pipelines, etc.

6. Excess Load on the Slope

The addition of weight on the slopes like dumping of debris or wastes and the construction of dams, reservoirs, buildings, etc., increases the intensity of the driving force and reduces the slope stability

V. Conclusion

Landslides are a very dangerous phenomenon that threatens the human life and it must be contained once detected authorities must take some cautionary steps to prevent them and that by effectuating the research and finding better solutions to contain them, certain steps can be taken to reduce the risk or damage from the landslides are following :

- Demarcating landslide prone areas and accordingly plan the future development activities.
- Reduce the slope angle.
- Place additional supporting material at the foot of the slope.
- Reduce the load on the slope (rock, soil or artificial structures)
- Stabilize near-surface soil by preferably fast growing plants with sturdy root system
- Build thick retaining walls at the toe of the slope (high thin walls have been less successful)
- Decrease the water content or pore pressure of the rock or soil;
- Sheet piling

- Use of rock bolts to stabilize rocky slopes (on thin slide blocks of very coherent rocks on low angle slope

I. Introduction :

Slope stability analysis is performed to assess the safe design of a man- made or natural slopes and the equilibrium conditions. Slope stability is the resistance of an inclined surface to failure by sliding or collapsing. The failure of a slope may lead to loss of life and property. It is therefore, essential to check the stability of proposed slopes. With the development of modern method of testing of soils and stability analysis, a safe and economical design of slope is possible. The geotechnical engineer should have a thorough knowledge of the various methods for studying the stability of slopes and their advantages and limitations. Two broad methodologies are in use when dealing with slope stability computation. These are the limit equilibrium methods and the numerical methods. The equilibrium methods have been developed to determine stability conditions, depending on the equations of equilibrium that are included and what assumptions are made (Bishop, 1954; Morgenstern and Price, 1965; Spencer, 1967; Duncan, 1996). In recent years, the advanced quantitative methods such as analytical finite elements and finite differences have been developed for this purpose. The key indicator in slope stability analysis is the factor of safety (FOS), which is commonly defined as the ratio of the resisting shear force to the driving shear force along a failure surface.

In slope stability computation one should distinguish between the planar failure which occurs mainly in rocks and along predefined discontinuity surfaces and the case in which the slip surface may be of curved, composite or of any arbitrary shape.

II. Limit equilibrium method

In the realm of landslide, limit equilibrium (LE) methods are the most widely used for analysing slope stability and designing engineered slopes. The simplicity and versatility of the of this methodology are based on the concept that the geometry of the potential failure surface in a slope is known a-priori and the slope can be discredited into finite vertical slices. Each slice is then analysed using principles of force and/or moment equilibrium (e.g., Bishop, 1954; Morgenstern and Price, 1965; Spencer, 1967; Duncan, 1996.

These methods investigate the equilibrium of a soil mass tending to slide down under the influence of gravity. As a general rule, if the value of factor of safety is less than 1.0, the slope is considered unstable. Nonetheless, due to the yielding of soils at a stress level far below the failure load, an accepted safety factor should not be below 1.2-1.4 regardless planar or circular failure.

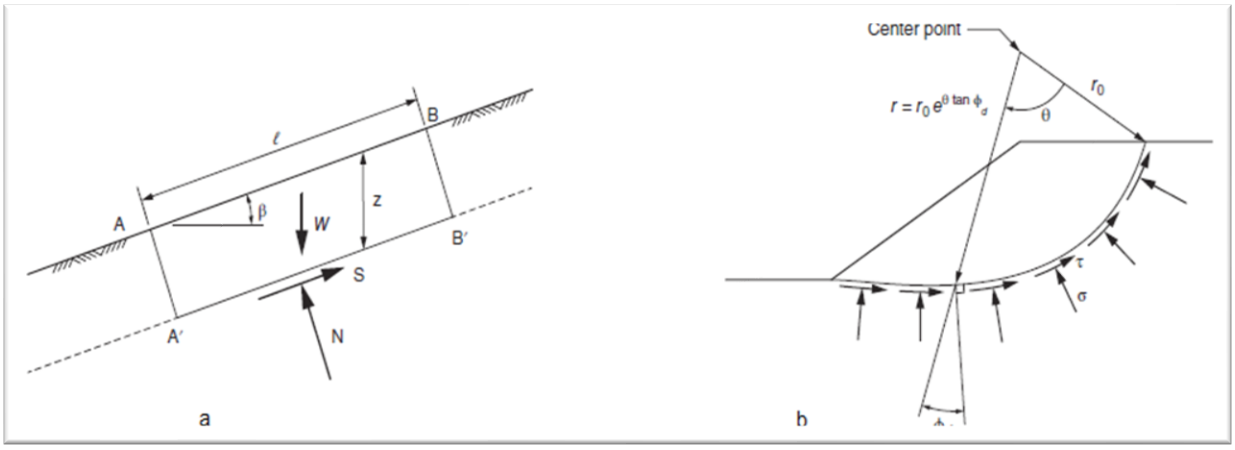

Figure1: Planar and circular failure of a soil

1. General assumption in limit equilibrium analysis:

The soil mass must be safe against slope failure on any conceivable surface across the slope. In this method using the theory of elasticity or plasticity are also being increasingly used, the most common method based on limit equilibrium in which it is assumed soil is at verge of failure. The limit equilibrium is statically indeterminate analysis. As the stress strain relationship along assume surface are not known, so necessary that system becomes statically determinant and it can be analyzed easily using the equation of equilibrium. Following assumption are generally made,

- The stress system is assumed to be two-dimensional. The stresses in the third direction (perpendicular to the section of the soil mass) are taken as zero.
- It is assumed that the column equation for shear strength is applicable and the strength parameters cand φ are known.
- It is further assumed that the seepage conditions and water level are known, and the corresponding pore water pressure can be estimated.
- The condition of plastic failure as assumed to be satisfied along the critical surface in other word shearing strains at all points of the critical surface are large enough to mobilize all the available shear strength.
- Depending upon the method of analysis some additional assumption are made regarding the magnitude and distribution of forces along various planes.

2. Planar failure

This type of slope failure occur most of the time along planar discontinuities and often referred to as *infinite slope* .The usual plane of failure for infinite slopes is typified by a relatively significant differences in the characteristics of the sliding mass and the bedrock along the plane of failure (e.g., a *clay* mass sliding over a *shale* formation). The sliding mass could be a cohessionless or cohesive soils, it may be contain seepage or no seepage. These considerations provide a good basis for the engineer to evaluate the stability.

a) Cohesive dry soil

Figure (21) shows the forces acting on an element from a slope of infinite extent. No seepage is assumed, and the material above the slip plane is assumed homogeneous and cohesive. The slip plane is parallel to the surface of the slope.

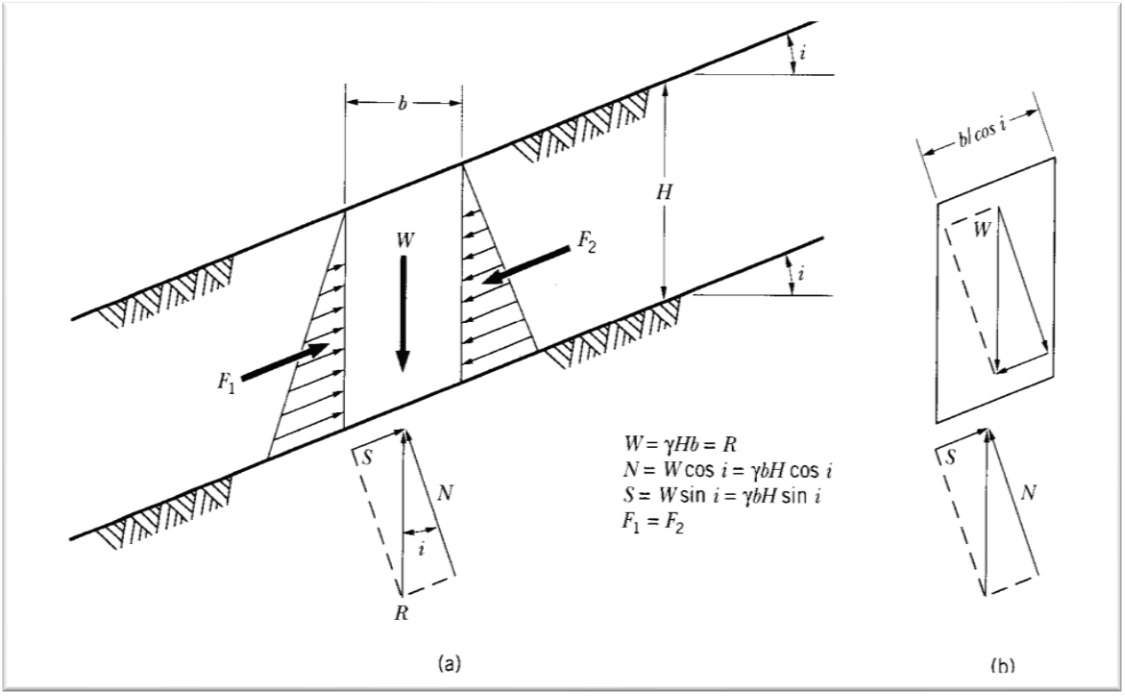

Figure 2: Forces on an element of infinite slope, (After Cernica 1995)

The normal effective stress on the sliding plane is given by:

$\boldsymbol{\sigma_n = \frac{N}{b/cosi} = \frac{\gamma bHcosi}{1!b/cosi} = \gamma hcos^2 i}$, Where $\mathbf{N} =$ normal force

$\boldsymbol{\sigma_n = \gamma hcos^2 i}$ Normal stress on the sliding plane

$\boldsymbol{\tau = \frac{s}{b/cosi} = \frac{\gamma bHsini}{b/cosi} = \gamma bHsini\ cosi}$, Where $\mathbf{S} =$ shear force

$\boldsymbol{\tau = \gamma bHsini\ cosi}$ Shear stress on the sliding plane

The shear strength of soil is defined by:

$$\mathbf{F} = \frac{\boldsymbol{available\ shear\ strength}}{\boldsymbol{shear\ stress\ on\ the\ sliding\ plane}} = \frac{\boldsymbol{resisting\ forces}}{\boldsymbol{driving\ forces}}$$

The available shear strength of the soil is given by Mohr-Coulomb failure criteria as:

$$\boldsymbol{\tau_{avab} = c_d + \sigma_n tan\emptyset}$$

The safety factor is then calculated:

$$\boldsymbol{F = \frac{\tau_{avble}}{\tau}}$$

$$\mathbf{F} = \frac{\mathbf{c_d}}{\boldsymbol{\gamma Hsini\ cosi}} + \frac{\mathbf{tan\emptyset}}{\mathbf{tani}}$$

$\boldsymbol{i}$ = slope inclination angle, $\mathbf{c_d}$=effective cohesion, $\boldsymbol{\gamma}$ = density of the material,

$\emptyset$= effective angle of internal friction of the material, $\boldsymbol{H}$ = height of the slope

b) Cohesive soil with seepage

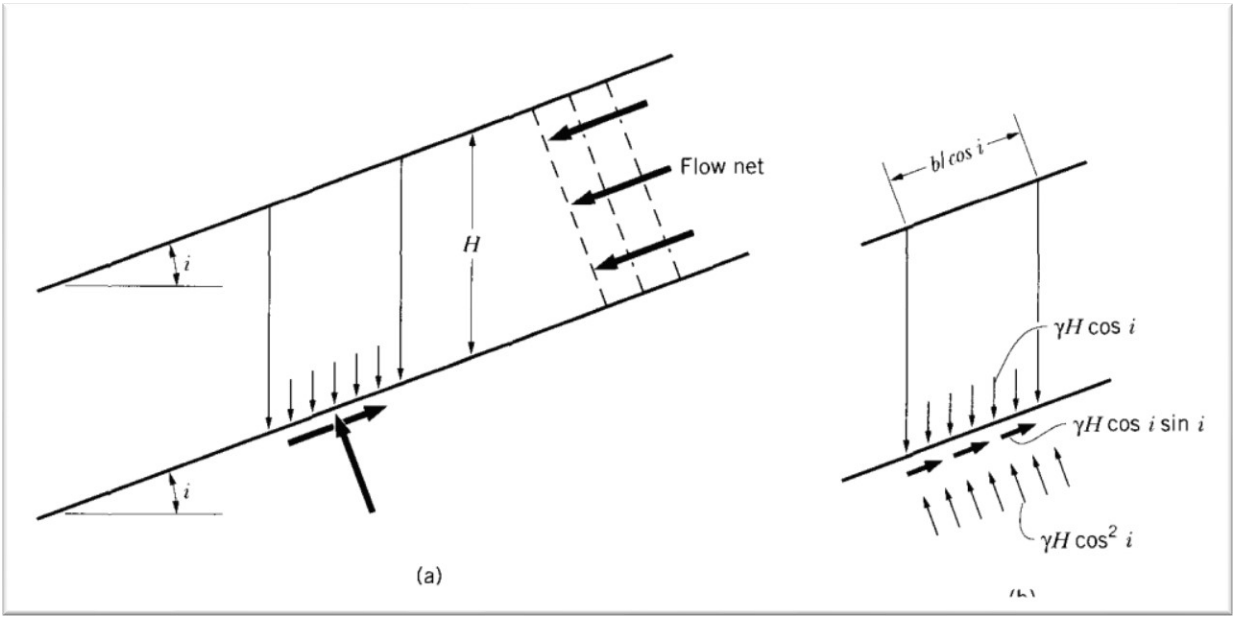

Figure 3: slope consisting of cohesive soil with seepage, Normal and shear stresses on an inclined plane. (After Cernica 1995)

When the slope is saturated with water and water percolate through it, this later comes under the seepage pressure and the effective normal stress is reduced which cause a significant increase in the soil shear strength.

$\boldsymbol{\sigma' = (\gamma - \gamma_w)cos^2 i, \tau = \gamma bHsini\ cosi,}$ $\boldsymbol{\tau_{avab} = c_d + \sigma' tan\emptyset_d}$

The factor of safety is then given by:

$$\mathbf{F} = \frac{\boldsymbol{c_d}}{\boldsymbol{\gamma Hsini\ cosi}} + \left(\frac{\boldsymbol{\gamma'}}{\boldsymbol{\gamma}}\right)\frac{\boldsymbol{tan\emptyset_d}}{\boldsymbol{tani}}$$

3. The circular arc analysis

Generally, for homogeneous cohesive soil slopes failure is usually a mixture of circular arcs and spirals. The work results of Petterson(1916) in connection with the slope failure at Stigberg Quay in the harbor of Gothenburg, Swedenand by other Swedish engineers, the analysis of slopes considering a circular failure surface became widely adopted. Site investigation by borings has shown the circular or curved rupture surfaces in failed homogeneous and isotropic soil slopes.

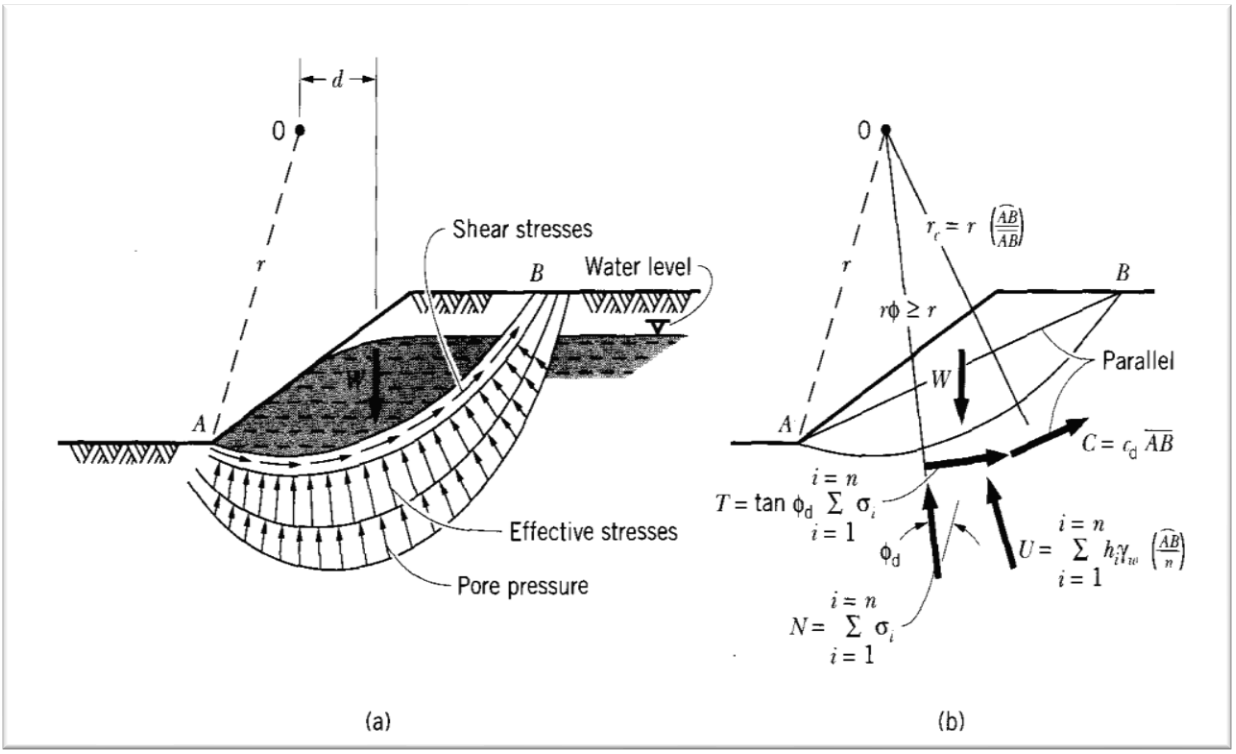

Figure 4: forces acting on a circular failure surface, a) stress distribution on failure circular surface, b) resultant forces acting on a failing soil element

In this case the factor of safety is defined as de ratio of the resisting moment to driving moment, along the failure curved surface.

$$F = \frac{r\left[c_d AB + \widehat{tan}\, \emptyset_d \sum_{i=1}^{i=n} \bar{\sigma}_i\right]}{W * d}$$

Where:

r: radius of circle,

AB: arc length,

Cd: average cohesion developed per unit length of arc,

$\boldsymbol{\phi_d}$: average friction angle developed,

$\bar{\boldsymbol{\sigma}}_{\mathbf{i}}$: Effective stress at a point I,

W: Total weight of wedge,

d: moment arm measured from center of rotation to vertical passing through centroid of mass

In view of the inaccuracy of this method of analysis, Fellenius (19xx) and Petterson (19xx),have advanced the *method of slices* as a more accurate method of stability analysis. It gives better results when applied in inhomogeneous soil slopes and seepage.

4. Ordinary Method of Slices

In this method, the slope is supposed to fail along a circular surface and the failing mass is subdivided into a number of vertical sections or slices. The stresses acting on a typical slice are the weight of the slice, the normal and shear stresses, the pore pressures, and the shear and normal effective stresses on the interface of the slice induced by deformation. These are shown in Fig 24. The latter two are rather indeterminate and, for the sake of simplifying the calculation efforts, are frequently neglected in the analysis.

For any given slice, the weight (*Wi)* could be determined as the product of the cross-sections of the slice times the unit weight times the unit thickness:

$$\mathbf{w}_i = \boldsymbol{\gamma} * \boldsymbol{A}_i * \mathbf{1}$$

It is assumed to act through the midpoint of the area, as shown in Fig. 24 b. From this figure,The normal force for a slice is given by: $\mathbf{N}_i = \boldsymbol{W}_i \cos \boldsymbol{\alpha}_i \quad \acute{\mathbf{N}}_i = \boldsymbol{W}_i \cos \boldsymbol{\alpha}_i - \boldsymbol{Ui}$

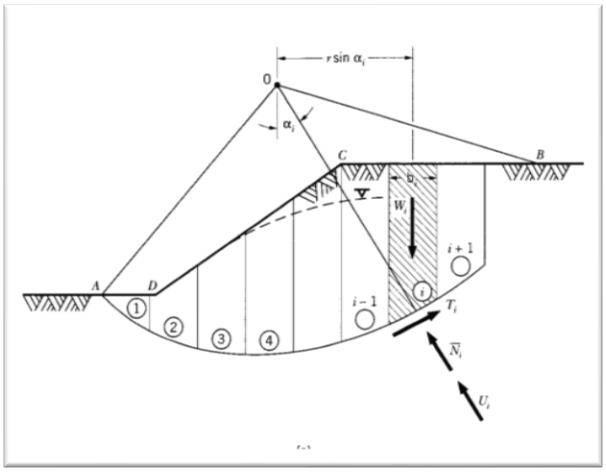

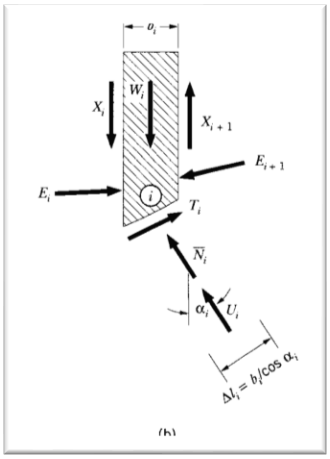

Figure 5 and 6: Method of slices: Sliding mass divided into slices. Forces acting on a slice **i**

The driving force is:

$\boldsymbol{T_i = W_i \sin \alpha_i}$ Driving force

$\boldsymbol{S = \acute{N}_i \tan \emptyset_i + c_d \Delta L_i = (W_i \cos \alpha_i - U_i) tan \emptyset_i}$ Resisting force

The factor of security is:

$\mathbf{F = \frac{resisting\ moment}{driving\ moment} = \frac{r \sum s_i}{r \sum W_i \sin \alpha_i}}$,

$\boldsymbol{F = \frac{\sum_{i=1}^{i=n} [c' \Delta L \acute{+} (W_\iota cos \alpha_i - U_i) tan \emptyset']}{\sum_{i=1}^{i=n} W_i \sin \alpha_i}}$

As mentionned earlier this method is not quite accurate as it violates the equilibrium requirement for translation as the side forces were neglegted. Bishop assumed the force resultant to be zero in a vertical direction as a way to remedy for the inaccuracy arising above.

$\boldsymbol{\acute{N}_i = W_i \cos \alpha_i - Ui}$ 1

$\boldsymbol{T_i = W_i \sin \alpha_i = \frac{\acute{N}_i \tan \emptyset_i + c_d \Delta L_i}{F}}$ 2

From the assumption of Bishop $\sum F_y = 0$

$\boldsymbol{U_i + N'_i (\cos \alpha_i - W_i + T_i \sin \alpha_i = 0}$ 3

$\boldsymbol{N'_i + N'_i \frac{tan \sigma_i + \tan \acute{\emptyset}}{F} = \frac{W_i}{cos \alpha_i} - U_i - \frac{c' \Delta L_i}{F} tan \alpha_i}$ 4

Substituting: $\boldsymbol{\Delta L_i = \frac{b_i}{cos \alpha_i}, U_i = u_i \Delta l_i = u_i \left(\frac{b_i}{cos \alpha_i}\right),}$

The equation above becomes:

$\boldsymbol{N'_i = \frac{W_i - u_i b_i - (c' b_i / F) \tan \alpha_i}{cos \alpha_i (1 + \frac{tan \alpha_i tan \emptyset'}{F})}}$ 5

We have from equation 1: $\boldsymbol{\acute{N}_i = W_i \cos \alpha_i - Ui}$ substituting into 5 we get

$$F = \frac{\sum_{i=1}^{i=n} \left\{ \frac{\bar{c} b_i}{\cos \alpha_i} + \left[\frac{W_i - u_i b_i - \bar{c} b_i \tan \alpha_i / F}{\cos \alpha_i (1 + \tan \alpha_i \tan \bar{\phi} / F)} \right] \tan \bar{\phi} \right\}}{\sum_{i=1}^{i=n} W_i \sin \alpha_i} \quad \text{.....6}$$

On simplification the factor of safety equation becomes:

$$F = \frac{\sum_{i=1}^{i=n} [\bar{c} b_i + (W_i - u_i b_i) \tan \bar{\phi}] [\sec \alpha_i / (1 + \tan \alpha_i \tan \bar{\phi} / F)]}{\sum_{i=1}^{i=n} W_i \sin \alpha_i}$$

The solution of this equation requires an iterative analysis since F appears on its both sides. Usually the first F is found using Fellenius method and then it is put in the equation. The iterative process goes on until the Fs on both sides are nearly equal. With the advancement of computer this method is quite easy to use.

5. Taylor's stability number

If the slope angle β, height of embankment, the effective unit weight of material γ, angle of Internal friction φ', and unit cohesion c' are known, the factor of safety may be determined. In order to make the unnecessary more or less tedious stability determinations, Taylor (1937) conceived the idea of analyzing the stability of a large number of slopes through a wide range of slope angles φ' and angles of internal friction, and then representing the results by an abstract number which he called the "stability number". This number is designated as N*s*. The expression used is

$$Ns = \frac{c'}{Fc\, \gamma H}$$

From this the factor of safety with respect to cohesion may be expressed as

$$Fs = \frac{c'}{Nc\, \gamma H}$$

Taylor published his results in the form of curves which give the relationship between *Ns* and The slope angles β for various values of φ' as shown in Fig 6-A. These curves are for circles passing through the toe, although for values ofβ less than 53°, it has been found that the most dangerous circle passes below the toe. However, these curves may be used without serious error for slopes down to β = 14°. The stability numbers are obtained for factors of safety withrespect to cohesion by keeping the factor of safety with respect to friction ($F\emptyset$) equal to unity. In slopes encountered in practical problems, the depth to which the rupture circle may extend is usually limited by ledge or other underlying strong material. The stability number *Ns* for the case when φ'=

0 is greatly dependent on the position of the ledge. The depth at which the ledge or strong material occurs may be expressed in terms of a depth factor nd which is defined as,

$$nd = \frac{D}{H}$$

Where, D = depth of ledge below the top of the embankment, H = height of slope above the toe. For various values of nd and for the φ'= 0 case the chart in Fig 26 gives the stability number Ns for various values of slope angle β. In this case the rupture circle may pass through the toe or below the toe. The distance x of the rupture circle from the toe at the toe level may be expressed by a distance factor nx which is defined as,

$$nx = \frac{X}{H}$$

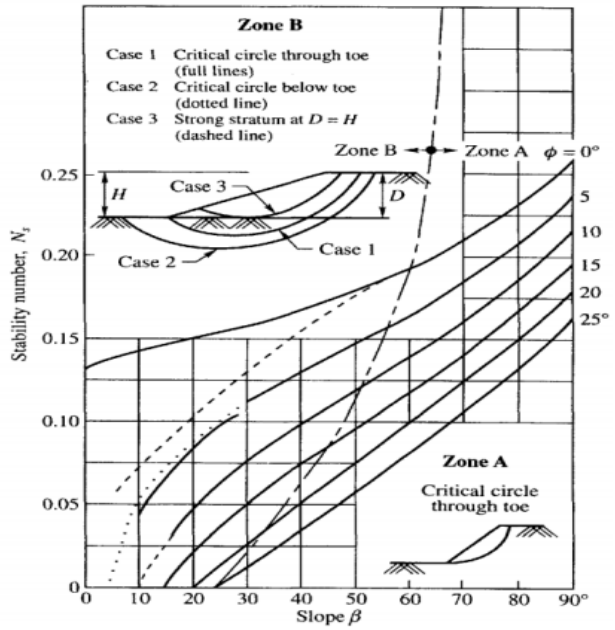

Figure 7: Taylor's stability number for circles passing through the toe and below or above the toe

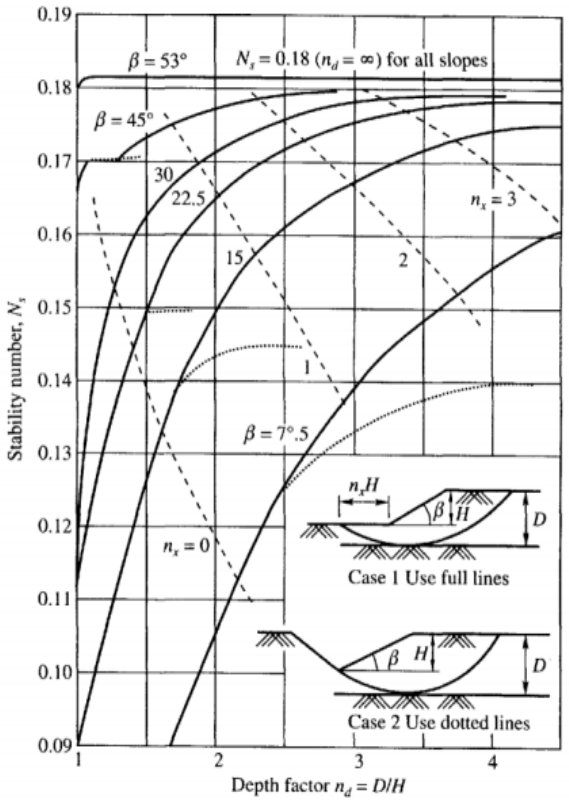

Figure 8: Taylor's stability number for φ' = 0

6. Factor of Safety with Respect to Strength:

The development of the stability number is based on the assumption that the factor of safety with respect to friction$F\emptyset$, is unity. The curves give directly the factor of safetyFc with respect to

cohesion only. If a true factor of safety Fs with respect to strength is required, this factor should apply equally to both cohesion and friction. The mobilized shear strength may therefore be expressed as,

$$sm = \frac{s}{Fs} = \frac{c\prime}{Fs} + \frac{\sigma \tan(\phi\prime)}{Fs}$$

In the above expression, we may write:

$$c\prime m = \frac{s}{Fs} \tan \varphi\prime m = \frac{\tan \phi\prime}{Fs} \qquad \text{Or,} \quad \varphi\prime m = \frac{\phi\prime}{Fs} \text{(approx).}$$

$c\prime$m And $\phi\prime m$ may be described as average values of mobilized cohesion and friction respectively.

III. Finite element method :

As computer performance has improved, the application of FE in geotechnical analysis has become increasingly common. These methods have several advantages: to model slopes with a degree of very high realism (complex geometry, sequences of loading, presence of material for reinforcement, action of water, laws for complex soil behaviour) and to better visualize the deformations of soils in place. However, it is critical to understand the analysis output due to the larger number of variables offered to the engineer. When developing the strength reduction methodology to be applied in Safe, a comparison was made between three differing techniques. For all techniques, an initialization run for a given slope model was carried out and the strains and displacements obtained in that run set to zero for the subsequent FOS assessment. In the first method, an incremental strength reduction was applied to the elastic Mohr-Coulomb material whereby for each follow-on increment the same reduction in global strength was applied. The second method involved specifying separate, independent model runs with revised material parameters corresponding to specific percentage reductions in material strength. The third method used a new feature in Safe, in which the program automatically applies the same strength reduction in successive analysis increments, but once failure is observed, reverts to the last converged increment and refines the strength reduction to obtain an estimate of FOS to an acceptable accuracy.

- Discontinuum modeling:

The Discontinuum approach is useful for rock slopes controlled by discontinuity behavior. Rock mass is considered as an aggregation of distinct, interacting blocks subjected to external load an

assumed of undergo motion with time. This methodology is collectively called as the discrete element method (DEM). Discontinuum modeling allows for sliding between the block and particles. The DEM is based on solution of dynamic equations of equilibrium for each block. Repeatedly until the boundary conditions and laws of contact and motion are satisfied. Discontinuum modeling belongs to the most commonly applied numerical approach to rock slope analysis.

- Hybrid/coupled modeling :

Hybrid codes involve the coupling of various methodologies to maximize their key advantages, e.g. limit equilibrium analysis combined with finite element groundwater flow and stress analysis adopted in GEO-STUDIO software; coupled particle flow and finite-difference analyses used in PF3D and FLAC3D. Hybrid techniques allow investigation of piping slope failures and the influence of high groundwater pressures on the failure of weak rock slope. Coupled finite-/distinct-element codes, e.g. ELFEN provide for the modeling of both intact rock behavior and the development and behavior of fractures. There other slope stability analysis methods such as the graphical method, the perturbation method and more.

IV. Conclusion

The causes and the nature of a slope failure should be understood before embarking on corrective action. Sowers (1979) mentioned that more than one cause is at the origin of the instability. What may seem to be the cause? In most of the time the trigger, The geological investigation, the boreholes, the back analysis may all together be used to determine the very cause of the failure. Once the cause determined, the appropriate solution must be chosen to heal the problem at its root. Among the solution to land sliding one can cite the drainage if water is the problem. Drainage can be surface drainage, well drainage, trench drainage and so on. Retaining structures can also be used to improve slope stability by applying stabilizing forces to slopes, thereby reducing the shear stresses on potential slip surfaces. Among these mechanical means of stabilisations we have pre stressed anchors and anchored walls, gravity walls, mechanically stabilised earth walls and soil nailed walls and reinforcing pile sand drilled shaf

I. Introduction:

The growing development that witness the region of souk ahras, has led authorities to consider locality arias for construction and road opening. These once considered marginally stable areas have caused severe damage to roads constructed upon them. It is the case of the road linking Souk Ahras to Mechrouha where the pavement has shown sever cracking and settlement due to the sliding of the entire slope. The undertaken remedial measure was the use of a cantilevered imbed sheet pile wall. The uses of sheet piles vary widely and are incredibly versatile. With that being said, let's get to know them in this chapter.

II. What is sheet pile?

They are sheets made of steel or other material (wood,reinforced concrete) with interlocking edges, flexible due to their thickness, their length is in practice limited to 30 m, they are driven into the ground to provide earth retention, excavation support and prevent water seepage.

III. The idea behind sheet piling:

Let's say that we want to separate a soil mass into two parts; we follow a certain process which consists of simply pushing in a vertical curtain in the ground from the surface separating the soil mass into two parts

As we cannot drive the curtain simultaneously over the entire length, it is cut into narrow vertical elements called sheet piles like piano keys that are going to set up one after the other as shown in figure 1and 2.

Figure 1: Sheet piles assembling

In order to ensure the solidity of these curtains, designers developed a groove called a “lock”; over the entire length of a sheet pile shown in figure 3 and 4, this “lock” is designed to be simple and resistant it secures each sheet pile with the other and ensures the rigidity of the entire curtain as a unit.

Figure 2 and 3: example of a lock

IV. Sheet piling applications:

The uses of sheet piles can be temporary or permanent. They may be used as a retaining walls for slope stabilization shown in figure 4, the reinforcement of banks, the creation of foundations,Cofferdam constructionas shown in figure 5 and provisional support.

Figure 4: backfill stabilized with sheet piles

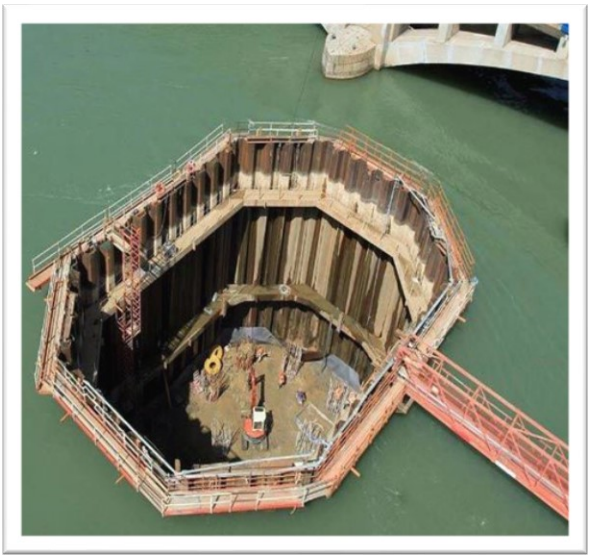

Figure 5: Cofferdam construction

V. Practical characteristics of sheet piles:

Sheet piles are most commonly made of deferent material like timber, reinforced concrete and steel.

Steel is the most common form of **sheet piles** as it has good resistance to high driving stresses, excellent water-tightness, and can be increased in length either by welding or bolting. They are connected by interlocking and they come into five basic forms as shown in figures 6, 7, 8, 9, 10: These include U and Z shaped **sheetpiles**, flat ones, HZ shapes mixture and finally the curtain mixed of tubes and piles.

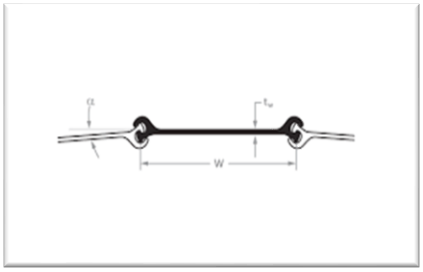

Figure 6: flat piles

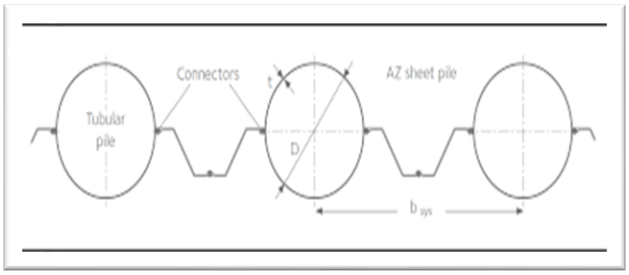

Figure 7 : tubes and piles curtain

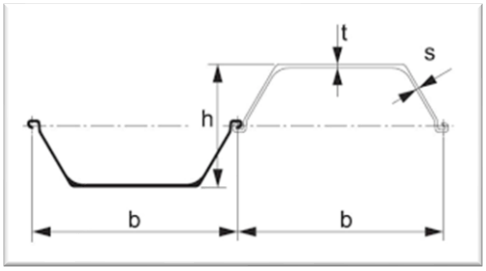

Figure 8 : U shaped piles

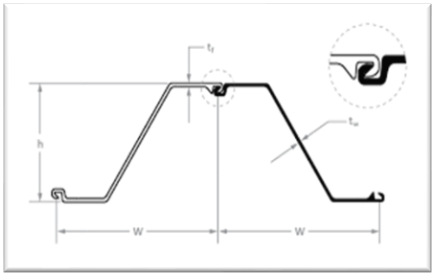

Figure 9 : Z shaped piles

Figure 10 : HZ shaped piles

VI. Installation:

Prior to installation, piles should be carefully inspected for straightness, cracks and the integrity of the interlocking components.

Driving must be carefully monitored and should stop immediately if the pile ceases to penetrate the soil, before moving on to the next pile along. In some cases, several adjacent piles will be unable to penetrate to the design depth. At this point, effort should be made to remove the obstacle, either by partial excavation or using a water jet. There is an acceptable number of 'under-driven' **sheet piles**, but this will vary according to the specific design requirements.

Sheet piles have a tendency to deviate from a vertical plane during driving and instead lean sideways. This is due to encountering obstacles within the soil which act as deflection. Guide controls should be used to counter this.

One technique is to drive piles in panels. This involves pitching and driving two piles to part or full-penetration at either end of a panel of piles. The panel is therefore supported by the 'bookended' piles during driving to their final position. The pair left on the end then forms the support of the next panel along.

Vibratory hammers are often used to install **sheet piles**, although if soils are too hard or dense, an impact hammer can be used. At certain sites where vibrations are not tolerated, the sheets can be hydraulically pushed into the ground .

VII. Sheet pile structure:

Steel sheet piles may conveniently be used in several civil engineering works. They may be used as: Cantilever sheet piles, Anchored bulkheads, Braced sheeting in cuts,Single cell cofferdams, Cellular cofferdams, circular type or Cellular cofferdams (diaphragm).

For this chapter we are going to focus on cantilever sheet piles.Cantilever sheet piles depend for their stability on an adequate embedment into the soil below the dredge line. Since the piles are fixed only at the bottom and are free at the top, they are called*cantilever sheet piles.* These piles are economical only for moderate wall heights, since the required section modulus increases rapidly with an increase in wall height, as the bending moment increases with the cube of the cantilevered height of the wall. The lateral deflection of this type of wall, because of the cantilever action, will be relatively large. Erosion and scour in front of the wall, i.e., lowering the dredge line, should be controlled since stability of the wall depends primarily on the developed passive pressure in front of the wall.

1. Summary of Rankine's lateral earth pressure theory:

The Rankine's theory assumes that there is no wall friction(φ = 0), the ground and failure surfaces are straight, and that the resultant force acts parallel to the backfill slope. In case of retaining structures, the earth retained may be backfill or natural soil. These backfill materials may exert certain lateral pressure on the wall. If the wall is rigid and does not move with the pressure exerted on the wall, the soil behind the wall will be in a state of elastic equilibrium. Consider the prismatic element E in the backfill at depth, z, as shown in Figure11:

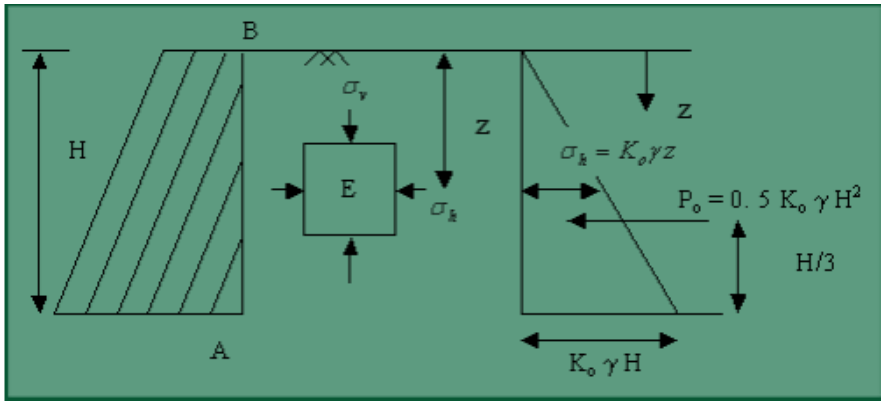

.

Figure11: Lateral earth pressure for at rest condition.

- **At rest conditions:**

The element E is subjected to the following pressures:

Vertical pressure $\sigma = \gamma z$ and lateral pressure $= \sigma h$, where γ' is the effective unit weight of the soil, If we consider the backfill is homogenous then both σh and σv increases rapidly with depth z. In that case the ratio of vertical and lateral pressures remain constant with respectto depth, that is $\frac{\sigma h}{\sigma v}$ $= \frac{\sigma h}{\gamma z}$constant= K_0, where$K_0$is the coefficient of earth pressure for at rest condition.

The lateral earth pressure acting on the wall of height H may be expressed as $\delta h = K_0 \gamma' H$

The total pressure for the soil at rest condition$P_0 = 0{,}5\ K_0\ \gamma' H^2$

The value K_0 depends on the relative density of soil and the process by which the deposit was formed. If this process does not involve artificial tamping, the value of K_0ranges from 0.4 for loose sand to 0.6 for dense sand. Tamping of the layers may increase it up to 0.8.

From elastic theory$K_0=\mu/(1-\mu)$, where μ is the Poisson's ratio.

According to Jaky (1944), a good approximation of K_0 is given by $K_0=1-\sin\theta$

- **Active earth pressure:**

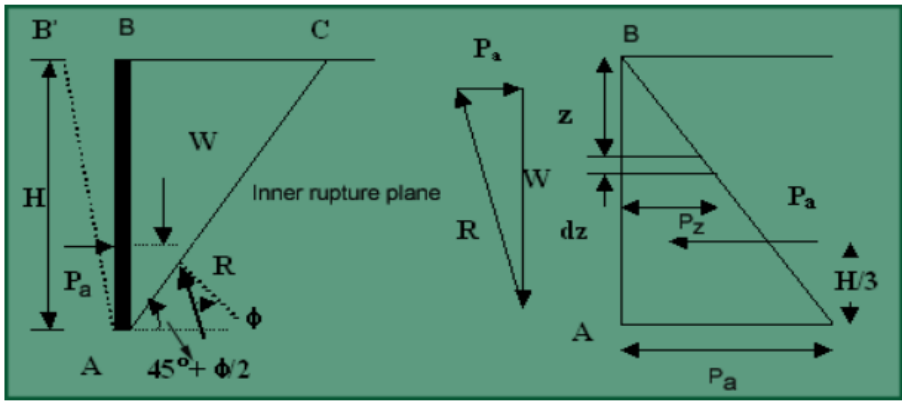

Figure 12: Rankine's active earth pressure in cohessionless soil

Rankine's Earth Pressure against a Vertical Section with a horizontal Surface and cohessionless Backfill

The lateral earth pressure acting against a smooth wall AB is due to mass of soil ABC above the rupture line AC which makes an angle of (45°- θ/2) with the horizontal. The lateral pressure distribution on the wall AB of height H increases in same proportion to depth.

The pressure acts normal to the wall AB.

The lateral active earth pressure at A is $P_a= K_a$, which acts at a height H/3 above the base of the wall. The total pressure on AB is therefore calculated as follows:

$Pa = \int_0^H Pz\, dz = \int_0^H Ka\,\gamma z\, dz$ = 0,5Ka γH^2, where Ka =$\tan^2(45° - \theta/2)$

❖ **Passive earth pressure:**

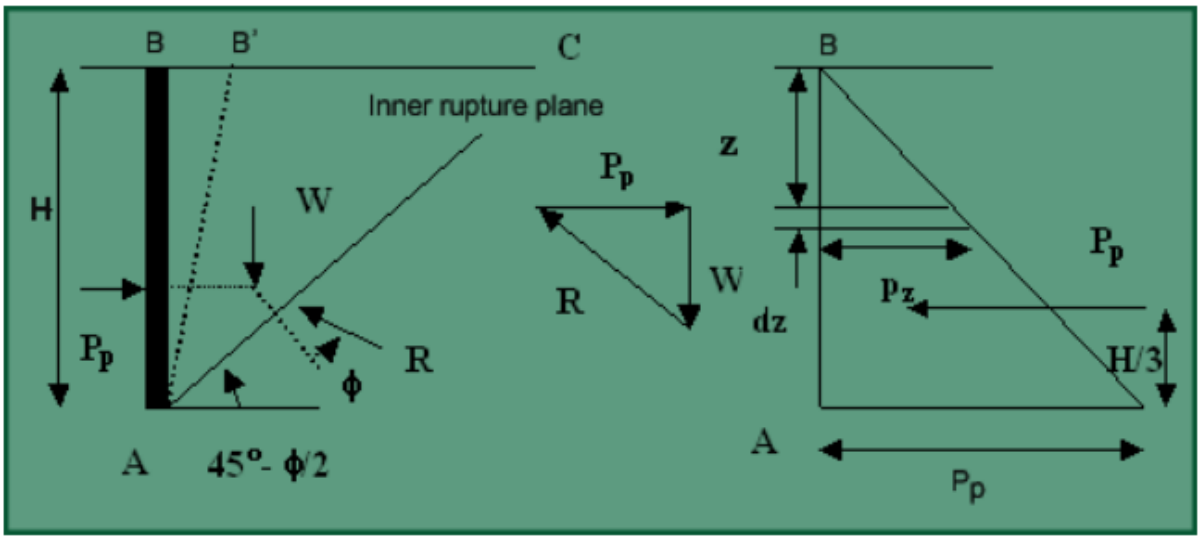

Figure 13: 0 Rankine's passive earth pressure in cohesionless soil

If the wall AB is pushed into the mass to such an extent as to impart uniform compression throughout the mass, the soil wedge ABC in fig. will be in Rankine's Passive State of plastic equilibrium. The inner rupture plane AC makes an angle (45°+ θ/2)with the vertical AB. The pressure distribution on the wall is linear as shown.

The lateral passive earth pressure at A is $P_p = K_p \gamma H$. which acts at a height H/3 above the base of the wall. The total pressure on AB is therefore

$Pp = \int_0^H Pz\, dz = \int_0^H Kp\, \gamma z\, dz = 0{,}5 K_p\, \gamma H^2$, where $K_p = \tan^2(45° + \theta/2)$

So In case of cohesionless soils, the active earth pressure at any depth is $P_a = K_a \gamma H$.the passive earth pressure is given by $P_p = K_p \gamma H$, andIn case of cohesive soils the cohesion component is included and the expression becomes $P_a = K_a \gamma H - 2c\sqrt{K_a}$and the passive earth pressure expression becomes $P_p = K_p \gamma H + 2c\sqrt{K_P}$.

2. Cantilever sheet pile wall design

In designing a cantilever sheet pile wall for earth stabilization, we use Rankin's active and passive earth pressure calculation method which is the most common used one. It consists in computing the value of land thrust against the wall surface. This approach assumes that the presence

of a wall does not disturb the distribution of vertical stresses in the ground in its vicinity on one hand and that the ground surrounding the wall is everywhere in a state of failure in active or passive mode on the other. With regard to these assumptions we can calculate the vertical stress at any point σv and the pore pressure u, from which we can deduce the effective stress σ'v = σv – u. we then evaluate that the σ'h = Kpσ'v or Kaσ'v .we conclude the value at all points of σh = σ'h + u that we integrate along the wall to obtain the resultant active and passive pressure. Active and passive earth pressures on cantilevered sheet pile: The basic principles for estimating the net lateral pressure distribution on a cantilever sheet-pile wall can be explained with the aid of Figure 14:

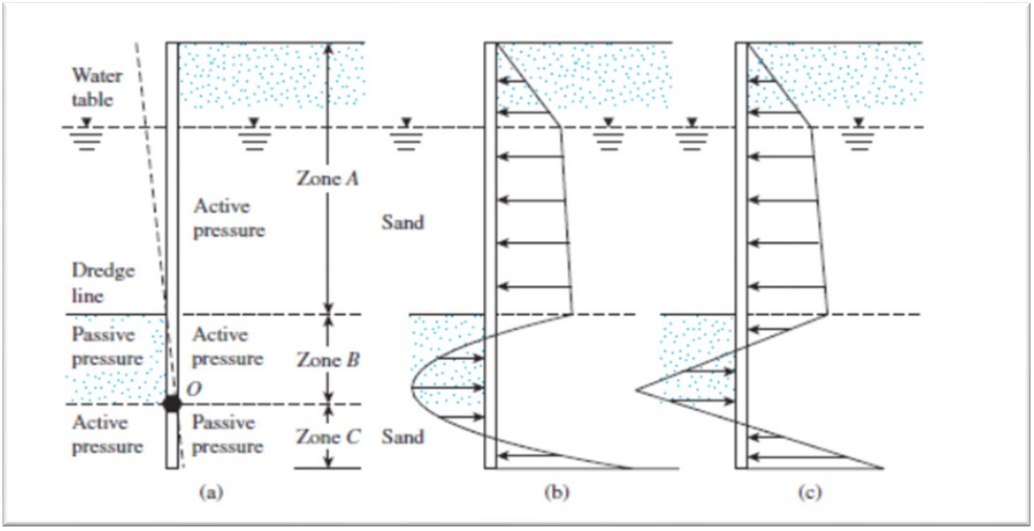

Figure 14: cantilevered sheet pile penetration sand

The figure shows the nature of lateral yielding of a cantilever wall penetrating a sand layer below the dredge line.

- The wall rotates about point O (Figure 14 a). Because the hydrostatic pressures at any depth from both sides of the wall will cancel each other, we consider only the effective lateral soil pressures.
- In zone A, the lateral pressure is just the active pressure from the land side. In zone B, because of the nature of yielding of the wall, there will be active pressure from the land side and passive pressure from the excavated side.
- The condition is reversed in zone C—that is, below the point of rotation, O.
- The net actual pressure distribution on the wall is like that shown in Figure 14 b.

3. Design steps of sheet pile walls:

In order to design a sheet pile we need to follow some steps: first we need to determine the lateral earth pressure acting on the wall, and then we do stability checks considering equilibrium of

total lateral forces and moment of the forces, after that we need to determine the depth of penetration and calculate the maximum bending moment value, finally we choose the necessary profile of the sheet piling according to the allowable flexural stress of the sheet pile material.

A. Cantilever type Sheet pile walls penetrating cohessionless Soils:

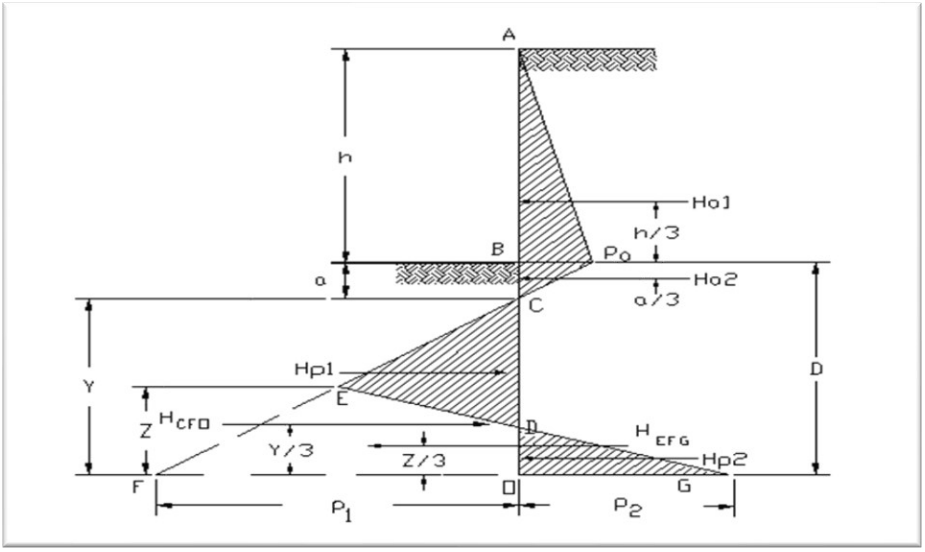

Figure 15: pressure distribution on a cantilever sheet pile in cohesionless soils

In cohesionless soil, C is zero. The active pressure at bottom of excavation can be calculated as $p_a = \gamma h K_a + q K_a$,

Where, γ is unit weight of soil, h is the height of excavation.

The lateral forces Ha1 is calculated as $H_{a1} = \gamma K_a h^2/2 + q K_a h$

Below the dredge line, the sheet pile is subjected to active pressure on the earth side and passive pressure on the excavation side. Since passive pressure is larger than active pressure, the earth pressure on the earth side decreases.

At some depth "a" below the dredge line, the earth pressure is zero.

The depth a can be calculated as $a = p_a / \gamma (K_p - K_a)$

Where K_p is passive earth pressure coefficient. When the sheet pile rotates away from the earth side, there are active pressure on the earth side and passive pressure on the excavation side. Therefore, the slope of BC is equal to $\gamma (K_p - K_a)$; The lateral forces Ha2 can be calculated as $H_{a2} = p_a * a/2$

- **Derive equation for depth Z from $\sum$ Fx = 0**

Summarize lateral forces, we have

$\sum F_x = H_{a1} + H_{a2} - H_{p1} + H_{p2} = 0$

From the diagram, we recognize that lateral force H_{p1} is the area of the triangle CDE and H_{p2} is area DOG. There is a common area DEFO between two areas, and

H_{p1}-H_{p2} = triangle CDE – triangle DOG = triangle CFO – triangle EFG = HCFO-HEFG

Where HCFO = p_1*Y/2, and HEFG = (p_1+p_2)*Z/2

Therefore the equation can be written asH_{a1}+ H_{a2} – p_1*Y/2+ (p_1+p_2)*Z/2 = 0

Solving the equation for Z, we have $Z = \frac{p1Y-2'(Ha1+Ha2)}{p1+p2}$

The pressure at bottom of sheet pile on the excavation side p_1 can be determined from the slope of line CEF. Since the slope of line CEF is $\boldsymbol{\gamma}$ (K_p-K_a), p_1 = g (K_p-K_a)*Y

The pressure at the bottom of sheet pile on the earth side p_2 can be determined from active and passive earth pressure coefficient and overburden pressure. When the sheet pile rotates, there are active pressure on the excavation side and passive pressure on the earth side at the bottom of sheet pile. The overburden pressure from bottom of excavation is(a+Y), the active pressure is $\boldsymbol{\gamma}$Ka(a+Y). The overburden pressure from the top to the bottom of sheet pile on the earth side is (h+a+Y), the passive pressure is $\boldsymbol{\gamma}$ K_p (h+a+Y). Therefore,

$p_2 = \gamma K_p (h+a+Y) - \gamma K_a (a+Y)$

If there a surcharge, $p_2 = \gamma K_p (h+a+Y)+q K_p - \gamma K_a (a+Y)$

Derive equation for Y from $\sum M_o = 0$

Both p_1 and p_2 are function of Y, to determine Y, we can take moment about bottom of sheet pile O. We have $\sum M_o = H_{a1}$*(h/3+a+Y)+ H_{a2}*(2a/3+Y) – HCFO*Y/3+HEFG*Z/3 = 0

OrH_{a1}*(h/3+a+Y)+ H_{a2}*(2a/3+Y) – p_1*Y2/6+(p_1+p_2)*Z^2/3 = 0

The depth Y can be determined from a trial and error process.

- **Calculating embed depth D**

Once Y is determined, the minimum embedded depth D is equal to Y+a. Usually a factor of safety of 1.2 is applied to D, and the length of sheet pile L is equal to h+D*FS. FS is factor of safety from 1.2 to 1.4.

- **Selection of sheet pile section**

The size of sheet pile is selected based on maximum moment and shear. Maximum shear force is usually located at D where lateral earth pressure change from active to passive.

Vmax = H_{a1}+H_{a2}

Maximum moment locates at where shear stress equals to zero between C and D.

Assume that maximum moment located at a distance y below point C, then

$(H_{a1}+H_{a2}) = \boldsymbol{\gamma}$ (Kp-Ka) $y^2/2$. Therefore,$y = \{2*(H_{a1}+H_{a2})/[\boldsymbol{\gamma}(Kp-Ka)]\}^{1/2}$

The maximum moment is$M_{max} = H_{a1}*(h/3+a+y)+ H_{a2}*(2a/3+y)-\boldsymbol{\gamma}$ (Kp-Ka)$*y^3/6$

The required section modulus is $S = M_{max} / F_b$,

F_b is allowable flessural strength of sheet pile.

The sheet pile section is selected based on section modulus

- **Design Procedure**

- Calculate lateral earth pressure at bottom of excavation, p_a and H_{a1}.
  $p_a = \boldsymbol{\gamma} K_a h$, $H_{a1}=p_a*h/2$
- Calculate the length a, and H_{a2}.
  $a = p_a / \boldsymbol{\gamma} (K_p-K_a)$, $H_{a2}=p_a*a/2$
- Assume a trial depth Y, calculate p1and p2.
  $p_1 = (K_p-K_a)*Y$,
  $p_2 = \boldsymbol{\gamma} K_p (h+a+Y) - \boldsymbol{\gamma} K_a (a+Y)$
- Calculatedepth $Z=\frac{p1Y-2'(Ha1+Ha2)}{p1+p2}$
- Let $R = H_{a1}*(h/3+a+Y)+ H_{a2}*(2a/3+Y) – p_1*Y^2/6+(p_1+p_2)*Z^2/3$

Substitute Y and Z into R, if R = 0, the embedded depth, D = Y + a.
If not, assume a new Y, repeat step 3 to 5.

- Calculate the length of sheet pile, L = h+1.2*D
- Calculate $y = \{2*(H_{a1}+H_{a2})/[\boldsymbol{\gamma}(K_p-K_a)]\}^{1/2}$.
- Calculate$M_{max} = H_{a1}*(h/3+a+y)+ H_{a2}*(2a/3+y)-\boldsymbol{\gamma}$ (Kp-Ka)$*y^3/6$
- Calculate required section modulus $S= M_{max}/F_b$.
- Select sheet pile section.

B. Cantilever type Sheet pile walls penetrating cohesive Soils:

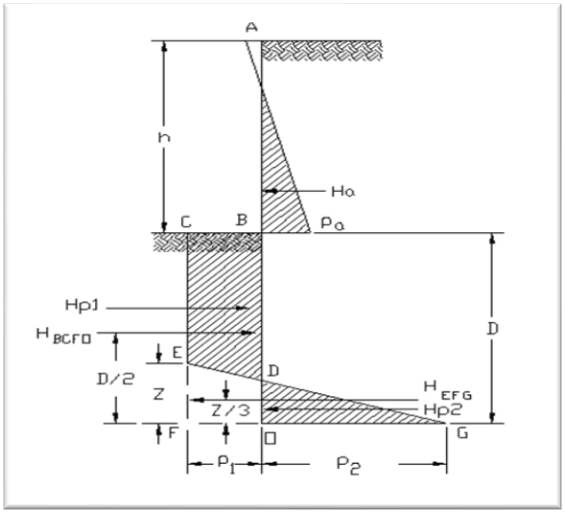

Figure 16: pressure distribution on a cantilever sheet pile in cohesive soils

❖ **Theory:**

For cohesive soil, friction angle, φ= 0, the sheet pile is supported by soil cohesion, C. Because of cohesion, the soil can stands by itself at certain height without the sheet pile support. Since f= 0, lateral earth pressure distributes uniformly below the excavation,

❖ **Calculating active earth pressure**

The active and passive lateral earth pressure of soil can be written as

$s_a=qK_a2C\ddot{O}K_a$, $s_p=qK_p+2C\ddot{O}K_p$

Where C is cohesion of soil and q is surcharge and

$K_a=\tan^2(45-\varphi/2)$, $K_p=\tan^2(45+\varphi/2)$ are active and passive lateral earth pressure, and φ is internal friction angle.

When friction angle, φ= 0, $K_a = K_p = 1$, and $\delta_a=q-2C$ and $\delta_p=q+2C$

If the unit weight of soil is $\boldsymbol{\gamma}$, the surcharge q at bottom of excavation on the earth side is $\boldsymbol{\gamma}$h, then, the lateral earth pressure, $p_a = \boldsymbol{\gamma}h - 2C$

The lateral pressure at top of excavation will be –2C. At a distance, d, below the top of excavation, the lateral pressure, $\delta_a=\boldsymbol{\gamma}d-2C = 0$, and $d = 2C/\boldsymbol{\gamma}$is the free-standing height of soil. The resultant force $H_a=p_ah/2$

❖ **Determine lateral earth pressure below excavation:**

Below the bottom of excavation, the sheet pile is subjected to both active and passive pressure. The active pressure is δ_a=gh-2C. The passive pressure is δ_p= 2C, since q = 0 Therefore, the net pressure isp_1= δ_p-δ_a= 2C-(γh-2C) = 4C-γh

At the bottom of sheet pile, the sheet pile is subjected to active pressure on the excavation side, and passive pressure on the earth side. The active pressure is δ_a=γD-2C, and the passive pressure is δ_p=(h+D)-2C. Therefore, the net pressure is

p_2= δ_p-δ_a= γD+2C-[(h+D)-2C] = 4C+γh

❖ **Derive equation for depth z from $\sum$Fx = 0**

Summarize horizontal forces, we have $\sum F_x = H_a - H_{p1} + H_{p2} = 0$; Where $H_a = p_a (h-d)/2$, and $H_{p1} - H_{p2}$ = HBCFO + HEFG; Since HBCFO = p_1*D,
and HEFG = (p_1+p_2)*Z/2=8C*Z/2 =4C*Z $H_a - p_1$*D +4C*Z= 0
Then, Z= (p_1*D- H_a)/4C

❖ **Derive equation for embed depth D from $\sum M_o = 0$**

Taking moment about point O at bottom of sheet pile, we have
$\sum M_o = H_a$*[(h-d)/3+D]- p_1*D^2/2+4C*Z^2/3 = 0

❖ **Structural design**

The maximum shear occurs at point B, at the bottom of excavation and or at point D. The maximum moment occurs at a distance y below the bottom of excavation where shear equal to zero. Then,H_a – p_1*y = 0, therefore, y = H_a/p_1

The maximum moment : M_{max}=H_a*[(h-d)/3+y]- p_1*y^2/2

The sheet pile section can be selected based on maximum moment and shear.

❖ **Design procedure:**

- Calculate free standing height, d = 2C/γ
- Calculate=(h-d)
- Calculate H_a=p_a*h/2
- Calculate p_1=4C-γh
- Assume a trial depth, D, Calculate Z=(p_1*D-H_a)/(4C)
- Calculate R=H_a[(h-d)/3+D]- p_1*D^2/2+4CZ^2/3
- If R is not close to zero, assume a new D, repeat steps 5 and 6

- The design length of sheet pile is L=h+D*FS, FS=1.2 to 1.4.
- Calculate y = H_a/ p_1.
- Calculate $_{Mmax}$=H_a[(h-d)/3+y]- p_1*y^2/2
- Calculate required section modulus S= $_{Mmax}$/F_b.
- Select sheet pile section

❖ **Numerical example for cohessionless soil**

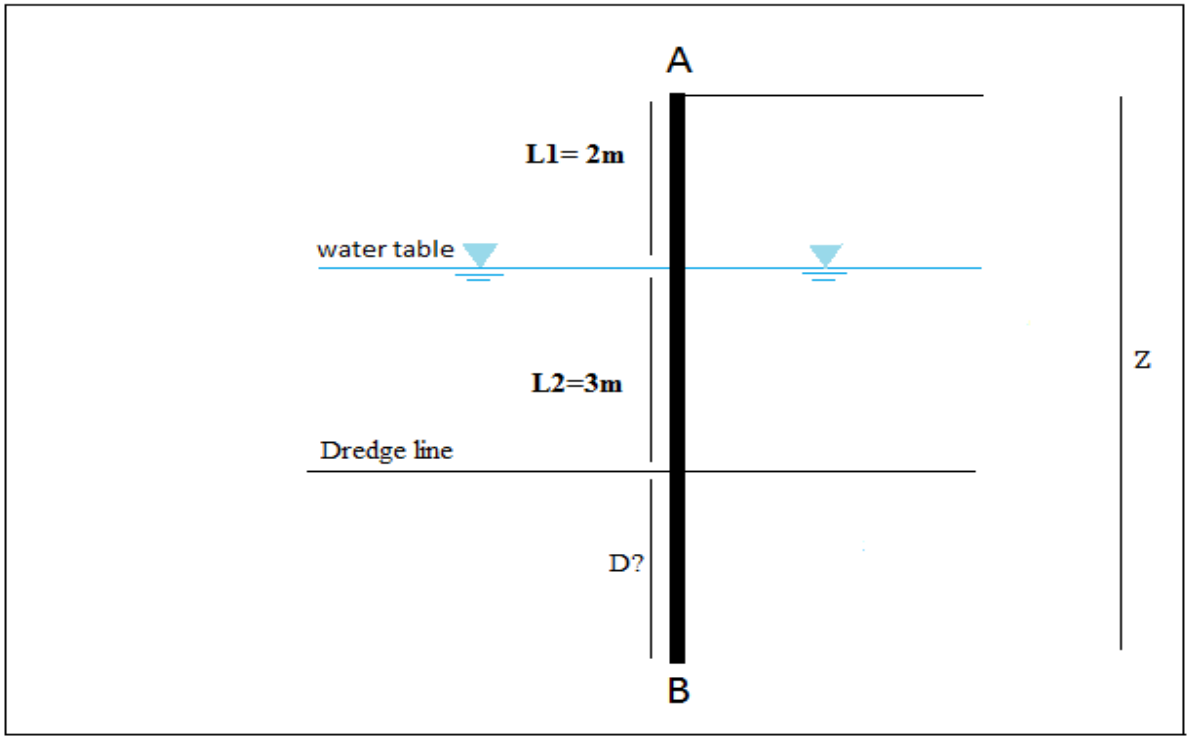

Figure 17: cantilever sheet pile in cohessionless soil

- For simplification purposes we consider the ground surface to be flat , water table to be at the same level on both sides and the soil is cohessionless, **AB** is the sheet pile penetrating the soil
- First thing required is to find theoretical depth of embedment **D**
- Second , determining the total length of sheet pile
- Finally, finding the minimum section modulus of the sheet pile with **σ** all is 172 MN/m²
- The soil in this case has on the first layer of **L1=2m** , **ϕ´= 32°** and **C = 0** and **γ = 15,09KN/m³**
- And the second layer of **L2= 3m**, **ϕ´= 32°** and **C = 0** and **γsat = 19,33KN/m³**

- ✓ Step 1: calculating **Ka** and **Kp**

Ka = 1-sin**ϕ**′/ 1+ sin **ϕ**′ therefore **Ka** = 1- sin 32 /1+ sin32 = 0. 307

Kp = 1+sin**ϕ**′/ 1-sin **ϕ**′ therefore **Kp** = 1+sin 32 /1- sin32 = 3. 25

- ✓ Step 2: calculating **σ** ′

At depth Z=0

σ′= **γ** L1 Ka = 15, 09 *0 .307 *0 = 0

At depth Z= 2m

σ1′=**γ** L1 Ka = 15, 09 *0 .307 *2 = 9,726 KN/m²

At depth Z=3m

σ2′= (**γ** L1 + **γ**' L2) Ka / **γ**sat – **γ**water = **γ**'

σ2′=18.53KN /m²

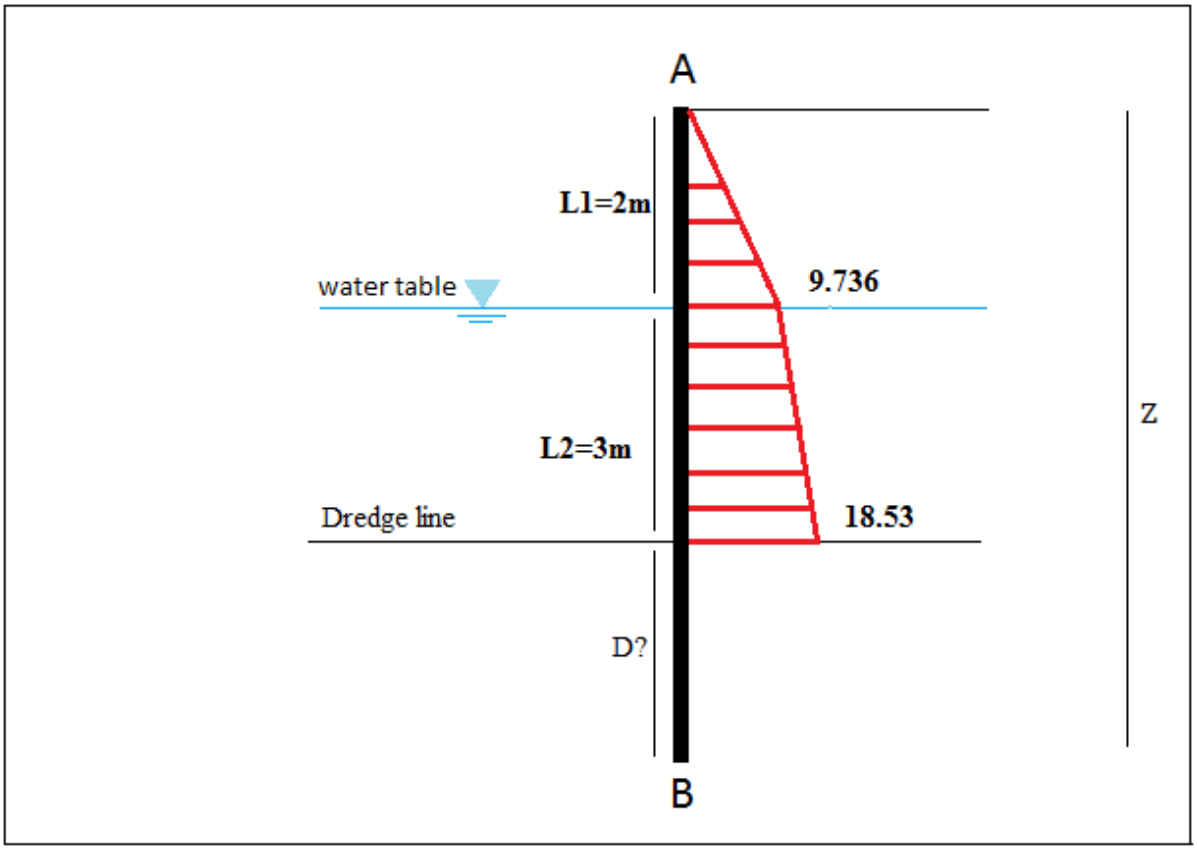

Figure 18: distribution of active pressure above dredge line

- ✓ Step 3: determine **L3**

At depth **L3** below dredge line net pressure is 0

The Net lateral pressure

σnet ′= σ ′a – σ ′p =0

Where σ ′p=[γ ′ (Z-(L1+L2))] Kp

And σ ′ a =[γ L1+γ ′ L2+ γ ′(Z-(L1+L2))] Ka

σnet ′=[γ L1+γ ′ L2+ γ ′(Z-(L1+L2))] Ka - [γ ′ (Z-(L1+L2))] Kp =0 /Z-(L1+L2)=L3

σ2′= (γ L1 + γ' L2) Ka

σ′ net = σ2′- γ ′(Z-L3) (Kp-Ka)=0

Therefore L3= σ2′/ γ ′ (Kp-Ka) so L3=18.53/9.52 (3. 25 -0. 307) = 0.66m

✓ Step 4 calculating P:

P = A1+ A2+ A3 +A4

P = 0.5*9.726*2 +9.726*3+0.5*18.53-9.726*3+0.5*18.53*0.66= 58.3KN/m

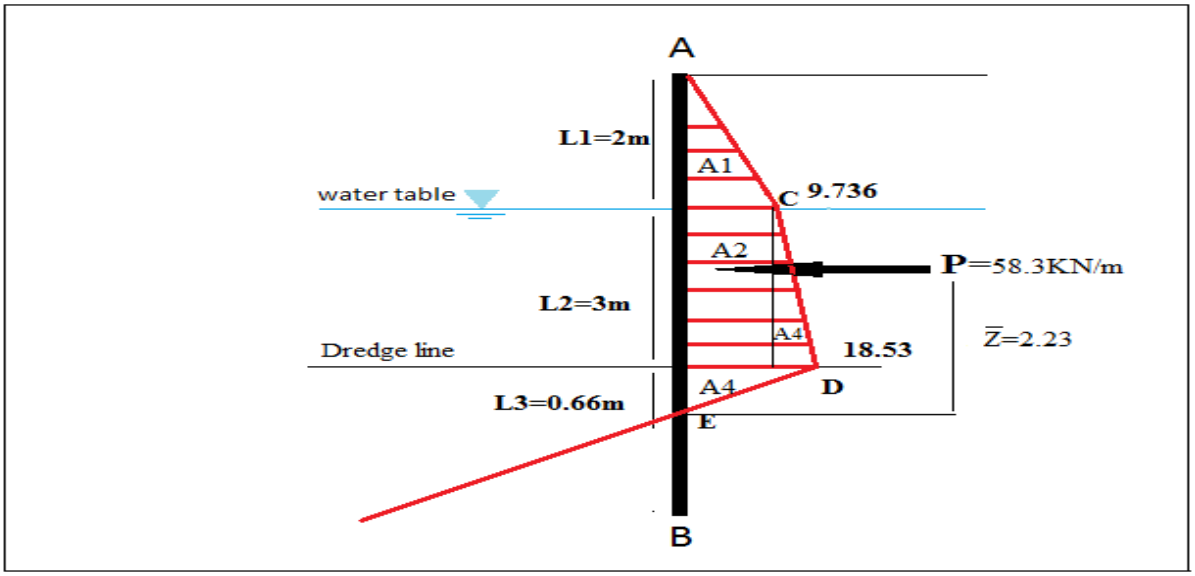

Figure 19: distribution of a arias and P

✓ Step5 calculating Z bar Σ ME= 0

Σ ME= 0

A1(3/2+3.66) +A2(1.5+0.66)+A3(3/3+0.66)+A4(2/3*0.66)-58.3Zbar =0

Zbar =2.23m

✓ Step 6Net pressure at the bottom of the sheet pile

σ ′ a= $\boldsymbol{\gamma}$ D Ka

σ ′ p= ($\boldsymbol{\gamma}$L1+ $\boldsymbol{\gamma}$'L2) Kp+ $\boldsymbol{\gamma}$'D Kp

σnet ′= σ ′p – σ ′a =0

σ ′net = ($\boldsymbol{\gamma}$ L1+ $\boldsymbol{\gamma}$ ′ L2) Kp+ $\boldsymbol{\gamma}$ ′ L3(Kp-Ka)+$\boldsymbol{\gamma}$ ′ L4(Kp-Ka)=0

σ ′5 = ($\boldsymbol{\gamma}$ L1+ $\boldsymbol{\gamma}$ ′ L2) Kp+ $\boldsymbol{\gamma}$ ′ L3(Kp-Ka)

σ ′5= 214.6KN/m²

✓ Step7 calculating L4

L⁴4+ A1 L³4 - A2 L²4 - A3 L 4 - A4 = 0

- A1= σ5′/ $\boldsymbol{\gamma}$ ′ (Kp-Ka) =7.66
- A2= 8P/ $\boldsymbol{\gamma}$ ′ (Kp-Ka) = 16.65
- A3= 6P[2Z $\boldsymbol{\gamma}$ ′ (Kp-Ka)+ σ5′] / $\boldsymbol{\gamma}$ ′² (Kp-Ka)² =151.93
- A4=P(6Z σ5′+4P) / $\boldsymbol{\gamma}$ ′² (Kp-Ka)² =230.72

Therefore L4 = 4,8m

✓ Calculate σ ′3

σ3′= $\boldsymbol{\gamma}$ ′ L4 (Kp-Ka) = 131 .28 KN/m²

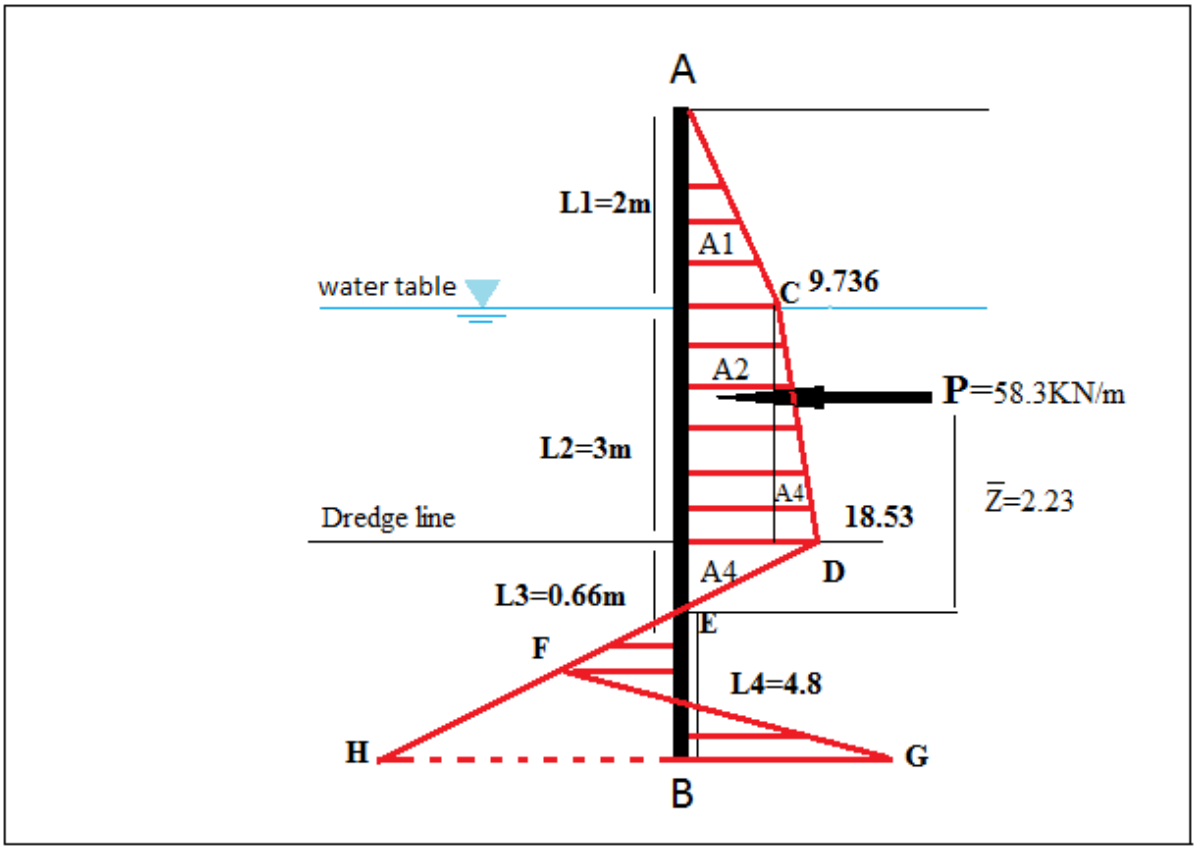

Figure20: Net pressure and L4 determining

- ✓ Step 9 calculate theoretical depth D

D= L3+L4=0.66+4.8= 5.46

For 30 % increase in D total length of pile would be

L1+L2+1.3(L3+L4) = 12.1m

- ✓ Step 10: calculate point of zero shear and Mmax

P – 0.5 *Z '² *γ'*(Kp-Ka)

Z ' = √2P/ γ'*(Kp-Ka) =2,04

Mmax =P(Z'+Z)-[0,5 γ' Z'² (Kp –Ka)]Z'/3= 209,39

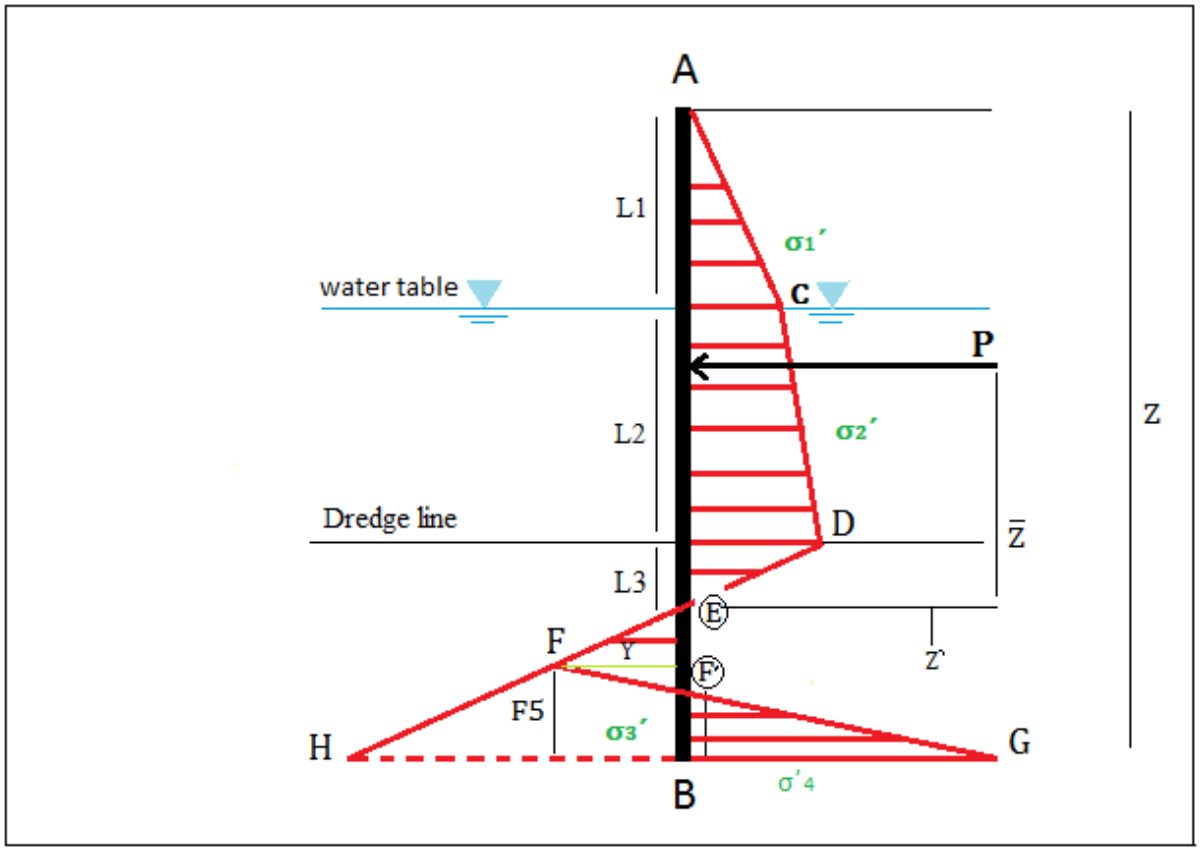

Figure21: point of zero shear and Mmax

Minimum section modulus of sheet pile

S= M max / σ all

S= 1.21 /10³m³ /m

VIII. Application to the study site

Before any mitigation measure is elaborated, one should have a clear picture of the tridimensional layout of the problematic slope. Not just that, but one should have representative physical and mechanical properties of soil and well as a good understanding of the mechanism of failure. All these data is gathered during the reconnaissance survey in the field and the tests in the laboratory.

Figure 22. is a cross section of the study area; it shows an upper cover of unconsolidated material mainly made of silt, clay, sand and an organic material responsible for the black aspect of the soil. This soil is not thick and can go up 30 cm. Below this cover comes a yellow brown to grey plastic layer mainly derived from weathering, erosion and deposition of trias, cretaceous marl and miocene

material. This is the horizon that causes most of the instabilities in the area; it is up to several meters thick. Then comes what we consider as bedrock constituted mainly by triasic material.

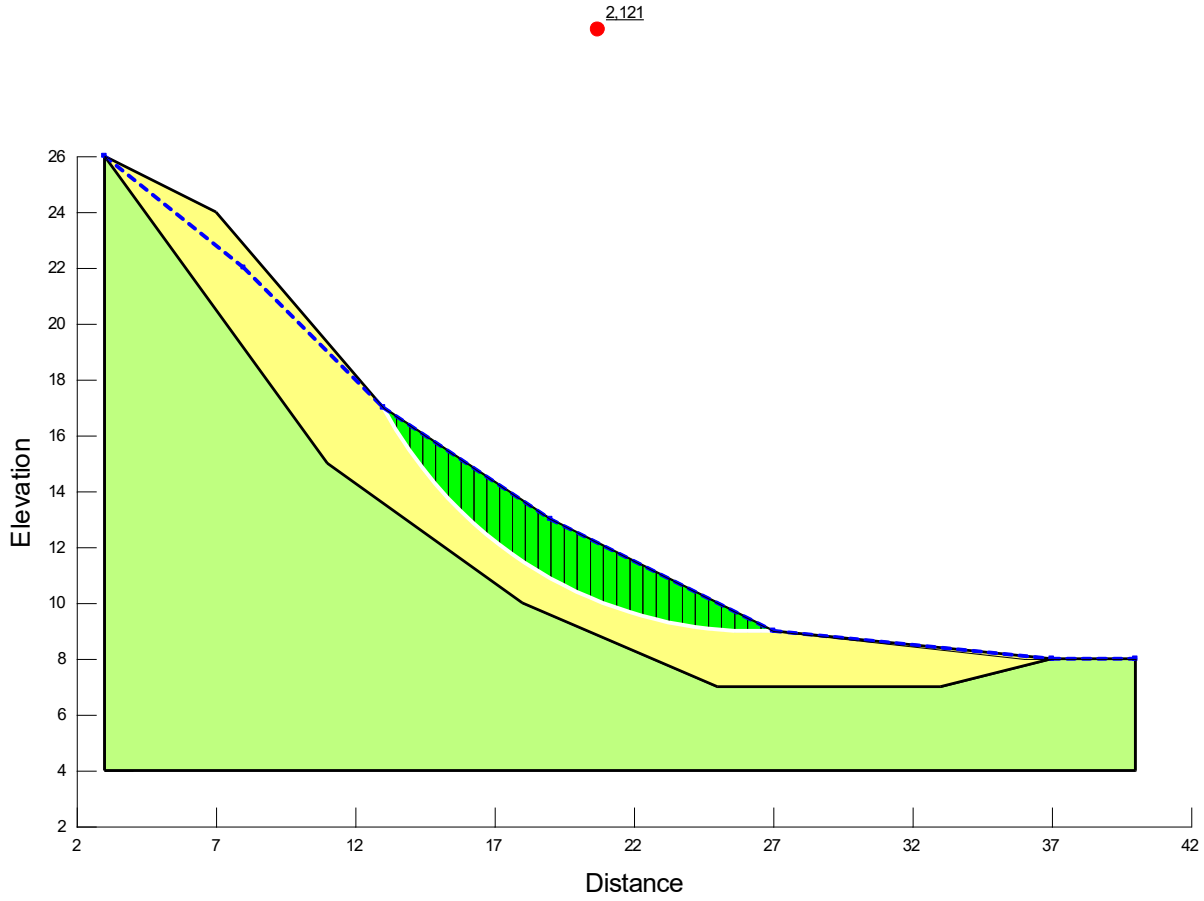

Figure 22: cross section of the study area.

The choice of the sheet pile characteristics such as the allowable flexural strength(yield bending moment), the section modulus and the length were hand calculated following the methodology presented earlier.Assuming the sheet pile acts as a continuous section, the maximum bending moments calculated in kN·m .

$\sigma_{all} = \frac{M_{max}}{s}$, σ_{all}= allowable yield stress = 266 MPa for steel, M_{max} = maximum moment, s = section modulus.

Sectional properties

Type	Dimension			Per pile				Per 1 m of pile wall width			
	Effective width W mm	Effective height h mm	Thickness t mm	Sectional area cm^2	Moment of inertia cm^4	Section modulus cm^3	Unit mass kg/m	Sectional area cm^2/m	Moment of inertia cm^4/m	Section modulus cm^3/m	Unit mass kg/m^2
NS-SP-10H	900	230	10.8	110.0	9,430	812	86.4	122.2	10,500	902	96.0
NS-SP-25H	900	300	13.2	144.4	22,000	1,450	113	160.4	24,400	1,610	126
NS-SP-45H	900	368	15.0	187.0	40,500	2,200	147	207.8	45,000	2,450	163
NS-SP-50H	900	370	17.0	212.7	46,000	2,490	167	236.3	51,100	2,760	186

Figure 23: Geometrical characteristics of sheet piles

Having the maximum moment calculated, and the σ_{all} allowable of the steel we can find the required section modulus from which we can select the appropriate sheet pile type.

The stability calculations have been carried out using two software, Praxis 8.2 and Geoslope 2018. Praxis 8.2 is finite elements software that computes the safety factor using the phi/c reduction method. Geoslope on the other hand uses on top of finite element analysis in its module sigma/w, it uses limit equilibrium methods to analyze and compute the safety factor before and after the reinforcement.

IX. Modeling using Geoslope software (slope/w)

In slope/w, the use of sheet pile load to reinforce a marginally stable slope is quite often. Hence, to carry out stability calculations, soil properties such as unit weight, cohesion angle of internal friction and so on, must be determined with a great accuracy. In the meantime, the properties of the reinforcing material should be specified. In slope/w the sheet pile contribute to stability by increasing the resisting shear force. The sheet has a shear strength of 200 kN. The length is not important provided that the pile is well embedded in the bedrock and cross the slip surface.

In this study, the geological model and the soil properties were first introduced and the factor of safety was determined using limit equilibrium method. Methods such as Morgenstern and price, Ordinary method, Jambu, Bishop all gave nearly similar safety factor. According to the soil properties we got the F is 1.378

On application of the reinforcement using a sheet pile wall with shear strength of 200 kN the safety factor jumped to 3.78.

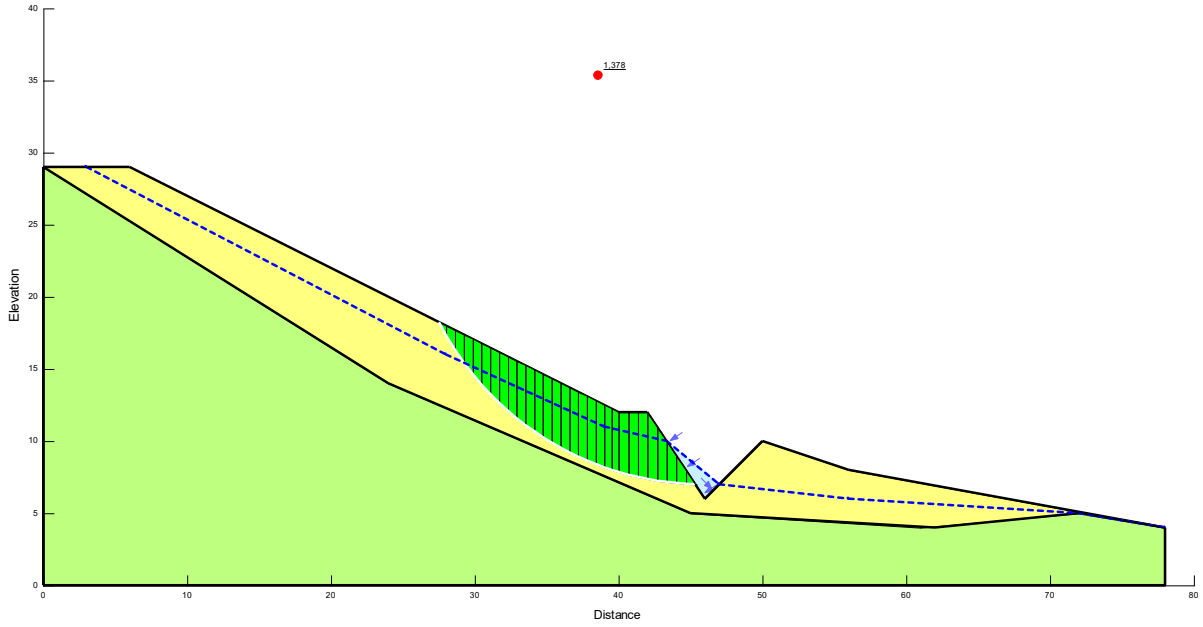

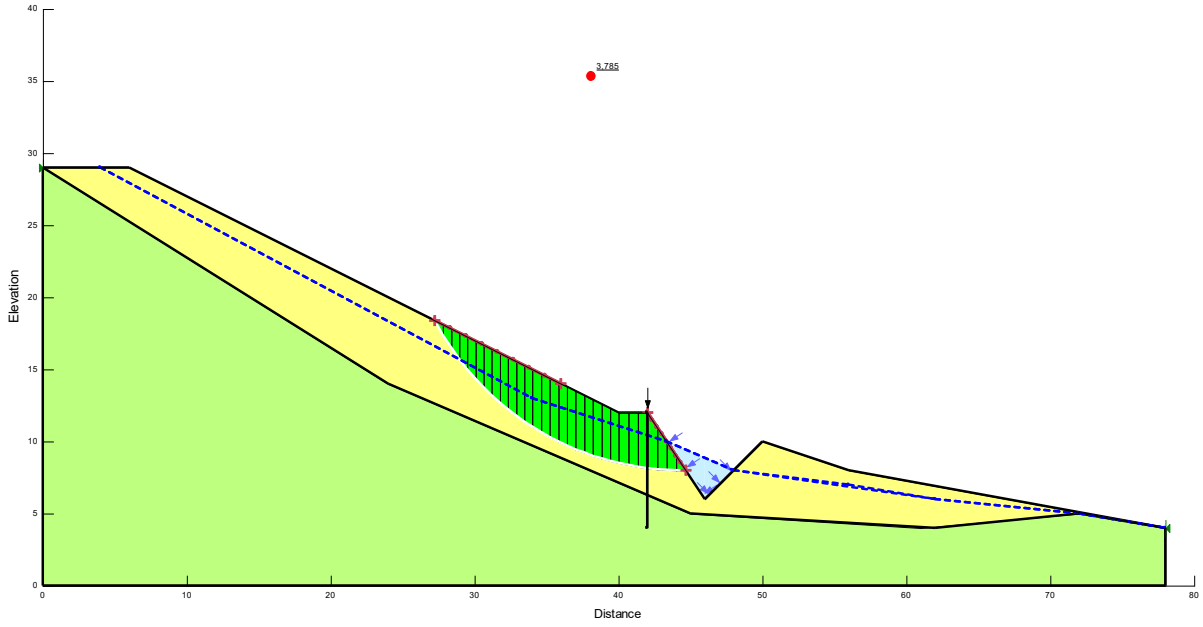

Figure 24 and 25: Stability analysis and factor of safety after reinforcing the slope

X. Plaxis Modeling :

In plaxis 8.2 finite elements analysis, the stability calculations are based on the balance between active thrust forces and passive and how the specified reinforcing material withstand the

resulting bending moment. But before the Plaxis analysis, hand calculations of the optimum depth of the sheet piles and the required allowable bending stress were carried out

In plaxis as in Geoslope (slope/w) the geological model was first introduced with soil physical and mechanical properties, hydrogeological conditions. Then comes the setup of calculation phases and the type of the soil behavior.

After the first run of the plaxis software taking in consideration the properties of the sheet pile such as flexural stiffness, normal stiffness, length of the pile, weight of the pile by meter long and so on.

The first calculation run without the introduction of the sheet pile show an instable slope with a factor of safety of the order of 0.99 (figure. 26 and 27)

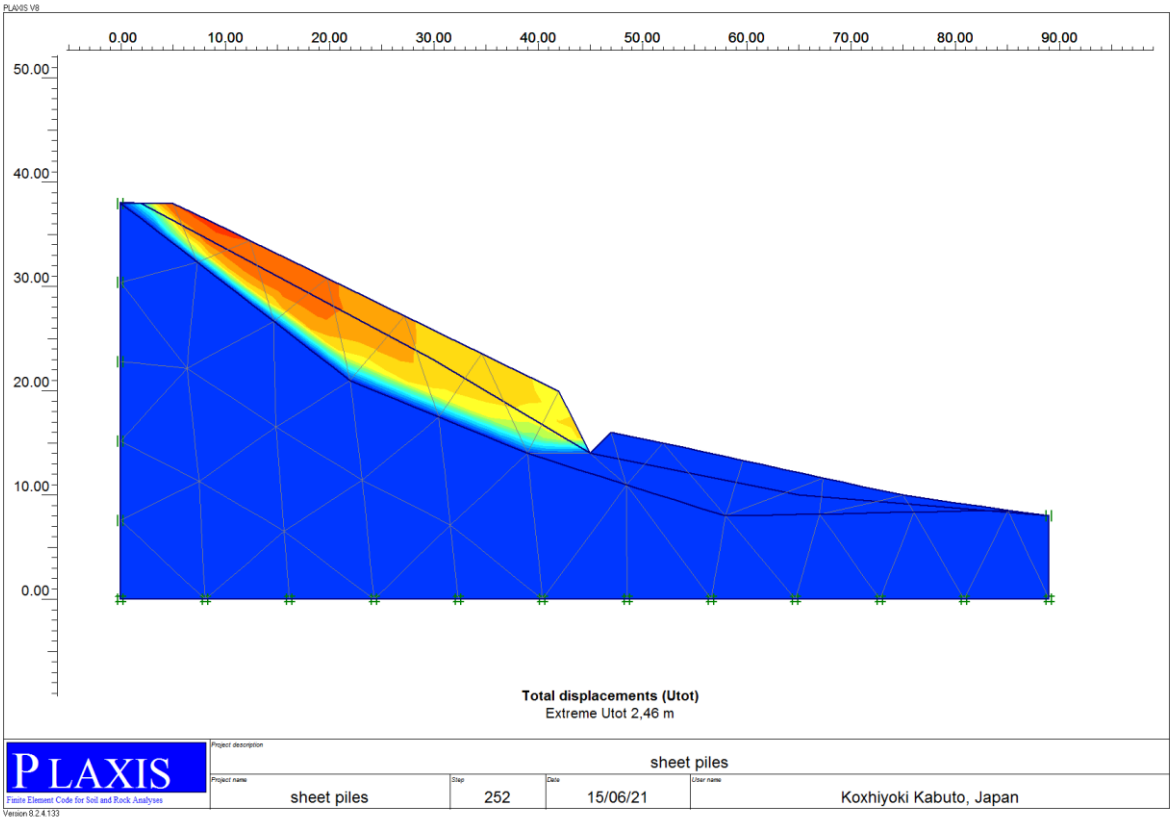

Figure 26: Slope stability calculation before reinforcement

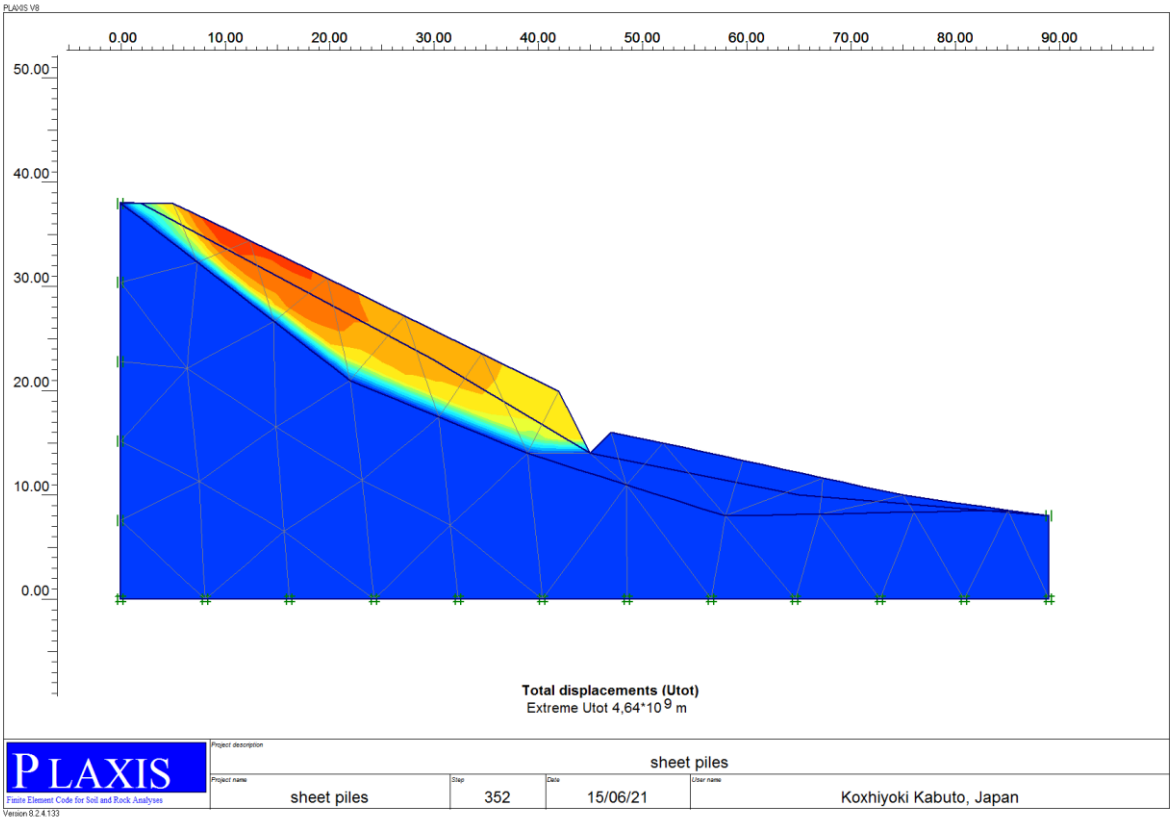

Figure 27: Slope stability calculation before reinforcement

Phi/C reduction method for slope stability computation

PLAXIS - Finite Element Code for Soil and Rock Analyses

Project description	: sheet piles	PLAXIS 8.0
User name	: Koxhiyoki Kabuto, Japan	
Project name	: sheet piles	Date : 15/06/2021
Output	: Calculation information	Step : 352 Page : 1

Step Info

Step 352 of 352	Incremental Multipliers		2,000	
PLASTIC STEP			0,000	

Prescribed displacements	Mdisp:	0,000	Σ-Mdisp:	1,000
Load system A	MloadA:	0,000	Σ-MloadA:	1,000
Load system B	MloadB:	0,000	Σ-MloadB:	1,000
Soil weight	Mweight:	0,000	Σ-Mweight:	1,000
Acceleration	Maccel:	0,000	Σ-Maccel:	0,000
Strenght reduction factor	Msf:	0,000	Σ-Msf:	0,992
Time	Increment:	0,000	End time:	0,991

Staged construction

Active proportion total area	Marea :	0,000	ΣMarea :	1,000
Active proportion of stage	Mstage :	0,000	ΣMstage :	0,000

Safety factor of 0.99 for the slope before reinforcement

The second calculation run in plaxis was done after the introduction of a sheet pile type of reinforcement.

The sheet pile is of length = 8 m

A flexural rigidity of = 60 10^6kNm^2/m

A normal stiffness of= 70 10^6kN/ m

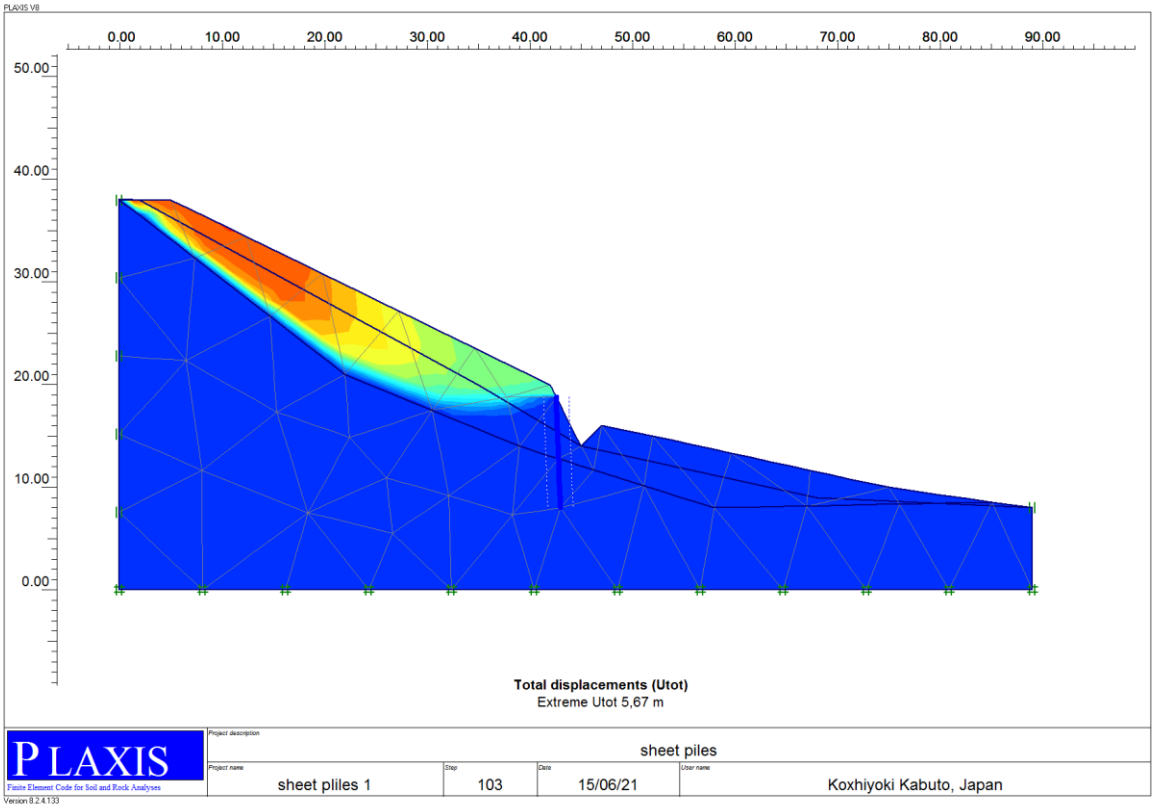

Figure 28: Slope stability computation after reinforcement

Figure 29: Total displacement diagram

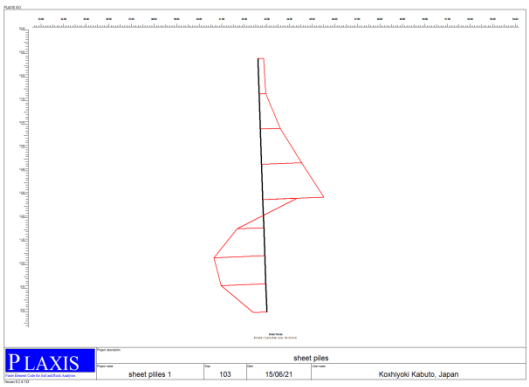

Figure 30: Shear forces diagram

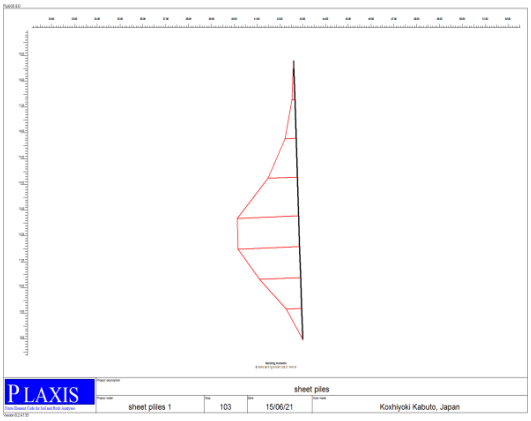

Figure 31: Bending moment diagram

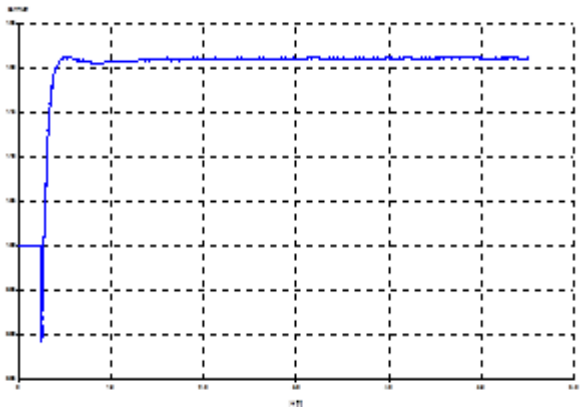

Figure 32: Factor of safety 1.2

Conclusion :

- The use of Cantilevered sheet pile in this case was accurate because the factor of safety jumped from low value to an ideal one
- Cantilevered sheet piles are also cheaper and easier to transport
- Retaining walls re heavy to the soil and can cause settlement and other issues in the soil that we do not desire ,while sheet piles do not due to their thinness and flexibility
- Sheet piles are also easier in the installation process

CONCLUSION

In this research program it has been dealt with one of the most challenging problem in geotechnical engineering which the stability assessment of natural slopes. It is challenging not because of the cumbersome analysis rather than the heterogeneity of the natural material. Knowing that the process of rock degradation and sedimentation of massifs along hill sides results very often in stratified crosscut and discontinuous soil with properties changing sometimes on few centimeters scale. Nevertheless, the heterogeneity becomes less pronounced on larger scale and one can suppose that the medium is homogeneous and continuous and accept the inherent inaccuracies in the results.

Souk Ahras area is known by the severity and the widespread of the landslide problem due to the weather on one side and the structural framework and the lithological nature of the geological formations. From a structural point of view, the area is located on a regional diapir which continues to rise up inducing high mountain picks, deep valleys and steep slopes. The lithological natures of the formations which are dominantly clay, marl, evaporate and limestone and the important rainfall have favored the erosion phenomenon and the deposition of relatively thick beds of clay, silt and degraded marl on the slopes. This later is highly susceptible to land sliding during rainy winters and springs.

In Zaarouria, at its north entrance, the road was cut parallel to a long slope face near a temporary ravine. After year of service, the road has shown longitudinal and parallel cracks and starts to subside. Field survey has revealed that all the slope is in fact instable and urgent remedial measures must be undertaken. A steel sheet pile was driven in the ground until it reaches the marl layer considered to be stable.

The present study is a reassessment of the efficiency of the steel sheet piles in stopping the instability. For this purpose a hand calculation procedure was undertaken for the determination of the maximum bending moment in order to determine the section modulus that allow to choose the sheet pile.

In plaxis, the calculation have shown that the slope is unstable in its natural state with an F = 0.99. Upon the introduction of the reinforcement by the sheet piles the F jumps to become 1.2. In geoslope, the reinforcement has increased F from 1.37 to 13.78.

BIBLIOGRAPHY

- analysis with conventional limit-equilibrium invistigation".(2003)University of Toronto, Toronto, Canada
- Carol Matthews and ZeenaFarook, Arup and Peter Helm, "Slope stability analysis – limit equilibrium or the finite element method?"(2014), ground engineering Newcastle University.
- Cernica geotechnical engineering soil mechanics
- Cours de mécanique des sols Notes de cours Rideaux de palplanches Année 2006-2007
- Dr. B. C. Punmia, Er. Ashok Kumar Jain, Dr. Arun Kumar Jain "Soil mec
- Dr. K. R. Arora "Soil mechanics and foundation engineering", (1987)Standerd publishers distrebuters,(2015) ISBN: 81-8014-112-8
- Dr. V. N. S. Murthy, ""
- Geotechnical engineering good book
- Hadji Rihab thesis of PHD
- https://pubs.usgs.gov/circ/1325/pdf/C1325_508.pdf
- https://www.dnr.wa.gov/geology(A Homeowner's Guide to Landslides)
- https://www.oregongeology.org/landslide/homeowners-landslide-guide.pdf
- https://www.preventionweb.net/files/25233_25102landslidesenglish1.pdf
- https://www.researchgate.net/publication/317328970_Landslides-Causes_Mitigation
- International Journal of Engineering Research & Technology (IJERT) Vol. 6 Issue 03, March-2017
- Khaled Farah, MounirLtifi and HediHassis. "A study of probabilistic FEMs for a slope reliability analysis using the stress fields" (2015), The Open Civil Engineering Journal, 9, 196-206.
- LysandorsPantelitides& D. V. Griffits, "Stability assessement of slopes using different factoring strategies." University of Newcast, Newcast. (2013)
- Mahdadi Fatna thesis of PHD
- R. Kourkoulis1, F. Gelagoti, I. Anastasopoulos, and G. Gazetas, M.ASCE "Hybrid method for analysis and design of slope stabilizing piles", (2012), 10.1061/(ASCE)GT.1943-5606 .0000546.
- ReginaldHammah, ThamerYacoub, Brent Corkum, John Curran, Lassonde Institute, "Comparision of finite elementslopestablity
- V. GRIFFITHS and P. A. LANE "Slope stability analysis by fnite elements". (1999). Geotechnique 49, No. 3, 387-403